

**Evaluating the Interactions of Crop Management, Carbon Cycling, and Climate
Using Earth System Modeling and Remote Sensing**

Michael William Graham

Dissertation submitted to the faculty of the Virginia Polytechnic Institute and State
University in partial fulfillment of the requirements for the degree of

Doctor of Philosophy
In
Geospatial and Environmental Analysis

Megan E. O'Rourke, Chair
R. Quinn Thomas, Co-Chair
James B. Campbell, Member
Brian D. Strahm, Member

August 1, 2019
Blacksburg, Virginia

Keywords: 'no-till', conservation tillage, soil carbon, land use change, crop residue,
emissions, agriculture, land management

CC BY-NC-ND 2019, Michael W. Graham

Evaluating the Interactions of Crop Management, Carbon Cycling, and Climate Using Earth System Modeling and Remote Sensing

Michael William Graham

ADADEMIC ABSTRACT

Crop management practices, such as soil tillage and crop residue management, are land management activities with potentially large impacts on carbon (C) cycling and climate at the global scale. Improvements in crop management practices, such as conservation tillage or 'no-till' (NT), have been proposed as climate change mitigation measures because such practices may alter C cycles through increased sequestration of soil C in agricultural soils. Despite their potential importance, regional to global scale data are lacking for many crop management practices, and few studies have evaluated the potential impact of the full range of crop management practices on C cycling and climate at the global scale. However, monitoring of crop management practices is crucial for assessing spatial variations in management intensity and informing policy decisions. Inclusion of crop management practices in Earth system models used for assessing global climate is a key requirement for evaluating the overall effects of different crop management practices on C cycling and their potential to mitigate climate change. Studies in this dissertation seek to address these issues by: (1) evaluating the efficacy of remote sensing methods for monitoring differences in soil tillage and crop residue management practices in Iowa; (2) incorporating soil tillage practices into an Earth system model and assessing the potential for soil C sequestration and climate change mitigation through adoption of NT practices; (3) assessing the historical impact of including the full range of crop management practices (residue harvest, grain harvest, soil tillage, irrigation, and fertilization) on changes in C cycling associated with land use and land cover change (LULCC) to crops in an Earth system model. The remote sensing study found that performance of the minimum Normalized Difference Tillage Index (minNDTI) method for assessing differences in tillage and residue management was below average compared to previous studies, even when using imagery from both Landsat 8 and Sentinel-2A sensors. Accurate assessment of these practices using minNDTI was hindered by issues with image quality and inability to obtain sufficient cloud-free, time series imagery during the critical planting window. Remote sensing research aimed at obtaining regional to global scale data on tillage and residue management practices is likely to continue to face these issues in the future, but further research should incorporate additional sensors and assess the efficacy of the minNDTI method for multiple locations and years. Adoption of NT practices in the Community Land Model, which is the land component of the Community Earth System Model, resulted in a cumulative soil C sequestration of 6.6 – 14.4 Pg C from 2015 – 2100 under a future climate change scenario (Representative Concentration Pathway 8.5), and cumulative soil C sequestration was equal to approximately one year of present-day fossil fuel emissions. Adjusting for areas where NT is already practiced had minor impacts on cumulative soil C storage, reducing gains in soil C from NT adoption by 0.4 – 0.9 Pg C globally. These results indicate that soil C sequestration and potential for climate change

mitigation through NT may be more limited than has been anticipated elsewhere. Soil C sequestration via NT adoption was highest in temperate regions of developed countries with high initial soil C contents, indicating these areas should be targeted for NT adoption. Simulating the full range of crop management practices in the Community Land Model resulted in an increase in C emissions due to LULCC of 29 – 38 Pg C compared to scenarios with generic crops and model defaults. Individual crop management practices with the largest impact on LULCC emissions were crop residue harvest (18 Pg C), followed by grain harvest (9 Pg C) and soil tillage (5 Pg C). Although implementation of crop residue harvest and soil tillage was extreme in this study, these results imply that Earth system models may underestimate emissions from LULCC by excluding the full range of crop management practices. Studies in this dissertation corroborate the importance of crop management practices for C cycling and climate, but further research on these management practices is needed in terms of data collection, improving process-level understanding, and inclusion of these practices in Earth system models.

Evaluating the Interactions of Crop Management, Carbon Cycling, and Climate Using Earth System Modeling and Remote Sensing

Michael William Graham

GENERAL AUDIENCE ABSTRACT

Agriculture is an important use of land by humans, and cropped areas account for 12% of Earth's ice-free land area. Management practices on cropped areas, such as soil tillage and crop harvest, can affect global climate and contribute to climate change by releasing greenhouse gases such as CO₂ to the atmosphere. Crop management can also diminish climate change by storing carbon (C) in soils and vegetation, thus reducing the amount of CO₂ in the atmosphere. Certain crop management practices, such as conservation tillage or 'no-till' (NT), have been widely promoted as means of mitigating climate change by storing more C in agricultural soils. However, there is limited information available on how various crop management practices differ between locations at the global scale. Additionally, some important crop management practices are not included in many Earth system models, which are used to assess global climate and form the basis of reports on climate change by the Inter-governmental Panel on Climate Change. Studies in this dissertation attempt to remedy these deficiencies by: (1) evaluating the effectiveness of satellite imagery for monitoring differences in soil tillage and crop residue management practices in Iowa; (2) incorporating soil tillage practices into an Earth system model and assessing the potential for soil C storage and climate change mitigation through adoption of NT practices; (3) assessing the impact of including the full range of major crop management practices (residue harvest, grain harvest, soil tillage, irrigation, and fertilization) on changes in C cycling and emissions in an Earth system model. The study monitoring tillage practices in Iowa used an index based on satellite imagery to assess differences in tillage and residue management, but found that performance of this index was below average compared to previous studies using similar methods. Accurate assessment of tillage and residue management practices using satellite imagery was hindered by issues with image quality and inability to obtain sufficient cloud-free, sequential imagery during the critical planting window. Efforts aimed at using satellite imagery to monitor tillage and residue management practices at the regional to global scale are likely to continue to face these issues in the future, but further research should include imagery from additional satellites, as well as assess the efficacy of the methods employed here for other time periods and locations. Adoption of NT practices in the Community Land Model resulted in soil C storage of 6.6 – 14.4 Pg C from 2015 – 2100, but these values were low relative to soil C gains from NT that have been anticipated by some studies and policy-makers. Cumulative soil C storage was equal to approximately one year of present-day fossil fuel emissions, which was well below objectives for soil C sequestration on agricultural land set out by international policy initiatives, such as the '4 per 1000' program. Simulating the full range of major crop management practices in the Community Land Model resulted in an increase in C emissions of 29 – 38 Pg C. Individual crop management practices with the largest impact on emissions were crop residue harvest (18 Pg C), followed by grain harvest (9 Pg C) and soil tillage (5 Pg C).

Although implementation of crop residue harvest and soil tillage was extreme in this study, these results imply that Earth system models may underestimate emissions from agriculture by excluding important crop management practices. Studies in this dissertation corroborate the importance of crop management practices for C cycling and climate, but further research on these management practices is needed in terms of data collection, improving basic understanding of these processes, and inclusion of these practices in Earth system models.

DEDICATION

For Mom & Dad, Nana & Papa, Gramps & Grandma

*“For in the end we will conserve only what we love,
We will love only what we understand,
And we will understand only what we [have learned]”*

- Baba Dioum, Senegalese conservationist
From “The Nature and Property of Soils” (Weil and Brady, 2016)

ACKNOWLEDGEMENTS

No one completes a PhD or accomplishes anything meaningful without a whole lot of investment from others. I would first like to extend my gratitude to my co-advisors, Megan O'Rourke and Quinn Thomas for their willingness to split advisory duties and for providing guidance over the years, as well as their faith in allowing me to follow my nose in developing a unique dissertation. I would also like to thank my committee members – Jim Campbell and Brian Strahm. Jim and the GEA program assisted in providing overall structure and guidance along the PhD path, and with the remote sensing aspects of this research in particular. Brian Strahm provided insights and feedback that impelled me to think more deeply about the wider context of my work with respect to soil carbon and tillage practices.

My co-authors and collaborators on the manuscripts in this dissertation also deserve recognition. Danica Lombardozzi served as my host at NCAR and was always willing to dig into the nitty gritty details of the CLM, and was instrumental in moving my modeling work forward. Baojuan Zheng provided valuable feedback and discussion on my remote sensing work, while Craig Daughtry at USDA-ARS provided the opportunity to undertake my remote sensing research in Iowa and provided feedback on the associated manuscript. Melannie Hartman, Sam Levis, Gordon Bonan, Dave Lawrence, and others at NCAR provided background and input on including tillage practices in the CLM. Carol Franco facilitated sharing of my work on tillage in the CLM with a wider, international audience through the Koronivia Joint Work on Agriculture under the UNFCCC.

Working with both Megan and Quinn allowed me to inhabit two different lab settings, and my support network and friendships during the PhD process extended to members of both. Firstly, Joshua Rady contributed to this work by providing another set of eyes on the code in the (several) instances when I was stuck, and helped with some of the code implementation (he was also instrumental in wildlife identification). Chris McCullough has been spying on me from his perch behind the lab bench for at least the last three years. This situation improved with the arrival of Jennie Wagner, whose periodic discussions with Chris have provided a welcome distraction from staring at my screen all day. Ben Ahlswede, Laura Puckett, and Wyatt McCurdy gave valuable feedback on my work, as well as insights on whether it is, in fact, acceptable to just walk up that 10% slope in the middle of a trail run. Velva Groover contributed a seemingly endless supply of snacks, baked goods, and field-work commiseration, and the afternoon sugar-rush from the former two likely kept me moving forward on many occasions (on the other hand, Max and Susan will not be on this list). Gina Angelella provided feedback and positive energy from afar.

Financial support for this research was provided in part by U.S. Dept. of Agriculture – National Institute of Food and Agriculture Project #2015-67003-23485, EASM-3: Decadal Prediction of Sustainable Agricultural and Forest Management.

Outside of academia Ellen and Charles Birx, along with the rest of the New River Zen Community, encouraged my sitting practice and provided camaraderie throughout my

time in Blacksburg. Shibabrat Naik ensured that we both had mutual couches to crash on if necessary, and also convinced me that cycling is a viable alternative to running. Arnab Gupta, Poorna Goswami, and the rest of the VT Bengali community continued their long-standing friendships from my previous tenure in Blacksburg, and finally gave me an excuse to visit South Asia in 2018. Trent Davis and members of the USO group provided emotional support and a welcome diversion from every day grad student life on a weekly basis. Honorary lab member Barslund Judd ensured that Chris, Jennie, and I were entertained on a regular basis.

None of this would have been possible without my parents, Ken and Patricia, who have been continually supportive throughout the PhD process, despite this work keeping me away from home for long time periods. All my friends and family have been very understanding and supportive, welcoming me back as though I never left whenever I returned to Boston. Dan and Vanessa Norton (plus Henry and Clementine) were emotionally reassuring and sympathetic about the PhD process and the (occasional) anxiety it causes, though I think procrastinating by playing online chess with Dan may have neutralized their overall impact in terms of getting this degree. Being perpetually trapped in the purgatory of Division 3 in FIFA with my brother Steve for the last four years, along with the accompanying phone calls every other day, made sure I didn't take anything too seriously, except *maybe* FIFA. Apologies to Chrissy and Bodhi for bringing them along against their will on that adventure. My sister, Christine, held down the fort at home and provided critical household IT support in my absence. Shout-outs to long-time friends at home include: Thilina Jayasekera, who I can always count on to let me come over and just hang out whenever I'm home; Joel Tenenbaum, for his commiseration, friendship, and activities with widely varying degrees of erudition; Sean Morris for his commiseration, friendship, and existential introspection; Chris Romanelli, for his commiseration, friendship, and letting me dogsit Eli. To all my other friends and family in Boston and elsewhere – you made sure I was never bored whenever we reconvened and that we maintained our friendships over years, despite the distances involved.

We're on to Nairobi.

TABLE OF CONTENTS

ADADEMIC ABSTRACT.....	ii
GENERAL AUDIENCE ABSTRACT	iv
DEDICATION	vi
ACKNOWLEDGEMENTS	viii
TABLE OF CONTENTS	x
LIST OF FIGURES.....	xii
LIST OF TABLES	xvi
CHAPTER 1. INTRODUCTION	1
CHAPTER 2. REMOTE SENSING OF TILLAGE INTENSITY IN IOWA USING MINNDTI METHOD AND HARMONIZED LANDSAT 8 SENTINEL-2 DATA	3
Abstract	3
Introduction	4
Materials and Methods	6
Study area	6
Field data collection	7
Remote sensing data acquisition	9
Image processing	10
Simple linear regression (SLR) and repeated K-fold cross validation (RKCV) analyses	10
Results	13
Time-series NDTI, NDVI, and WI.....	13
Models and accuracy assessment	16
Discussion	20
Conclusions & Recommendations	21
CHAPTER 3. MODELING SHOWS MODEST CAPACITY OF ‘NO-TILL’ AGRICULTURE TO OFFSET EMISSIONS	24
Abstract	24
Introduction	24
Methods	25
Model description.....	25
Tillage implementation.....	26
Data and experimental design	28
Results & Discussion.....	29

Acknowledgements	37
Supplementary Information.....	38
CHAPTER 4. ADDING FULL RANGE OF CROP MANAGEMENT PRACTICES INCREASES LAND USE CHANGE EMISSIONS AND REDUCES SOIL CARBON IN THE COMMUNITY LAND MODEL.....	48
Abstract	48
Introduction	48
Materials & Methods.....	51
Model Description.....	51
Experimental Design	52
Framework for Partitioning and Analysis of LULCC Flux.....	54
Results	56
Analysis of Net LULCC Flux for Three Main Simulations	56
Attributing Changes in Net LULCC Flux to Individual Crop Management Practices.....	56
Partitioning of Net LULCC Flux into Component Fluxes	59
Analysis and Attribution of Changes in Soil Carbon Stocks.....	62
Discussion	68
Analysis of Net LULCC Flux for Three Main Simulations	68
Attributing Changes in Net LULCC Flux to Individual Crop Management Practices.....	69
Partitioning of Net LULCC Flux into Component Fluxes	71
Analysis and Attribution of Changes in Soil Carbon Stocks.....	71
Conclusions	73
Acknowledgments	74
Supplementary Information.....	75
CHAPTER 5. CONCLUSIONS AND RECOMMENDATIONS.....	86
Remote sensing of tillage and crop residue management practices	86
Soil carbon sequestration and climate change mitigation potential of ‘no-till’ adoption based on Earth system modeling	86
Effects of including full range of crop management practices on LULCC emissions and SOC in the an Earth system model.....	88
REFERENCES.....	90

LIST OF FIGURES

Figure 1-1 Location of the South Fork watershed of the Iowa River in central Iowa within U.S. Corn Belt region	7
Figure 1-2 Area planted (%) in corn and soybean in central Iowa over the mid-April to late June in 2016 (a) and 2017 (b). Precipitation (cm) over time is included on the secondary axis. Dates for imagery and field surveys in 2016 (a) and 2017 (b). Area planted based on USDA NASS Crop Progress Reports for 2016 and 2017.....	8
Figure 1-3 Sentinel-2A false color composite imagery of SWIR 2 (Band 12), SWIR 1 (Band 11), and narrow NIR (Band 8A) bands at 30m resolution. Imagery was collected for two separate, overlapping HLS tiles – 15TVG and 15TVH – overlaying the South Fork watershed for two dates in 2016.....	9
Figure 1-4 Example time-series values for individual field data points for Landsat 8/OLI (a,b), Sentinel-2A/MSI (c,d), and combined datasets (e,f) for three remote sensing indices.	14
Figure 1-5 Time-series NDTI values of individual field sampling location with low CRC (<30%) and high CRC (>70%). NDTI time-series values for Landsat 8/OLI (a,b), Sentinel-2A/MSI (c,d), and combined Landsat 8/OLI & Sentinel-2A/MSI (e,f), are displayed from top to bottom for 2016 (a,c,e) and 2017 (b,d,f). Filled markers indicate the date and image on which the minimum NDTI value occurred for each field location.....	16
Figure 1-6 Measured versus predicted plots of crop residue cover (CRC) for 2016 (a,c,e) and 2017 (b,d,f). Showing plots for Landsat 8/OLI (a,b), Sentinel-2A/MSI (c,d), and combined datasets (e,f).	19
Figure 2-1 Time-series of global changes in soil organic carbon stocks in Gt C subtracted from the control scenario from 1850 to 2100	31
Figure 2-2 Maps showing the distribution of losses in soil organic carbon (Mg C ha ⁻¹) per hectare of cropland subtracted from the control scenario for each individual grid cell in the ‘moderate (A) and ‘high’ (B) intensive tillage (IT) scenarios over the 1850 - 2014 time period.	32
Figure 2-3 Maps showing the distribution of increases in soil organic carbon (SOC) for ‘no-till’ (NT) relative to intensive tillage (IT) scenarios over the 2015-2100 time period.	34
Figure 2-4 Maps showing the geographic distribution of reductions in soil organic carbon (SOC) after accounting for areas where ‘no-till’ (NT) is already practiced as of 2012 ...	36
Supplementary Figure S-1. Time-series plot showing changes in irrigated, rain-fed, and total area in crops in millions of hectares (million ha) globally in the Community Land	

Model for the 1850 – 2015 historical time period. Land use change is based on Land Use Harmonized, version 2 (LUH2) data (<http://luh.umd.edu/data.shtml>)..... 39

Supplementary Figure S-2. Map showing the total area in crops as a proportion of each individual grid cell in the Community Land Model. Proportional crop area is averaged for the 1990 to 2010 time period. Land use distribution is based on Land Use Harmonized, version 2 (LUH2) data (<http://luh.umd.edu/data.shtml>) 40

Supplementary Figure S-3. Map showing the initial distribution of average soil organic carbon stocks in 1850 (i.e. prior to implementation of intensive tillage practices) for each individual grid cell in the Community Land Model. Soil carbon stocks based on Harmonized World Soil Database v1.2. 41

Supplementary Figure S-4. Maps showing the distribution of losses in soil organic carbon as a percentage of initial carbon stocks for each individual grid cell in the ‘low’ (A) and ‘high’ (B) intensive tillage scenario over the 1850 -2014 time period..... 42

Supplementary Figure S-5. Maps showing the distribution of the annual rate of increase in soil organic carbon (SOC) for ‘no-till’ (NT) relative to intensive tillage (IT) scenarios over the 2015-2100 time period..... 43

Supplementary Figure S-6. Bar plots showing the proportion of absolute change in SOC accounted for by each quintile of cropped area in the Community Land Model for ‘no-till’ simulations over the 2015-2100 time period..... 44

Supplementary Figure S-7. Time-series of changes in soil organic carbon stocks subtracted from the control scenario for two grid cells with high proportional crop area over the entire 1850 -2100 time frame..... 44

Supplementary Figure S-8. Global map showing the mask for ‘no-till’ practices as a proportion of total cropped area for each grid cell in CLM5 as of 2012. 46

Supplementary Figure S-9. Plot showing the cumulative soil carbon gains over the 2015- 2100 time period for the low (blue lines) and high (red lines) scenarios. Dotted lines show reductions in SOC due to the tillage mask for each scenario. 47

Figure 4-1. Plot (A) showing cumulative change in Net LULCC Flux between the three main simulations over the historical time period (1850 – 2014) 57

Figure 4-2. Plot (A) showing cumulative change in Net LULCC Flux for the five subtractive simulations of individual crop management practices relative to the full AM simulation over the historical time period (1850 – 2014)..... 58

Figure 4-3. Time-series plots of cumulative change in Net LULCC Flux and components fluxes (Direct, Indirect, GrowthProdC) over the historical time period (1850 – 2015) for

the three main simulations: generic crops (GC) (a), CLM 5.0 default (CLM5) (b), and all management practices (AM) (c) 60

Figure 4-4. Bar plots showing the cumulative difference over the historical time period (1850 – 2015) for components of the Indirect Flux (Δ NPP, Δ HR, Δ Fire, Δ CropProdC) between LULCC on (LU) and LUC off (NOLU) runs of the three main simulations: generic crops (GC) (a), CLM 5.0 default (CLM5) (b), and all management practices (AM) (c)..... 61

Figure 4-5. Bar plot (A) showing cumulative change in soil organic carbon (SOC) between LULCC on (LU) and LUC off (NOLU) runs of the three main simulations over the historical time period (1850 – 2014)..... 64

Figure 4-6. Geographical distribution of the cumulative difference in soil organic carbon (SOC) per hectare of cropland (Mg C/ha) over the historical time period (1850 – 2015) for all management minus generic crops (AM – GC) (a) and all management minus CLM 5.0 default (AM – CLM5) (b) simulations..... 65

Figure 4-7. Bar plot (A) showing cumulative change in soil organic carbon (SOC) between LULCC on (LU) and LUC off (NOLU) runs of the AM simulation and five subtractive simulations over the historical time period (1850 – 2014)..... 66

Figure 4-8. Geographical distribution of the cumulative difference in soil organic carbon (SOC) per hectare of cropland (Mg C/ha) over the historical time period (1850 – 2015) for all management (AM) simulations minus AM – Residue (a), AM – Grain Harvest (b), AM – Tillage (c), AM – Irrigation (d), and AM – Fertilizer (e). Note the different scale for AM – Irrigation and AM – Fertilizer plots..... 67

Supplementary Figure S-10. Spatial distribution of annual mean Net LULCC Flux ($g\ C/m^2/yr$) averaged over the historical time period (1850 – 2014) for the three main simulations: generic crops (GC) (a); CLM 5.0 default (CLM5) (b); all management practices (AM) (c)..... 75

Supplementary Figure S-11. Spatial distribution of annual mean Direct LULCC Flux ($g\ C/m^2/yr$) averaged over the historical time period (1850 – 2014). The distribution and magnitude of the Direct Flux is identical across all simulations in this study..... 76

Supplementary Figure S-12. Geographical distribution of annual mean Indirect LULCC Flux ($g\ C/m^2/yr$) averaged over the historical time period (1850 – 2014) for the three main simulations: generic crops (GC) (a); CLM 5.0 default (CLM5) (b); all management practices (AM) (c)..... 77

Supplementary Figure S-13. Bar plots showing the cumulative difference over the historical time period (1850 – 2015) for components of the Indirect Flux (Δ NPP, Δ HR, Δ Fire, Δ CropProdC) between LULCC on (LU) and LUC off (NOLU) runs of two

simulations: all management practices (AM) (a) and all management without tillage (AM – Tillage) (b).	78
Supplementary Figure S-14. Geographical distribution of the cumulative difference in soil organic carbon (SOC) per hectare of cropland (Mg C/ha) over the historical time period (1850 – 2015) for CLM 5.0 default minus generic crops (CLM5 – GC) simulations.	79
Supplementary Figure S-15. Plot showing the annual change in Net LULCC Flux, Direct Flux, and Indirect Flux for the all management (AM) simulation over the historical time period (1850 – 2015).....	80
Supplementary Figure S-16. Geographical distribution of annual mean flux due to wildfire ($\Delta\text{Fire}_{\text{LU-NOLU}}$) ($\text{g C/m}^2/\text{yr}$) averaged over the 2010 – 2015 time interval for the all management simulation.	81
Supplementary Figure S-17. Plot showing the annual change in $\Delta\text{HR}_{\text{LU-NOLU}}$, $\Delta\text{Fire}_{\text{LU-NOLU}}$, $\Delta\text{NPP}_{\text{LU-NOLU}}$, and $\Delta\text{CropProd}_{\text{CLU-NOLU}}$ for the all management (AM) simulation over the historical time period (1850 – 2015).....	82
Figure S-18. Geographical distribution of the average difference in grain yields (tonnes/ha) for major cereal crops between the full management (AM) and CLM 5.0 default (CLM5) simulations for the 2000 – 2015 time interval.....	83
Supplementary Figure S-19. Plot showing the annual change in absolute cumulative global SOC stocks for LULCC on (LU) simulations only over the historical time period (1850 – 2015) for the three main simulations.	84
Supplementary Figure S-20. Map showing the initial distribution of average soil organic carbon stocks (Mg C/ha) in 1850 (i.e. prior to implementation of intensive tillage practices) for each individual grid cell in the Community Land Model. Soil carbon stocks based on Harmonized World Soil Database v1.2.	85

LIST OF TABLES

Table 1-1 Comparison of sensor characteristics for Landsat 8 Operational Land Imager (OLI) and Sentinel-2A and Sentinel-2B MultiSpectral Instrument (MSI)	6
Table 1-2 Table of various remote sensing indices used in this study	12
Table 1-3 Analysis of 2016 and 2017 data for simple linear regression models (SLR) of minNDTI and crop residue cover (CRC), overall classification accuracy of SLR models, and repeated K-fold cross validation procedure	18
Supplementary Table S-1. Decomposition rate multipliers for various soil carbon pools based on DayCent tillage implements for ‘high’ and ‘low’ intensive tillage treatments..	38
Supplementary Table S-2. List of simulations run for various tillage scenarios, plus associated treatments and time intervals.....	38
Table 4-1. List of all simulations in this study with number, name, and description. Simulations are divided into three ‘main’ and five ‘individual crop management’ simulations.	53

CHAPTER 1. INTRODUCTION

Anthropogenic climate change represents a critical threat to the sustainability of agriculture and human societies over next century. Broad-scale conversion of natural ecosystems to agriculture has been an important driver of historical anthropogenic CO₂ emissions, and emissions from land use and land cover change (LULCC) account for approximately one-third of all historical anthropogenic CO₂ emissions (Ciais et al., 2013; Houghton and Nassikas, 2017). Human impacts on ecosystems and climate have increased substantially over the last several centuries, and three-quarters of Earth's ice-free land area is now in some form of human management aimed at meeting growing demands for food, fuel, and fiber (Luyssaert et al., 2014). Of this land area, 12% is managed as croplands and additional 35% as grasslands and pasture (Monfreda et al., 2008).

Agricultural management activities, and crop management specifically, play a key role in global C cycling and can potentially exacerbate climate change by releasing CO₂ and other greenhouse gases to the atmosphere. Alternatively, cropland ecosystems have the capacity to store C in vegetation and soils, and improvements in crop management practices, as such as conservation tillage or 'no-till', have been widely promoted as tools for climate change mitigation and land radiative management (Bai et al., 2019; Seneviratne et al., 2018). Monitoring of crop management practices is therefore critical for informing policy decisions on land management, but there is limited data available on how different crop management practices vary between locations at the global scale. Additionally, fundamental process understanding regarding the climatic effects of many crop management practices is lacking, making it difficult to assess the aggregate impacts of these practices at the global scale and potentially creating uncertainty in the global carbon budget (Erb et al., 2017; Le Quéré et al., 2018).

Inclusion of crop management practices in Earth system models (ESMs) used for assessing global climate is a key requirement for evaluating the aggregate effects of different crop management practices on C cycling and their impacts on climate. But, the addition of crop management practices to ESMs has been hindered by the foregoing issues with data availability and process understanding, and several critical crop management practices are present in less than half of current generation ESMs submitted to Coupled Model Intercomparison Project 6 (CMIP6) in advance of the forthcoming round of Inter-governmental Panel on Climate Change (IPCC) reports (Pongratz et al., 2018). Some research has shown that exclusion of crop management practices in ESMs may lead to underestimation of emissions from LULCC and contribute to uncertainty in the global carbon budget, potentially leading to inappropriate actions and policies with respect to management practices on croplands based on CMIP6 ESM simulations (Pugh et al., 2015; Arneeth et al., 2017)

Crop management activities and other components of the biosphere have historically been included in ESMs mainly to advance scientific understanding of the physical basis of climate change, with a focus on increasing model agreement with historical

observations and improving model predictions of future climate change. As the pace of Earth system model development accelerates and more agricultural processes are included in ESMs, the traditional separation of climate change science into three broad categories – namely, establishing the physical basis of climate change, assessing of vulnerability, impacts, and adaptation (VIA), and evaluating mitigation activities – has become blurred (Bonan and Doney, 2018). Biosphere processes that have been previously included in ESMs to establish the physical basis for climate change, particularly land management activities, often overlap with activities proposed for mitigation (Smith et al., 2014). Bonan and Doney (2018) suggest that a broad Earth system framework, which emphasizes the paramount role of ESMs, may be useful in integrating historical effects of management activities on climate processes with assessments of the potential for these activities to mitigate climate change.

Studies in this dissertation employ an overarching Earth system framework to address the foregoing issues, with particular focus on soil tillage and crop residue management practices. Soil tillage is a ubiquitous management activity on croplands globally and is thought to impact climate by accelerating decomposition of soil organic carbon (SOC) on cropped soils. Conservation tillage practices, such as ‘no-till’ (NT), which minimize soil disturbance and leave more crop residue on the soil surface, have been shown to increase SOC sequestration in many circumstances and have been promoted as a potential climate change mitigation measure (Minasny et al., 2017). However, global scale data on variations in tillage practices are largely unavailable, and there is considerable uncertainty regarding the magnitude of increases in SOC due to adoption NT practices (Powlson et al., 2014; Prestele et al., 2018). Few global studies have assessed the climate change mitigation potential of NT practices at the global scale, and soil tillage has not been included as a standard management activity in any major ESM (Levis et al., 2014). Further, there has been minimal research examining how tillage and other crop management practices, such as crop residue and grain harvest, affect emissions from LULCC, and no studies have evaluated the effects of including the full range of crop management practices on C cycling in ESMs. This dissertation attempts to address these issues through the following objectives:

- (1) Evaluate the efficacy of remote sensing methods for monitoring differences in soil tillage and crop residue management practices in central Iowa.
- (2) Incorporate soil tillage practices into an Earth system model and assess the potential for soil C sequestration and climate change mitigation through adoption of NT practices.
- (3) Determine the historical impact of including the full range of crop management practices (residue harvest, grain harvest, soil tillage, irrigation, and fertilization) on changes in C cycling associated with land use and land cover change (LULCC) to crops in an ESM.

CHAPTER 2. REMOTE SENSING OF TILLAGE INTENSITY IN IOWA USING MINNDTI METHOD AND HARMONIZED LANDSAT 8 SENTINEL-2 DATA

Graham, M.W., C.S.T, Daughtry, J.B. Campbell, B. Zheng, M.E. O'Rourke, R.Q. Thomas

Abstract

Conservation tillage practices retain more crop residue cover (CRC) on the soil surface and improve many cropland ecosystem services compared to intensive tillage. Information on tillage practices at broad scales – a requirement for assessing environmental impacts – is largely unavailable. Remote sensing approaches, such as the minimum Normalized Difference Tillage Index (minNDTI) method, have been developed for this purpose, but have been hindered by a lack of timely cloud-free imagery. This research aims to assess: (1) the relationship between NDTI and CRC using Harmonized Landsat 8 Sentinel-2 project (HLS) data for Landsat 8 and Sentinel-2A individually; and (2) the relationship between NDTI and CRC using combined HLS data for Landsat 8 and Sentinel-2A . We measured field-level CRC for >40 fields in a watershed in central Iowa in the United States for 2016 and 2017, then developed simple linear regression models of time-series data for NDTI, as well as applying a repeated k-fold cross validation procedure. In 2016, overall model accuracy for Landsat 8 alone was 50% ($R^2=0.74$), while Sentinel-2A alone had an overall accuracy of 43% ($R^2=0.66$). Combining Landsat 8 and Sentinel-2 data in 2016 did not improve overall accuracy (50%) ($R^2=0.72$). Overall accuracy in 2017 improved for Landsat 8 and combined data to 73% ($R^2=0.79$), and for Sentinel-2A to 59% ($R^2=0.79$). Repeated K-fold cross validation found an increased overall model accuracy, particularly for LS8/OLI (81% in 2016; 83% in 2017) and combined datasets (75% in 2016; 81% in 2017), potentially indicating that underlying data quality may be high. Poor performance was likely due to the small number of “clean” field points for model calibration and validation and to issues with image quality. Models for LS8/OLI and combined datasets performed better than S2A/MSI in both years due to a larger number of cloud-free images during the time period when tillage operations were performed. We found that it is still challenging to obtain a good number of observations in a time series using combined LS8/OLI and S2A/MSI data for mapping tillage practices over broad areas. Future research should investigate incorporating Landsat 7 and Sentinel-2B/MSI into the existing harmonized Landsat 8 and Sentinel-2A data to detect CRC and map tillage practices over broader areas.

Introduction

Conservation tillage is an alternative method of soil tillage that reduces soil disturbance and retains more crop residue on the soil surface compared to conventional, intensive tillage practices (USDA-NRCS, 2006a). Conservation tillage practices, such as ‘no-till’, generally reduce soil erosion and some studies have shown potential for climate change mitigation via increasing soil C sequestration compared to intensive, conventional tillage practices (Lal, 1998; Stockmann et al., 2013). As a result, conservation tillage practices have been widely promoted on croplands globally to reduce soil erosion and improve other ecosystem services (Powlson et al., 2010; Palm et al., 2014).

Although conservation tillage has been adopted in many regions, there is a paucity of geographical data on the extent of conservation tillage practices (Erb et al., 2017). Accurate monitoring of tillage practices is essential for providing inputs to environmental and Earth system modeling tools, such as the Soil and Water Assessment Tool (SWAT) and the Community Earth Systems Model (CESM), which are used to assess the broad-scale environmental impacts of management practices and inform policy decisions (Gassman et al., 2007; Oleson et al., 2013).

Tillage intensity and residue management practices can be assessed at the field scale by estimating the percent of crop residue cover (CRC) in fields shortly after planting (USDA-NRCS, 2006a). The Conservation Technology Information Center (CTIC) has evaluated tillage intensity in the past for selected counties using roadside surveys, but such surveys are costly and subjective (Thoma et al., 2004). Satellite remote sensing methods have the potential to accurately detect differences in CRC and provide information on tillage practices on a field by field basis over broad geographic areas and in a timely manner.

A number of remote sensing indices have been developed to detect differences in CRC levels and tillage intensity, and these indices typically on spectral differences between soils and crop residues, particularly the cellulose absorption feature at 2100 nm found in crop residues (Nagler et al., 2000; Serbin et al., 2009). However, most previous remote sensing work has relied on a single image to detect these differences at the field scale. Detection of CRC and tillage intensity from a single image has proven difficult because multiple field conditions can exist in the same image for dates early in the growing season, when tillage operations are performed (Zheng et al., 2012). Moreover, since not all fields are planted and tilled simultaneously, fields that have yet to be tilled when an image is captured provide an inaccurate assessment with respect to the ultimate CRC and tillage intensity of a given field (Zheng et al., 2014).

Time-series images collected early in the growing season, when crops are planted, have shown success in detecting differences in tillage intensity and CRC using Landsat. In this regard, the minimum Normalized Difference Tillage Index (minNDTI) method has emerged as an approach for accurately detecting CRC and tillage intensity at broad-scales (Zheng et al., 2012; Zheng et al., 2013a; Zheng et al., 2013b). The Normalized Difference Tillage Index (NDTI) is computed using two short-wave infrared (SWIR) bands at approximately 1610 nm and 2200 nm, for which there are analogous bands on several

multi-spectral satellites, including Landsat (<https://landsat.gsfc.nasa.gov/landsat-8/>) and Sentinel-2 (<https://sentinel.esa.int/web/sentinel/missions/sentinel-2>) (van Deventer et al., 1997). The minNDTI approach uses multi-temporal imagery acquired around the time of planting to extract a minimum value for NDTI, which then serves as a proxy for CRC level and tillage intensity for a given pixel. Models developed from minNDTI time-series data can then be used to estimate CRC and tillage intensity over broader geographic areas (Zheng et al., 2013b). However, widespread use of the minNDTI method has been restricted due to several obstacles.

Firstly, obtaining a sufficient number of cloud-free images during the critical planting window, when tillage operations are performed, has frequently proven difficult (Zheng et al., 2014). The planting window in many locations is fairly narrow (one to two months), and high cloud cover and precipitation are often common during this time period. Detection of CRC is also affected by in-field weathering of crop residues over time, and presence of green vegetation due to crop growth following planting and tillage operations can obscure the spectral signature from CRC (Daughtry et al., 2005). High levels of soil moisture can also substantially reduce the reflectance of both soils and crop residues, undermining assessments of CRC in time-series imagery (Quemada and Daughtry, 2016). Relatively low revisit frequency and data quality issues for multispectral sensors, such as data gaps in Landsat 7 ETM+ imagery, compound these issues because only a limited number of high quality images can be acquired during this restricted planting window. Finally, the potential for regional-scale mapping of tillage practices using minNDTI has not been realized for logistical reasons: models developed using minNDTI for a given location and year have not been successful in estimating CRC at other locations, or even at the same location in different years, thus necessitating extensive in situ field data collection on CRC annually for a given location in order to validate minNDTI-based estimates of CRC (Zheng et al., 2013a).

The Harmonized Landsat 8 Sentinel-2 (HLS) project

The recent launch of moderate resolution Landsat 8 and Sentinel-2 sensors portends the possibility of improving capacity to obtain high-quality, multi-temporal imagery for assessing CRC and tillage intensity using the minNDTI method (Zheng et al., 2014). The Harmonized Landsat 8 Sentinel-2 (HLS) project is a NASA initiative aimed at creating harmonized, pre-processed surface reflectance data by combining data from Landsat 8 Operational Land Imager (LS8/OLI) and Sentinel-2A and Sentinel-2B MultiSpectral Instrument (S2/MSI). Characteristics of LS8/OLI and S2/MSI systems are similar, with analogous bands in the SWIR region and comparable spectral, spatial, and temporal resolution (Table 1-1). The temporal gap between which imagery is collected for combined LS8/OLI and S2/MSI sensors is low, but will vary between 0-10 days until imagery from Sentinel-2B becomes available (Mandanici and Bitelli, 2016). Combining LS8/OLI and S2/MSI data from the HLS project may increase opportunities to acquire the sequential cloud-free imagery required for monitoring tillage practices using the minNDTI method.

To our knowledge, no studies have evaluated the minNDTI method using Landsat 8 or Sentinel-2 data, either independently or in combination. Therefore, we propose the following research questions:

- (1) What is the relationship between minNDTI derived from separately collected HLS Landsat 8 OLI and Sentinel-2 MSI imagery and field-measured CRC?
- (2) What is the relationship between minNDTI derived from combined HLS Landsat 8 OLI and Sentinel-2 MSI imagery and field-measured CRC, and does combining imagery from both sensors improve this relationship?

Table 1-1 Comparison of sensor characteristics for Landsat 8 Operational Land Imager (OLI) and Sentinel-2A and Sentinel-2B MultiSpectral Instrument (MSI). Note that the revisit frequency for Sentinel-2A and Sentinel-2B together is five days.

Sensor	Launch	Swath width	Resolution	
			Spatial	Temporal
Landsat 8/OLI	2013	180 km	30 m	16 d
Sentinel-2A/MSI	2015	290 km	10 m/20 m/60 m	10 d
Sentinel-2B/MSI	2017			

Materials and Methods

Study area

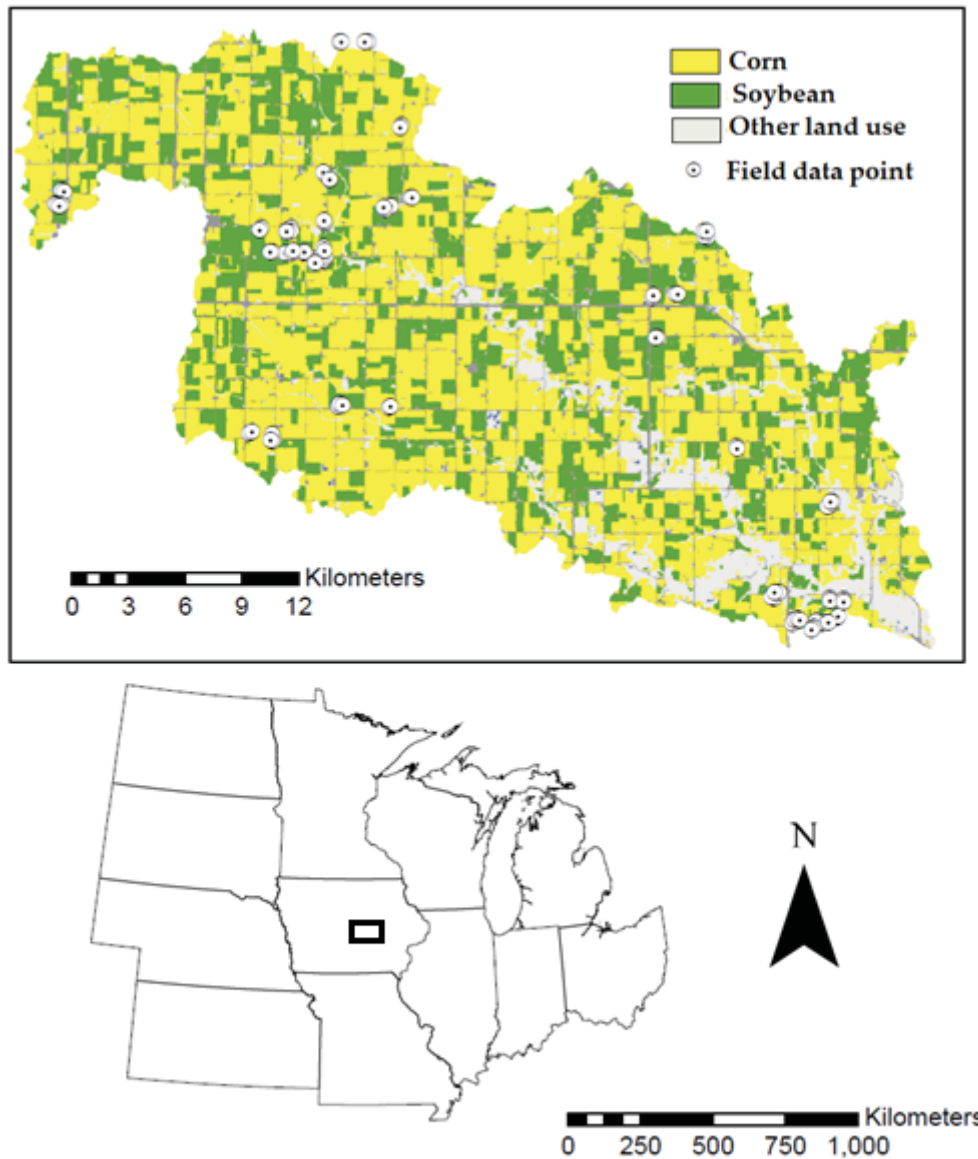
The South Fork watershed of the Iowa River is a long-term research watershed of the U.S. Dept. of Agriculture – Agricultural Research Service (USDA-ARS) located in Iowa in the U.S. Corn Belt region (42°25'N, 93°55'W) (Figure 1-1). The majority (>85%) of the watershed is under intensive row crop production of corn (*Zea mays* L.) and soybean (*Glycine max* (L.) Merr.). Tillage operations typically occur in both the fall and spring, while the planting window for corn and soybean is generally between mid-April and late May (USDA-NASS, 2016; USDA-NASS, 2017).

Soils in the watershed consist of moderately well-drained to poorly drained Mollisols (NRCS, 2006b). The watershed falls within the prairie pothole region and is characterized by regular occurrence of very poorly drained depressions (potholes or kettles) formed by uneven distribution of post-glacial meltwater (NRCS, 2006b). Due to poor drainage, the majority of soils in the watershed are artificially drained via subsurface tiles (Tomer and James, 2004).

Soil erosion and water quality associated with intensive row crop production are major concerns in the watershed, and conservation tillage and residue management are widely practiced. Historical data on cropping and tillage practices extend for more than 10 years,

with 43% of the cropped area in some form of conservation tillage as of 2011 (Tomer et al., 2008; Beeson et al., 2016).

Figure 1-1 Location of the South Fork watershed of the Iowa River in central Iowa within U.S. Corn Belt region. Inset shows watershed with three land use classes and location of field data points measured in 2017. Land use classes are derived from USDA National Agricultural Statistics Service (NASS) CropScape – Cropland Data Layer for 2017 (<https://nassgeodata.gmu.edu/CropScape/>).

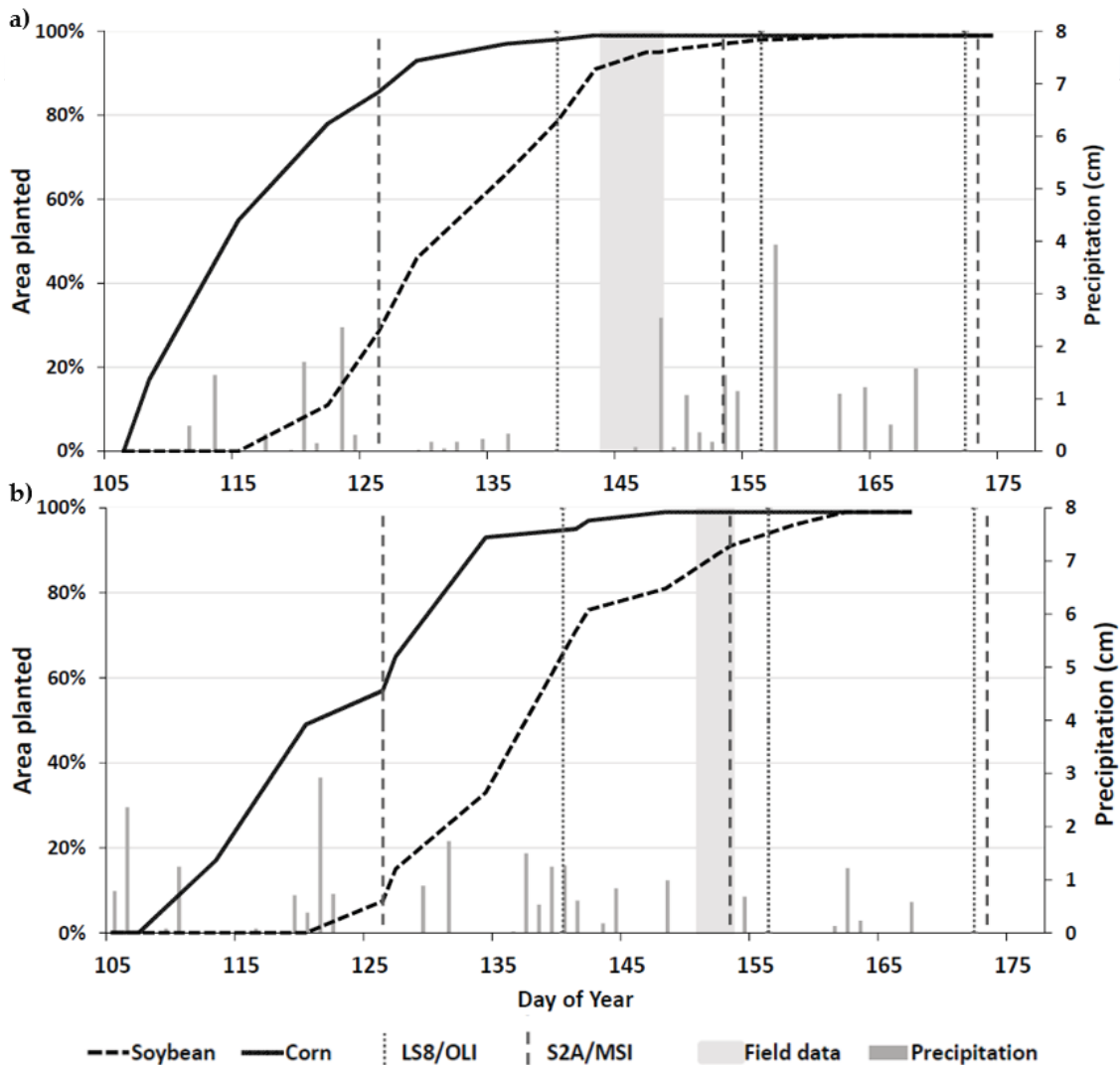


Field data collection

Crop residue cover was measured using the line-point transect method for multiple fields throughout the watershed in 2016 and 2017 (Morrison et al., 1993). In 2016, a total of 42

fields (99 points) were sampled, while in 2017 there were 49 fields (106 points). At least two random locations within each field were selected that were >100 m from the field boundary and >100 m apart. At each location, 2 to 4 line-point transects using 15.2 m long strings with 100 evenly spaced markers were stretched diagonally across the rows, and presence or absence of crop residue at each marker was noted to obtain CRC percentage. The center position of each transect pair was recorded with a GPS receiver with wide area augmentation. Current crop and the previous year's crop (corn or soybean) were recorded, along with crop growth stage at time of sampling. Dates for field surveys are shown in Figure 1-2 and were conducted following completion of most tillage and planting operations in the watershed (USDA-NASS, 2016; USDA-NASS, 2017).

Figure 1-2 Area planted (%) in corn and soybean in central Iowa over the mid-April to late June in 2016 (a) and 2017 (b). Precipitation (cm) over time is included on the secondary axis. Dates for imagery and field surveys are shown as dashed and shaded vertical lines, respectively, in 2016 (a) and 2017 (b). Area planted based on USDA NASS Crop Progress Reports for 2016 and 2017.



Remote sensing data acquisition

Multispectral remote sensing data was obtained from NASA Harmonized Landsat and Sentinel-2 (HLS) project (<https://hls.gsfc.nasa.gov/>) for LS8/OLI and S2A/MSI imagery. HLS provides harmonized Level-2A surface reflectance products for both LS8/OLI S2/MSI with considerable pre-processing, thus facilitating ease of comparison between systems. Pre-processing operations performed by HLS algorithms include atmospheric correction, geometric resampling, bidirectional reflectance distribution function (BRDF) normalization, band pass adjustment, and temporal compositing (Claverie et al., 2018). HLS algorithms resolve reported issues with co-registration between LS8/OLI and S2/MSI imagery in the pre-processing phase (Storey et al., 2016). Initial comparisons of HLS products indicate that there is good agreement amongst sensors at 30m spatial resolution and that cloud-masking algorithms for S2/MSI imagery represents the main issue with HLS data (Claverie et al., 2018). HLS products are gridded based on the S2A/MSI tiling system using UTM/WGS84 projection and tile size of 109.8×109.8 km.

Figure 1-3 Sentinel-2A false color composite imagery of SWIR 2 (Band 12), SWIR 1 (Band 11), and narrow NIR (Band 8A) bands at 30m resolution. Imagery was collected for two separate, overlapping HLS tiles – 15TVG and 15TVH – overlaying the South Fork watershed for two dates in 2016. Panel A shows imagery obtained on Day 153 (June 1) in 2016 and demonstrates S2A/MSI imagery unaffected by data gaps. Panel B demonstrates data gaps present in both tiles for S2A/MSI imagery for Day 126 (May 5) in 2016. Dots represent field data points. The expected areal coverage of the imagery is demarcated by the border and the large whitespace in the image demonstrates the data gap for imagery obtained on this date, as well as imagery acquired on Day 106 (April 15) in 2016.

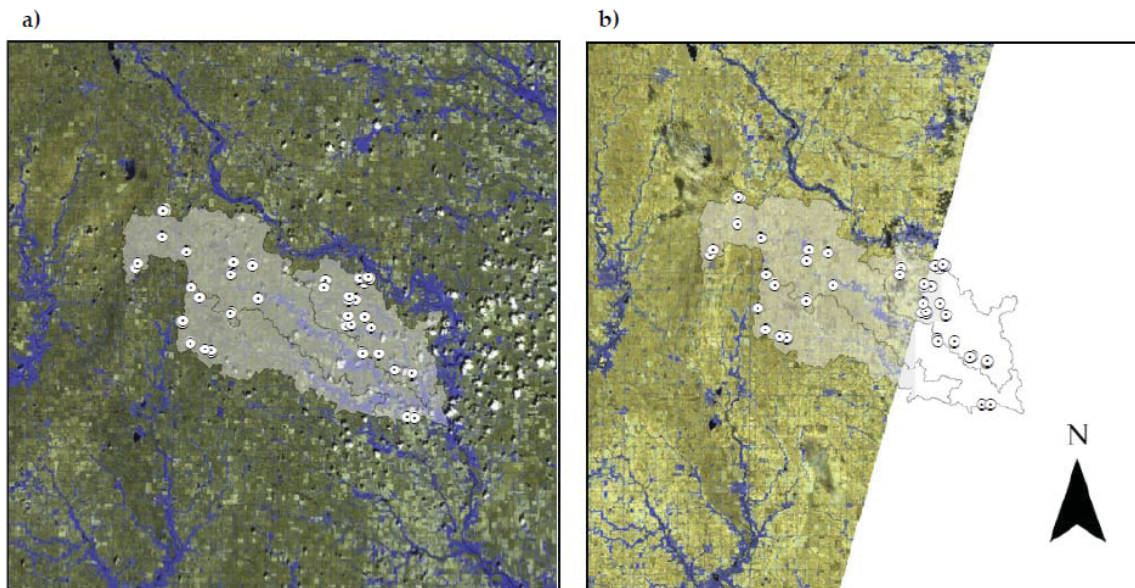


Image processing

Three separate indices were calculated for single pixels directly underlying each field data point in a given image to create time-series imagery. NDTI was computed separately for LS8/OLI and S2A/MSI per equations in Table 1-2. Based on equations in Table 1-2, the Normalized Difference Vegetation Index (NDVI) was calculated to detect the presence of green vegetation, and simple water index (WI) was computed based on SWIR bands to discern the potential effects of soil moisture on NDTI.

Layers for NDTI, NDVI, and WI for dates with imagery were split by sensor and year, then stacked to form a time-series dataset. Combined NDTI and other index datasets were created by merging LS8/OLI and S2A/MSI imagery into a single stack for each year. Index calculations and other operations were performed using R, ENVI (Harris Geospatial), and ArcMap 10.5 (ESRI) software packages. Individual sensor and combined sensor datasets were processed to remove clouds, cloud shadows, and data gaps by combining HLS Quality Assessment (QA) bands for each date within the stack into a single QA layer. This created a single QA layer shared by both sensors in each year, which was then applied to all time-series datasets.

To ensure valid comparisons between sensors, only “clean” field sampling points that were shared between LS8/OLI and S2A/MSI were used in subsequent analysis (i.e. field data points not affected by clouds, shadows, or data gaps on any image date for either sensor). Minimum values were extracted from each NDTI dataset to obtain minimum NDTI (minNDTI) values. The single pixel directly underlying each “clean” field point was used in extracting minNDTI values. If pixel NDVI values were >0.3 for an image date on which minNDTI occurred, the point was removed from the dataset to reduce confounding effects of green vegetation on NDTI (Zheng et al., 2013a). This resulted in a total of 28 “clean” field data points in 2016 and 45 “clean” points in 2017.

Simple linear regression (SLR) and repeated K-fold cross validation (RKCV) analyses

A manual data split method was used to develop simple linear regression (SLR) models of field-measured CRC versus minNDTI values for each year, sensor, and combination thereof. Points were sorted by field-measured CRC and every other point was selected to manually split points into separate datasets for calibration and validation. CRC values for points used in calibration data were used to develop SLR models. The SLR equations were applied to remaining (validation) points to estimate CRC using minNDTI values. To assess SLR model performance, accuracy assessments were conducted by dividing field-measured CRC into three categories based on CTIC conventions: $CRC < 30\%$ (non-conservation tillage), $30\% < CRC < 70\%$ (conservation tillage), and $CRC > 70\%$ (conservation tillage – no-till) (CTIC, 2019).

Due to small number of “clean” points in both years, a cross validation approach using a machine learning model was also applied to evaluate the accuracy of minNDTI as a predictor of CRC. A repeated K-fold cross validation (RKCV) procedure was followed using a Naïve Bayesian model, with $k=10$ and repeated three times. The RKCV procedure operates by dividing data into k groups, with data from one group used as test

data and the remaining groups as training data. A $k=10$ is commonly used and the procedure in general is considered less biased in estimating model accuracy than other methods (Kuhn and Johnson, 2013).

Table 1-2 Table of various remote sensing indices used in this study.

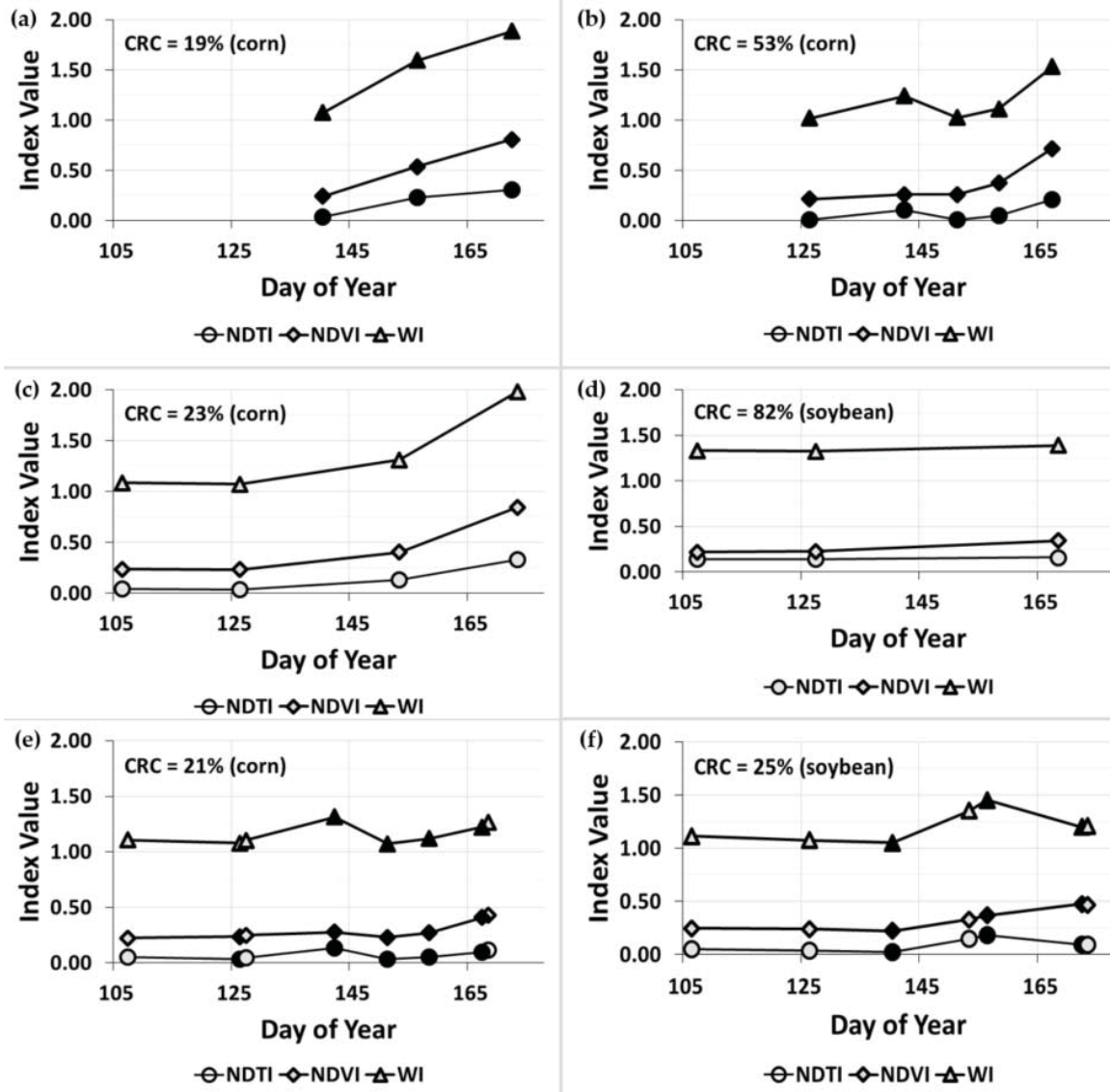
Sensor	Index	Bands	Wavelength, nm	Equation	Reference
Landsat 8/OLI	Normalized Difference Tillage Index (NDTI)	B6	1560-1660	$(B6 - B7) / (B6 + B7)$	Van Deventer et al., 1997
		B7	2100-2300		
Sentinel-2A/MSI		B11	1613.7	$(B11 - B12) / (B11 + B12)$	Van Deventer et al., 1997
		B12	2202.4		
Landsat 8/OLI	Normalized Difference Vegetation Index (NDVI)	B4	0.630-0.680	$(B5 - B4) / (B5 + B4)$	
		B5	0.845-0.885		
Sentinel-2A/MSI		B4	664.6	$(B8A - B4) / (B8A + B4)$	
		B8A	864.7		
Landsat 8/OLI	Water Index (WI)	B6	1560-1660	$(B6 / B7)$	Quemada and Daughtry, 2016
		B7	2100-2300		
Sentinel-2A/MSI		B11	1613.7	$(B11 / B12)$	Quemada and Daughtry, 2016
		B12	2202.4		

Results

Time-series NDTI, NDVI, and WI

Combined time-series profiles of NDTI, NDVI, and WI displayed variability within and between years (Figure 1-4). Planting of corn and soybeans (Figure 1-2) occurred one week earlier on average in 2016 relative to 2017, which may have affected the relative timing of increases in NDVI and NDTI between years. NDTI tended to be lower for the first few images collected from mid-April to mid-May, likely due to tillage operations. NDTI generally increased over time, presumably in association with increases in green vegetation, as evidenced by increases in NDVI. Changes in WI also indicate that increases in soil moisture due to precipitation events around the time of image acquisition inflated NDTI values for several image dates in both years

Figure 1-4 Example time-series values for individual field data points for Landsat 8/OLI (a,b), Sentinel-2A/MSI (c,d), and combined datasets (e,f) for three remote sensing indices – Normalized Difference Tillage Index (NDTI), Normalized Difference Vegetation Index (NDVI), and simple Water Index (WI). Individual field points and indices are shown for both 2016 (a,c,e) and 2017 (b,d,f). Markers indicate dates on which images were acquired. Dark-filled markers indicate Landsat 8/OLI imagery, while light-filled markers are for Sentinel-2A/MSI images.

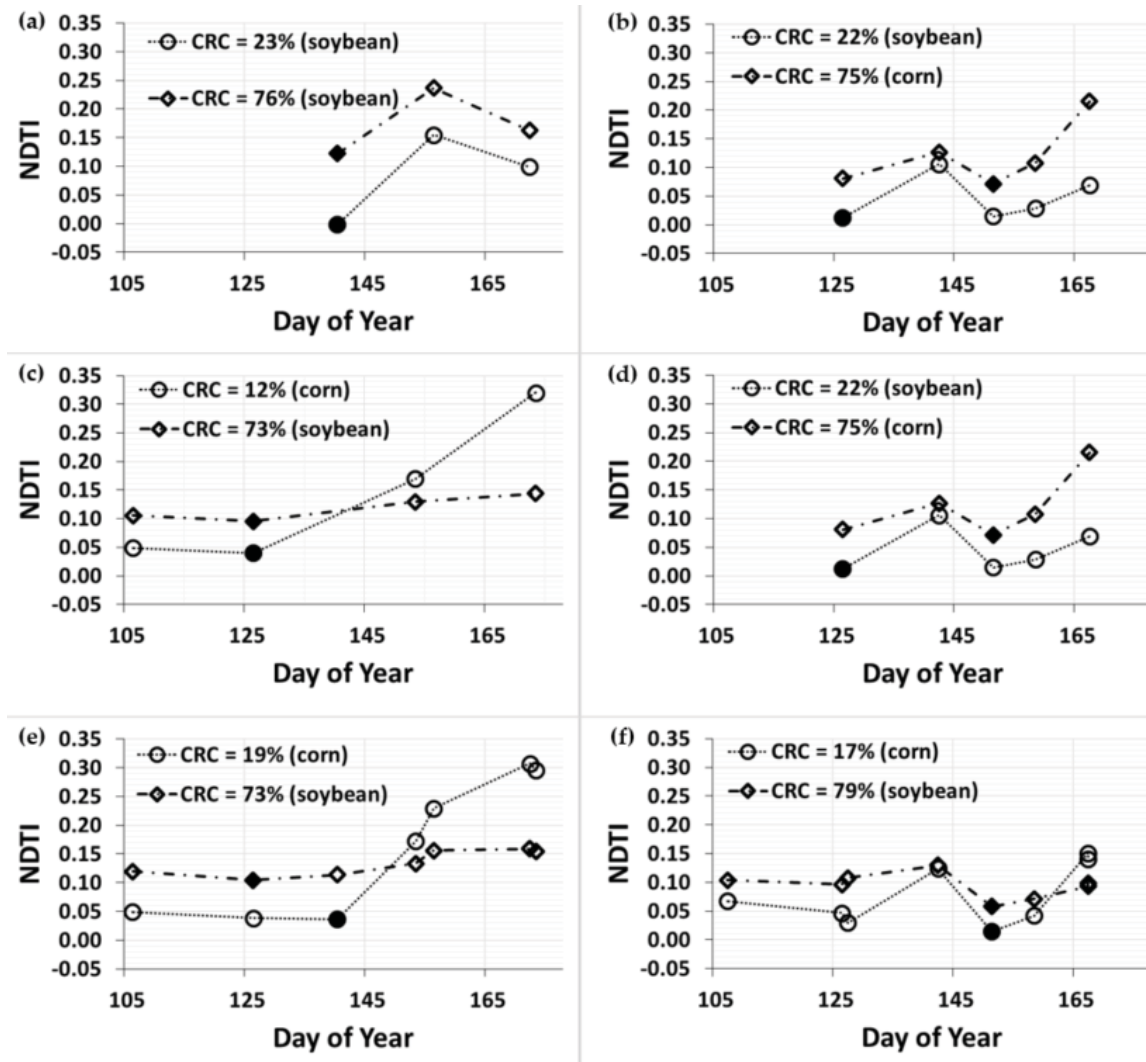


Time-series NDTI values for fields with high and low CRC for separate and combined sensors in both 2016 and 2017 are shown in Figure 1-5. Values for NDTI in 2016 increased following congruent changes in NDVI and WI, likely due to presence of green vegetation and soil moisture, respectively (Figure 1-5 a,c,e). Relatively few images were available for LS8/OLI early in the planting window in 2016 (Figure 1-5a), and almost all minimum NDTI values were associated with the first image available for LS8/OLI. S2A/MSI had better temporal coverage (Figure 1-5c), but NDTI values for images

acquired later in the planting window were likely inflated by increases in green vegetation and soil moisture. As a result, minimum NDTI values for S2A/MSI in 2016 occurred primarily on imagery for dates that were quite early (Day 105 – April 15; Day 125 – May 5) relative to the crop area planted at the time. Combined LS8/OLI and S2A/MSI data resulted in more a complete NDTI time-series than either sensor alone (Figure 1-5e), and minNDTI values tended to fall on dates between the first and last image acquired for combined data.

Values for NDTI (Figure 1-5 b,d,f) in 2017 followed a similar pattern to 2016. Dates for LS8/OLI image acquisition were spread more evenly throughout the planting window compared to 2016 (Figure 1-5b). The LS8/OLI time-series was more complete for 2017, although precipitation events prior to image acquisition on Day 142 (May 22) (Figure 1-2b) likely caused an increase in soil moisture and inflated NDTI values. Virtually no cloud-free imagery for S2A/MSI was available in 2017 for dates later in the planting window, despite the higher revisit frequency of S2A/MSI compared to the LS8/OLI sensor (Figure 1-5d). Combined LS8/OLI and S2A/MSI data resulted in more a complete NDTI time-series than either sensor (Figure 1-5f), but was dominated by the large number of available dates with imagery from LS8/OLI.

Figure 1-5 Time-series NDTI values of individual field sampling location with low CRC (<30%) and high CRC (>70%). NDTI time-series values for Landsat 8/OLI (a,b), Sentinel-2A/MSI (c,d), and combined Landsat 8/OLI & Sentinel-2A/MSI (e,f), are displayed from top to bottom for 2016 (a,c,e) and 2017 (b,d,f). Filled markers indicate the date and image on which the minimum NDTI value occurred for each field location.



Models and accuracy assessment

The relationship between minNDTI and crop residue cover (CRC) was weak in 2016, as indicated in Table 1-3 and in measured versus predicted CRC plots (Figure 1-6). Overall correlation between CRC and minNDTI using manual data split simple linear regression (SLR) models was lowest for S2A/MSI data, with coefficient of determination (R^2) of 0.63 (Table 1-3). CRC and minNDTI were more strongly correlated for LS8/OLI and combined models with $R^2=0.66$ and $R^2=0.72$, respectively. Overall classification accuracy for LS8/OLI was 50% in 2016 with a Kappa coefficient ($K\text{-hat}$) of 20%. S2A/MSI had lower overall accuracy (43%) and $K\text{-hat}$ (13%) in 2016, while overall accuracy (50%) and $K\text{-hat}$ (23%) were slightly higher for combined LS8/OLI and

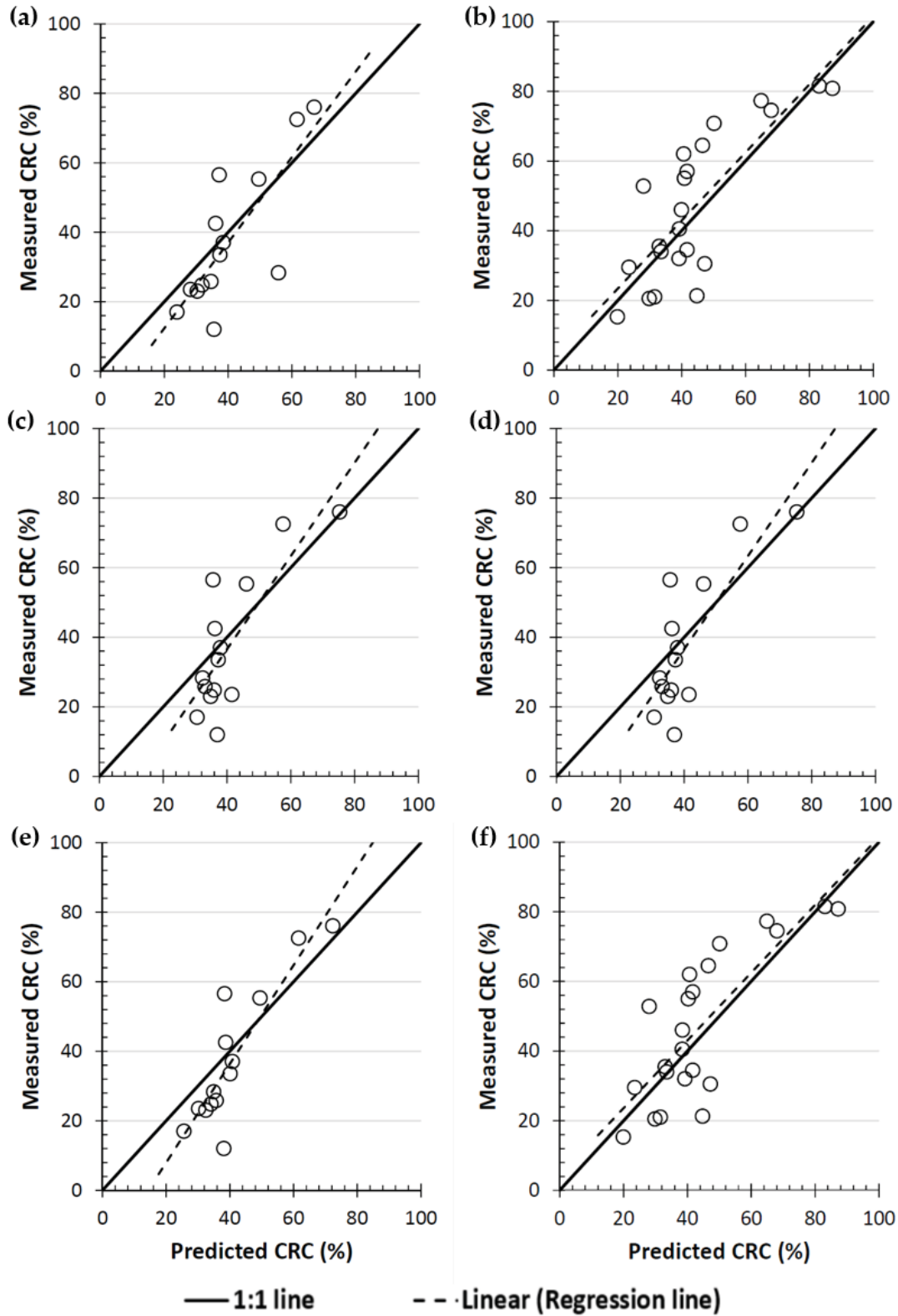
S2A/MSI datasets. Repeated K-fold cross validation (RKCV) substantially improved classification accuracy and demonstrated a greater capacity of underlying minNDTI data to accurately classify CRC for all three datasets, particularly for LS8/OLI and combined data.

There was a stronger relationship between CRC and minNDTI for all datasets in 2017 (Table 1-3, Figure 1-6). LS8/OLI and combined SLR models were virtually identical for 2017 because almost all minNDTI values in the combined dataset were derived from LS8/OLI imagery. Combined and LS8/OLI overall models had an overall $R^2=0.71$, while the correlation for the S2A/MSI overall model was somewhat lower ($R^2=0.65$). Plots of measured CRC versus predicted CRC in 2016 are displayed in Figure 1-6. Overall classification accuracy of the models also improved from 2016 to 2017. Overall accuracy for combined and LS8/OLI models was 73% with $K\text{-hat}=50\%$. Accuracy for the S2A/MSI model was lower at 59%, with a corresponding $K\text{-hat}=33\%$. The RKCV procedure improved classification accuracy for all three datasets, as the overall accuracy and Kappa coefficients for combined (81%, $K\text{-hat}=66\%$) and LS8/OLI (83%, $K\text{-hat}=68\%$) was similar between 2017 and 2016. The magnitude of improvement in accuracy metrics was slightly lower for S2A/MSI data (66%, $K\text{-hat}=42\%$).

Table 1-3 Analysis of 2016 and 2017 data for simple linear regression models (SLR) of minNDTI and crop residue cover (CRC), overall classification accuracy of SLR models, and repeated K-fold cross validation procedure. Classification and accuracy were determined using three categories of tillage intensity/CRC levels (Low <30% CRC; Medium 30-70% CRC; High >70% CRC).

Variable	2016			2017		
	Landsat 8	Sentinel-2	Landsat 8, Sentinel-2 combined	Landsat 8	Sentinel-2	Landsat 8, Sentinel-2 combined
Overall model R ²	0.66	0.63	0.72	0.71	0.65	0.71
<i>Manual data split calibration</i>						
R ²	0.74	0.66	0.73	0.79	0.79	0.79
RMSE	9.50	10.70	11.96	10.12	10.10	10.12
Samples	14	14	14	23	23	23
<i>Manual data split validation</i>						
R ²	0.62	0.64	0.78	0.63	0.53	0.63
RMSE	11.94	11.7	9.22	12.69	14.42	12.74
Overall Accuracy	0.50	0.43	0.50	0.73	0.59	0.73
Kappa	0.20	0.13	0.23	0.50	0.33	0.50
Samples	14	14	14	22	22	22
<i>Repeated k-fold cross validation</i>						
Overall Accuracy	0.81	0.58	0.75	0.83	0.66	0.81
Kappa	0.65	0.20	0.56	0.68	0.42	0.66
Samples	28	28	28	45	45	45

Figure 1-6 Measured versus predicted plots of crop residue cover (CRC) for 2016 (a,c,e) and 2017 (b,d,f). Showing plots for Landsat 8/OLI (a,b), Sentinel-2A/MSI (c,d), and combined datasets (e,f).



Discussion

Combined HLS data provided similar temporal coverage in the planting window compared to previous work using minNDTI method. Results of combined time-series data were on par with those obtained by Zheng et al. (2013a) using the minNDTI method and Landsat 5 TM and Landsat 7 ETM+ imagery, which reported four to seven cloud-free images per year for multiple locations in the U.S. Corn Belt region. However, frequency of image acquisition and quality were less consistent in the present study because the combined revisit frequency of LS8/OLI and S2A/MSI varies between 0 to 10 days. Results obtained using HLS data from individual sensors (i.e. LS8/OLI and S2A/MSI) tended to yield relatively few images and were less reliable in terms of providing a complete time-series of NDTI compared to the previous research for similar reasons (Zheng et al., 2012; Zheng et al., 2013a; Zheng et al., 2013b). The exception to this was for LS8/OLI data in 2017, for which there were five relatively cloud-free images spread evenly throughout the planting window. There was a paucity of imagery in the critical later portion of the planting window for S2A/MSI in both 2016 and 2017, likely leading to reduced performance of associated models.

Models showed weak relationships between field-measured CRC and minNDTI compared to the literature, particularly for 2016. Most studies examining the minNDTI method have obtained overall accuracy of at least 70% and Kappa coefficients demonstrating moderate agreement (i.e. $K\text{-hat} = 40\text{-}80\%$) (Zheng et al., 2012; Zheng et al., 2013a). Studies based on NDTI from single Landsat images acquired at the end of the planting window for two classes of CRC have found overall accuracies $>70\%$ and $K\text{-hat} >40\%$, which exceeded those reported here for 2016 (Beeson et al., 2016). Only the LS8/OLI and combined datasets in 2017 had classifications with agreement in this range (overall accuracy=73%, $K\text{-hat}=50\%$). The repeated K-fold cross validation procedure dramatically strengthened the relationship between CRC and minNDTI, and outputs were more in line with those from previous research. The exception to this was S2A/MSI data in 2016, which still had fairly low overall classification accuracy ($<60\%$) and Kappa coefficient ($<40\%$).

The relatively weak relationship between minNDTI and field-measured CRC found in this study is likely due to a combination of study design and lack of high quality, cloud-free time-series imagery. This study restricted analysis to only shared, “clean” data points to ensure valid comparison between sensors, which dramatically reduced the sample size in both 2016 ($n=28$) and 2017 ($n=45$) for developing SLR models using the traditional data split method. Small sample size likely contributed to weak relationships between measured CRC and predicted CRC values (Figure 1-6), particularly in 2016, where major data gaps in S2A/MSI imagery eliminated nearly half the field sampling points from consideration in the subsequent analysis (Figure 1-3). Eliminating this restriction would likely improve the relationship between minNDTI and CRC, as evidenced by the repeated K-fold cross validation procedure, which had model performance metrics comparable to those in the literature for classification of CRC using minNDTI for LS8/OLI and combined data. This indicates that underlying data quality may be high despite low number of available points for these sensors and years.

Weak relationships between minNDTI and CRC are also likely attributable to image availability and quality, particularly the timing of image acquisition relative to completion of tillage and planting operations. In both years, nearly all minimum NDTI values for S2A/MSI were associated with imagery acquired early in the growing season (before mid-May), at which point less than 60% of crops had been planted (Figure 1-2). In 2016, another S2A/MSI image was available at the end of the planting window, but the quality of this image was poor due to the confounding effects of soil moisture and green vegetation (Figure 1-3a) (Daughtry et al., 2005). Time-series imagery for S2A/MSI in both years therefore likely captured changes in NDTI and CRC for fields that were planted relatively early, while missing a large proportion of fields planted between mid- and late-May. S2A/MSI data also suffered from known issues with both data gaps and the HLS-generated cloud mask, for which there were major issues in at least one image in 2017 (Claverie et al., 2018). By contrast, LS8/OLI time-series images were spread more evenly throughout the planting window and, critically, had high quality images available shortly after completion of most tillage and planting operations in 2016 (Day 140 – May 19) and 2017 (Day 151 – May 31). The minimum NDTI values associated with these dates provided most of the inputs to models for LS8/OLI and combined datasets in both years, resulting in higher agreement between measured and predicted CRC (Figure 1-6).

Domination of the combined datasets by outputs from LS8/OLI is likely responsible for the lack of improvements in predicting CRC using combined imagery. In the combined datasets, relationships between minNDTI and CRC may have been weaker compared to previous research because the revisit frequency of combined LS8/OLI and S2A/MSI sensors varies between 0 – 10 days, rendering it more difficult to obtain high quality time-series imagery compared to other sensor combinations (e.g., LS5 and LS7; S2A and S2B). However, the preponderance of imagery from LS8/OLI in the combined data is likely due to chance, and combining data still ought to provide the ‘best bet’ for obtaining cloud-free imagery staggered throughout the planting window in the future despite issues with revisit frequency for combined sensors (Mandanici and Bitelli, 2016).

Conclusions & Recommendations

Relationships between crop residue cover and NDTI with Harmonized Landsat 8 Sentinel-2 data were relatively weak using the minNDTI method. The Sentinel-2A/MSI data was less reliable than Landsat 8/OLI and combined data, and combining LS8/OLI and S2A/MSI data did not increase the performance of the minNDTI method compared LS8/OLI alone due to large number of shared points. Despite fairly high temporal resolution using both LS8/OLI and S2A/MSI sensors, the capacity of the minNDTI and associated regression models to predict CRC was also poor compared to previous studies using the minNDTI methods, though results of the repeated K-fold cross validation procedure were more in line with those found in the literature. Poor performance of the minNDTI method in this study is likely attributable, in part, to study design and the resulting very small sample size for field points available in subsequent analysis. Performance was also negatively affected by lack of high quality, cloud-free imagery, particularly for S2A/MSI, and clouds remain a major issue when using the minNDTI method.

However, the study design employed here was restrictive, and results of repeated K-fold cross validation procedure indicate that the underlying quality of data may be reasonably high. Future studies could improve the relationship between CRC and minNDTI with HLS data by using less restrictive study designs which, consequently, may obtain more “clean” field data points for analysis. Combining LS8/OLI and S2A/MSI also resulted in a fairly thorough time-series NDTI throughout the planting window, so combining sensors may still represent the “best bet” for acquiring sequential cloud-free imagery.

Although these results could be improved upon in the future research, this study ought to serve as a cautionary tale for using the minNDTI method and combined Harmonized Landsat 8 Sentinel-2 imagery, as well as future efforts aimed at broad-scale mapping of tillage intensity and CRC more generally. Firstly, cloud cover will likely continue to be an issue for the minNDTI method and other time-sensitive remote sensing applications, particularly for agriculture – where planting and tillage operations often coincide with increased precipitation and cloud cover, even with combined time-series HLS data (Zheng et al., 2014). Similarly, the deleterious effects of soil moisture and green vegetation during this time period can reduce image quality to the point where NDTI is no longer a useful proxy for CRC and tillage intensity (Daughtry, 2001). The variable revisit frequency (0 – 10 days) of combined HLS data for LS8/OLI and S2/MSI is likely to cause irregularities and make obtaining sufficient time-series imagery more challenging (Li and Roy, 2017).

Additionally, HLS data, particularly for Sentinel-2, has technical and post-processing problems. Data gaps for Sentinel-2 imagery can result in large portions of scenes and sampling locations being unusable for analysis (Cai, 2019). HLS Sentinel-2 imagery has well-documented problems with the cloud mask algorithm, which results in both false positives and false negatives for cloud cover and renders analysis of Sentinel-2 imagery difficult (Claverie et al., 2018).

Finally, previous work has shown that equations relating minNDTI to CRC for one location and year do not perform well for different locations and at the same location for different years, limiting the applicability of the minNDTI approach for broad-scale mapping of tillage practices. Use of the minNDTI method with HLS data to assess tillage and CRC still needs to be validated through extensive field campaigns over multiple years and locations in order to verify its utility for mapping tillage practices over larger areas and time periods (Zheng et al., 2013b).

Therefore, while future work using the minNDTI method in tandem with HLS data could be promising, much work remains to be done in order to corroborate the efficacy of the minNDTI approach for monitoring tillage practices over broader areas and for time periods longer than a year. Future work with the minNDTI method should focus on validation of combined HLS data across multiple locations and years, with a particular emphasis on developing regional-scale models for detecting differences in CRC and tillage intensity (Zheng et al. 2013b). If successful, regional-scale mapping of tillage practices could eventually be used to replace inventory data on tillage practices as inputs to environmental and Earth systems models (Prestele et al., 2018).

Operationalization of the Sentinel-2B/MSI sensor ought to provide additional opportunities for cloud-free image acquisition in the future, but issues with data gaps for Sentinel-2A/MSI imagery are likely to persist. Timing of image acquisition appears to be critical and it is highly recommend that any future efforts using the minNDTI method obtain at least one cloud-free image immediately after completion of tillage and planting operations for best results. Future work with the minNDTI method could also benefit from recent work on developing remote sensing indices that adjust for soil water content to minimize effects of precipitation events and soil moisture on NDTI to ameliorate issues with image quality (Quemada et al., 2018).

CHAPTER 3. MODELING SHOWS MODEST CAPACITY OF ‘NO-TILL’ AGRICULTURE TO OFFSET EMISSIONS

Graham, M.W., R.Q. Thomas, D.L. Lombardozzi, M.E. O’Rourke

Abstract

Conservation tillage practices, such as ‘no-till’ (NT), have been widely promoted as a means of soil organic carbon (SOC) sequestration with the potential to mitigate climate change. However, the magnitude of increases in SOC using NT practices is uncertain and few global studies have attempted to estimate the potential of NT to offset emissions. Here we use a land surface model to simulate historical losses of SOC due to intensive tillage, followed by future scenarios (2015 – 2100) assessing the SOC sequestration potential of adopting NT globally. Cumulative SOC sequestration in future NT scenarios was equivalent to approximately one year of current fossil fuel emissions, and ranged between 6.6 – 14.4 Gt C (0.08 – 0.17 Gt C yr⁻¹). Potential SOC sequestration under NT was concentrated in temperate regions, and overlapped with some areas where NT is already practiced. Adjusting for lower SOC gains in areas currently in NT reduced cumulative SOC sequestration slightly, by 0.4 – 0.9 Gt C globally. Our results imply that the global potential for SOC sequestration from broad-scale adoption of NT is more limited than anticipated by some studies and policy-makers. Policies aimed at mitigating climate change through NT should target adoption in developed countries, where potential SOC storage appears to be highest.

Introduction

Agricultural practices that increase SOC storage have been widely researched as a means of offsetting emissions and mitigating climate change while also improving soil health and food security (Lipper et al., 2018). Mitigating climate change through SOC sequestration on agricultural land underpins major international initiatives, such as ‘4 per 1000’ program introduced at the United Nations Framework Convention on Climate Change Conference of the Parties (COP22) in 2015, and represents a key component of many countries’ National Determined Contributions to reducing emissions under the Paris Agreement (Minasny et al., 2017; Soussana et al., 2017).

Conservation tillage practices, such as ‘no-till’ (NT), have been shown to effectively increase SOC in many circumstances, but estimating the total global SOC sequestration potential of NT adoption has been hindered by uncertainty in the magnitude of gains under NT (Powlson et al., 2014). Methods for estimating changes in SOC at the global scale based on activity data typically rely on linear scaling methods, which are not capable of capturing non-linear changes in SOC over time (Ogle et al., 2019). Process-based models, such as DayCent, can simulate non-linear changes in SOC over time in a

spatially explicit manner, but their application has been limited by their geographical scope and inability to represent land use change (LUC) (Jain et al., 2005; Lugato et al., 2014; Lugato et al., 2018).

Global land surface models (LSMs), the land component of Earth system models, are process-based models that can comprehensively simulate non-linear biogeochemical and biogeophysical processes in a spatially explicit manner for Earth's entire land surface (Bonan and Doney, 2018). Recent advances in LSMs allow for changes in LUC and explicit simulation of agricultural management practices over time at global scales, as well as atmospheric forcing associated with changes in climate and concentrations of greenhouse gases (McDermid et al., 2017; Pongratz et al., 2018).

Methods

Here we address the effects of historical, intensive tillage practices on cumulative changes in SOC on croplands, then assess the potential for SOC sequestration and climate change mitigation via adoption of NT practices on all croplands globally by running the first global-scale scenarios of these practices in an uncoupled, land surface model. We use the Community Land Model, version 5 (CLM5), which is the land component of the Community Earth System Model (CESM), to run scenarios simulating both historical, intensive tillage (IT) and NT practices. CLM5 includes time-varying global distributions of explicit crop types and management practices, such as fertilization and irrigation (Levis et al., 2012). CLM5's soil biogeochemistry is based on DayCent and we build on previous work (Levis et al., 2014) using DayCent-based decomposition multipliers for SOC to run idealized scenarios simulating the impact of IT on SOC stocks on all cropland over the historical time period (1850 – 2014) prior to implementing NT practices. To account for variability in intensity of tillage practices historically, we ran two scenarios simulating IT as an increase in decomposition rates of SOC at two levels of intensity (high, moderate) (Supplementary Table 2-1). Historical scenarios with IT were run on all cropland globally beginning in 1850, with prescribed historical LUC and 20th century climate and CO₂ forcing. For NT scenarios we assumed that adoption of NT practices in the model begins in 2015. Following completion of the historical scenarios with IT, we simulated NT in an idealized manner by 'turning off' the enhanced decomposition of SOC associated with IT for 2015 – 2100, and continued to run scenarios for IT at two levels over the same interval for comparison (Supplementary Table 2-2). To account for the reduced potential for SOC sequestration in cropped areas where NT practices have already been adopted, we applied a post-hoc mask that reduced gains in SOC based on the present-day fractional area in NT using a globally gridded data product (Prestele et al., 2018). All future scenarios were run with land use fixed at 2015 distributions and driven by a Representative Concentration Pathway 8.5 (RCP 8.5) climate change scenario. A control scenario without tillage practices (i.e., default CLM5) was run for the entire 1850 – 2100 interval.

Model description

The Community Land Model (CLM) is the land surface component of the Community Earth System Model (CESM). In this study, we used CLM version 5.0 (CLM5) coupled to the Community Atmosphere Model (CAM) (version 5.0) in Community Earth System

Model version 2.0 (CESM 2.0) (Lawrence et al., 2019). CESM 2.0 is a state-of-the-art coupled climate model with capacity to simulate the entire Earth and climate system (<https://escomp.github.io/cesm/release-cesm2/index.html>), and is the primary Earth system model (ESM) contributed by the United States to Coupled Model Intercomparison Projects for the Inter-Governmental Panel on Climate Change. CESM 2.0 includes multiple component capable of comprehensively representing the Earth system and consists of sub-models for atmosphere (i.e., Community Atmosphere Model), land, ocean, land-ice, sea-ice, and river run-off. CESM 2.0 can be run fully coupled with interactive components to simulate feedbacks between model components, or uncoupled with a focus on a specific sub-model. Uncoupled or offline runs with specific sub-model(s) can be performed using slab components for unused sub-models and typically rely on prescribed forcing data (e.g., prescribed forcing data for climate and radiative gases in uncoupled/offline simulations).

CLM5 is capable of representing land surface biogeochemistry and biogeophysics for many land surface processes, with components for simulating land use change (LUC), dynamic vegetation and phenology, hydrology, human management activities, and ecosystem dynamics (Lawrence et al., 2019). CLM5 also allows for changes in LUC over time, with multiple land use time-series datasets available depending on the simulation of interest. CLM5 biogeochemistry is based on the DayCent/CENTURY model (Parton et al., 1996), with multiple distinct litter and soil pools for representation of soil organic carbon, as well as vertically resolved soil data columns to a depth of 47 m. As in DayCent, decomposition and accumulation within various SOC pools in CLM5 is calculated on a daily time-step, and is a function of temperature, moisture, depth, and aeration within the soil.

The CLM5 crop sub-model (CLM5-CROP) is derived from the AgroIBIS land surface model and is among the most well-developed crop sub-models within major ESMS (Pongratz et al., 2018). CLM5-CROP dynamically simulates crop growth and phenology as four phenological growth stages based on growing degree-days, corresponding to planting, leaf emergence, grain-fill, and grain harvest. The crop sub-model simulates several important management practices, including crop-specific plant functional types (CFTs) for individual crop species, grain harvest, crop product pools, fertilization, and irrigation. Within CLM5-CROP, CFTs have crop-specific growth and phenology based on individual crop-specific models for major crops. Each CFT is allocated a separate soil column for irrigated and rain-fed CFTs, both of which are separate from the natural vegetation column; this precludes crop management practices from spilling over and indirectly impacting natural vegetation. More comprehensive descriptions of the CLM-CROP model and associated processes can found in Levis et al. (2012) and in the CLM5.0 User's Guide (https://escomp.github.io/ctsm-docs/doc/build/html/users_guide/).

Tillage implementation

We simulated different tillage practices as a proportional change in decomposition rates to existing SOC litter and soil organic matter C pools within CLM5. Since CLM5 biogeochemistry and SOC pool structure is based on DayCent (Parton et al., 1996; Del Grosso et al., 2006), we simulated tillage by applying decomposition multipliers for

tillage that had been calibrated and validated in previous DayCent studies on the impacts of tillage on SOC pools in the top 20 cm of the soil profile (Hartman et al., 2011; Parton et al., 2015). More specifically, implementation of multipliers in CLM5 model code was based on previous work by Levis et al. (2014). To represent uncertainty in the model representation of the tillage, we applied two levels of DayCent-based decomposition multipliers for several SOC pools in CLM5, with different multipliers for individual SOC pools, as shown in Supplementary Table 1. Although tillage practices are variable in space and time, with more recent and industrialized cropping systems tending to maintain more intensive tillage practices (i.e. increased decomposition rates) compared to historical and subsistence tillage practices, we applied uniform multipliers at the two levels of intensity (moderate, high) over the entire historical time period (1850 – 2015). In order to capture uncertainty and variability in tillage practices spatially and over the historical time period, values for decomposition multipliers were obtained from a thorough perusal of the literature on DayCent decomposition multipliers for tillage to represent a range of tillage intensities across time and space.

Decomposition multiplier values for the ‘high’ intensity tillage scenarios were based on DayCent version 4.5 simulations conducted for the U.S. Great Plains region and are intended to represent high intensity tillage systems in more recent, industrialized cropping systems (Hartman et al., 2011). The decomposition multipliers for “moderate” intensity simulations are derived from default multipliers for DayCent version 4.0, and are intended to represent the comparatively lower tillage intensity in historical, subsistence, and non-mechanized cropping systems (Metherell et al., 1993; Metherell et al. 1996; Manies et al., 2000; Leite et al., 2004; Chang et al., 2013). In all cases, we represented soil disturbance from tillage in the CLM as three discrete, sequential events, with each event corresponding to individual tillage management practices that are common across many cropping systems. In both the ‘high’ and ‘moderate’ scenarios, these three events were intended to simulate ‘primary tillage’, ‘cultivation’, and ‘planting and weeding’. Here ‘primary tillage’ refers to major disturbance of the soil and incorporation of crop residue conducted prior to planting in order to prepare the soil; ‘cultivation’ corresponds to lower intensity soil disturbances following ‘primary tillage’ with the goal of removing weedy vegetation and creating a uniform seedbed; ‘planting and weeding’ consists of a final event wherein crops are planted and additional, low-intensity clearing of weedy vegetation is performed.

Each of the three main tillage events occurs in sequence annually for each crop (i.e., CFT) in CLM5. Following crop planting in the model, the increase in decomposition rates for cropped soils in CLM5 is implemented for period of 75 days, an interval which largely agrees with the literature on the time period over which enhanced decomposition from tillage is effective (Abdalla et al., 2013; Abdalla et al., 2016). Planting in CLM5 occurs based on growing degree-day (GDD) thresholds, and we chose to implement tillage practices after planting rather than using an earlier, lower GDD threshold because future changes to the CLM5-CROP model may alter planting dates to depend on both GDD and moisture. Therefore, while our simulation is less realistic than might be optimal, since tillage events generally occur before planting in most cropping systems, the implementation of intensive tillage in the CLM5 code is more robust to future

changes in model structure related planting date thresholds for CLM5-CROP. Additionally, since the “plow layer” is generally considered to be between 25 – 30 cm in most cropping systems, we limited enhanced decomposition due to tillage to the top 26 cm of each crop-specific soil column in the model.

We performed multiple sensitivity tests to verify model behavior and assess the effects of different methods for implementation of enhanced decomposition due to tillage in CLM5. For example, we examined the impact of uniform versus differential decomposition rates for different SOC pools, prescribed versus planting date-based tillage event timing, LUC on versus LUC off. Although tillage is implemented in a simple manner in this study, we found that results of sensitivity tests were as expected in terms of model behavior and relatively robust to changes in specific details of implementation.

Implementation of ‘no-till’ practices was performed in a similarly simple manner in CLM5 based on DayCent, which simply turns tillage multipliers ‘off’ by setting values equal to one. We also ran future scenarios of NT adoption with LUC turned off and constant crop area at 2015 levels. We therefore assumed that NT adoption would occur exclusively on existing cropland, and that any new cropland converted due to LUC after 2015 would be under intensive tillage. This assumption seems justified given the rarity with which NT practices are implemented on newly cleared croplands and the associated difficulty in implementing these practices on recently cleared crop areas (Schob, 1973; Lal et al., 2007; Fujisaki et al., 2016; Fujisaki et al., 2018). Further, issues with monitoring LUC to crops for NT implementation, as well as uncertainty with respect to where future LUC to crops might occur, would add further complexity to model assumptions (Prestele et al., 2016). We did not include the impacts of conversion to NT on SOC losses in historical simulations using the mask of present-day NT practices from Prestele et al. (2018), since almost all conversion to NT is comparatively recent and future NT adoption will occur on the much larger fraction of cropland currently under intensive tillage.

Changes in SOC due to differences in tillage practices between scenarios were calculated by subtracting simulated quantities of SOC in treatment scenarios from the corresponding quantity in the ‘control’ scenario. CO₂ equivalents for changes in SOC were calculated by multiplying the quantity of carbon by 3.67 as per (Smith et al., 2014).

Data and experimental design

Scenario simulations were performed using coupled Community Land Model 5.0 and Community Atmosphere Model 5.0 (CAM5; Neale et al., 2012) sub-components of CESM 2.0, as discussed in the “Model description” section. CLM and CAM simulations were conducted in offline mode, with slab (i.e., uncoupled) ocean and ice sub-models at 1.9° x 2.5° resolution. All simulations used CLM5 component sets with active carbon and nitrogen biogeochemistry and prognostic crops (CLM5.0-BGC-CROP).

Since the CLM was not fully coupled, all historical scenarios for the 1850 – 2015 interval were simulated using prescribed atmospheric forcing for radiative gases and climate was simulated using repeated 20th century climate data from the Global Soil Wetness Project

(GSWP; Dirmeyer et al., 1999). Forcings for CO₂ and other radiative gases for future simulations used Representative Concentration Pathway 8.5 (RCP 8.5), which represents the most extreme RCP scenario for both climate change and atmospheric concentrations CO₂ and other gases, providing an interesting scenario for testing the impacts of differences in tillage practices. Future climate forcings were based on monthly climate anomalies acquired from several years of historical climate data at the end of the 20th century (1996 – 2005) for temperature, precipitation, atmospheric pressure, short- and long-wave radiation, relative humidity, and wind speed (Lombardozzi et al., 2018). Monthly anomalies were obtained by subtracting present-day anomalies from those simulated in RCP8.5 for Coupled Model Intercomparison Project 5 (CMIP5) using the Community Climate System Model, version 4 (CCSM4), then adding this difference to historical climate data produced by the Global Soil Wetness Project (GSWP) for the 1996 – 2005 interval (Dirmeyer et al., 1999; Meehl et al., 2012).

Land use change in CLM5 for historical scenarios was prescribed based on Land Use Harmonized version 2 data (LUH2; <http://luh.umd.edu/data.shtml>), and was held constant at 2015 distributions for all future scenarios. CLM5 default settings maintain both crop fertilization and irrigation. Fertilization (N only) was applied by adding N directly to the soil mineral N pool and is prescribed in a spatially explicit fashion according to transient LUH2 data for fertilizer use globally (Lawrence et al., 2016). Irrigation was prescribed using spatially explicit, transient data for locations with requisite equipment for irrigation based on Portmann et al. (2010).

We ran three scenarios over the historical time period (1850 – 2015), with treatments consisting of: a control scenario without tillage practices (CLM5 default settings) and intensive tillage (IT) practices at two levels of intensity ('high' and 'moderate') (Supplementary Table 2), as described in the preceding section on implementation of tillage practices in CLM5. Scenarios with IT treatments were initiated following model spinup to 1850 land use distribution and equilibrium SOC conditions, with decomposition multipliers for tillage going into effect beginning in 1850. After running scenarios with IT for the historical time period, we ran two sets of future scenarios for each historical IT scenario for the 2015 – 2100 time period. Future simulations were branched from scenarios with continued IT at 'high' and 'moderate' intensities to two 'no-till' scenarios where tillage decomposition multipliers from historical IT scenarios were "turned off" (i.e., set equal to one). The CLM5 default 'control' scenario without tillage practices was run for the 2015 – 2100 for comparison.

Results & Discussion

Implementation of IT scenarios over the historical time period resulted in a cumulative 'carbon debt' between 6.8 and 16.8 Gt C (25.0 – 61.3 Gt CO_{2e}), and SOC losses strongly depended on the level of tillage intensity (Fig. 2-1). SOC stocks begin declining shortly after implementation of tillage practices in 1850 and drop continuously through the 20th century in association with increasing LUC to crops during this time period (Supplementary Fig. S-1; Supplementary Fig. S-2).

Cumulative losses of SOC per hectare were unevenly distributed geographically (Fig. 2-2a; Fig. 2-2b), and the highest SOC losses were concentrated in temperate regions. The geographic distribution and magnitude of SOC losses are within the range of those reported in a spatially explicit analysis of SOC losses due to historical agricultural practices (Sanderman et al., 2017), corroborating that broad patterns observed here are realistic. Areas with high per hectare losses accounted for a disproportionate share of the ‘carbon debt’ accrued on a percentile basis: the top quintile of cropped areas accounted for >76% of the total cumulative SOC losses due to IT globally, regardless of tillage scenario (Fig. 2-2c.). The geographical pattern of historical SOC losses appears to be driven primarily by initial SOC stocks and climate – locations with large losses were generally in mid-latitude regions with high initial SOC in CLM5 (Supplementary Fig. S-3.), indicating that areas with high initial SOC may have more SOC to lose. However, the distribution of losses as a percentage of initial SOC stocks was inconsistent with the pattern of absolute losses per hectare (Supplementary Fig. S-4.).

Figure 2-1 Time-series of global changes in soil organic carbon stocks in Gt C subtracted from the control scenario for 1850 to 2100. Dark red lines denote intensive tillage (IT) scenarios with ‘high’ decomposition rates for the historical (1850-2014) and future (2015-2100) time periods. Dark blue lines denote IT scenarios with ‘moderate’ decomposition rates for the historical (1850-2014) and future (2015-2100) time periods. Light red lines denote changes in soil carbon stocks for ‘no-till’ (NT) scenarios following the ‘high’ historical IT scenarios. Light blue lines denote changes in soil carbon stocks for NT scenarios following the ‘moderate’ historical IT scenarios.

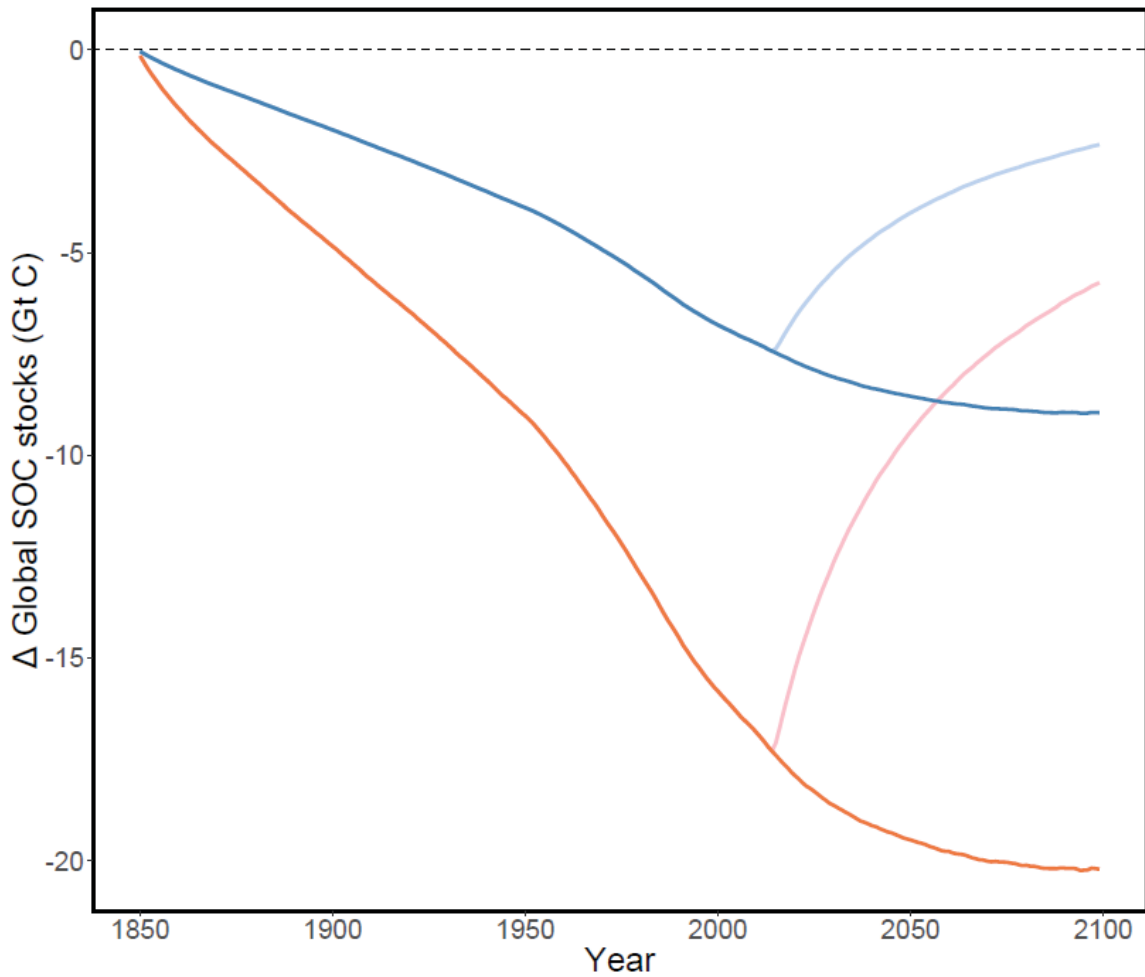
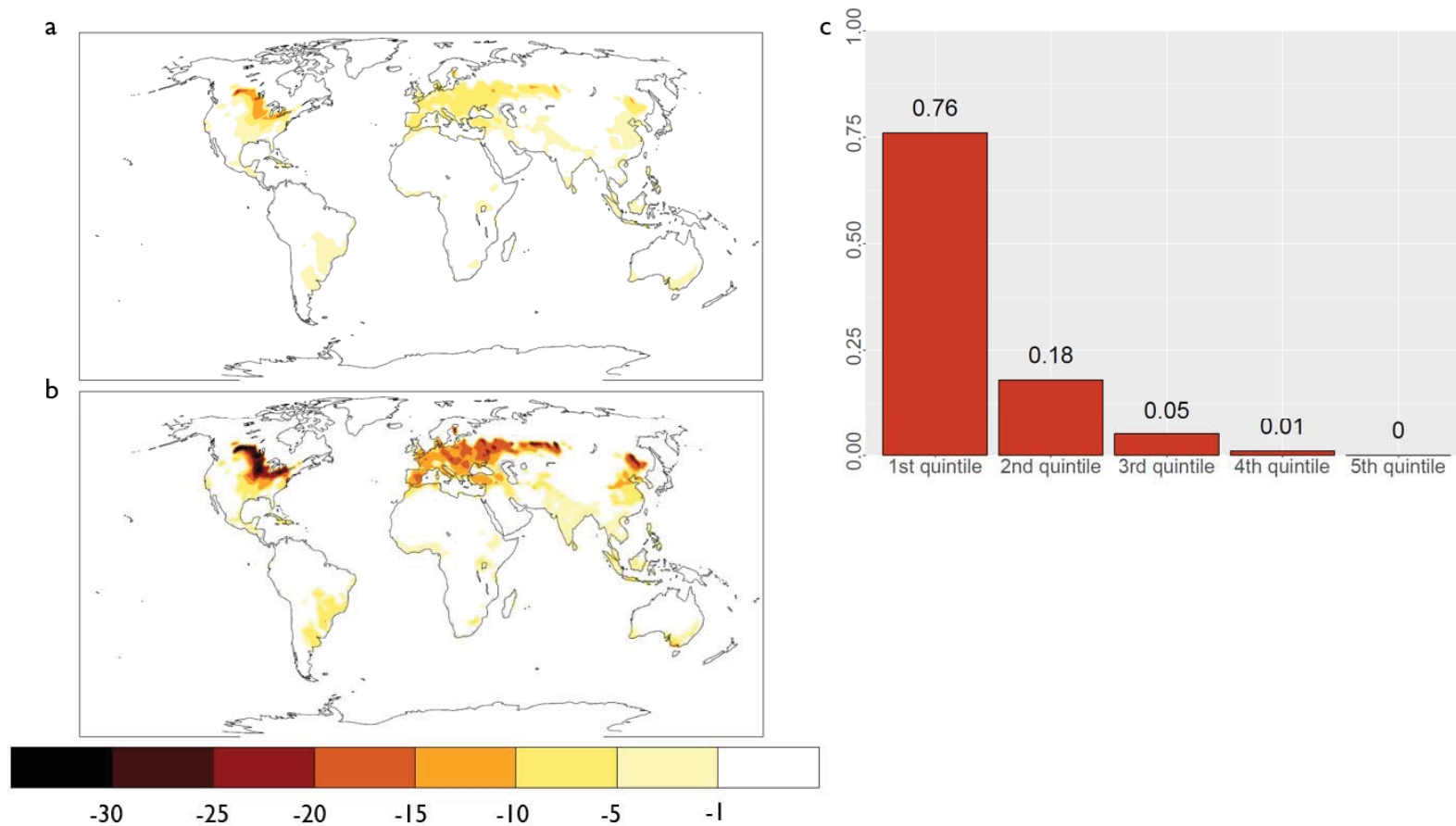


Figure 2-2 Maps showing the distribution of losses in soil organic carbon (Mg C ha⁻¹) per hectare of cropland subtracted from the control scenario for each individual grid cell in the ‘moderate (A) and ‘high’ (B) intensive tillage (IT) scenarios over the 1850 - 2014 time period. Areas with less than 15% crops are masked out. Bar plots in (C) show the proportion of total global losses in SOC accounted for by each quintile of cropped area in the Community Land Model. Cropped areas with high per hectare losses in (a) and (b) accounted for a large proportion of the cumulative global change in SOC by quintile, shown in (c), over the historical time period (1850 - 2014).



Conversion from intensive tillage practices to NT resulted in an accumulation of 6.6 – 14.4 Gt C (24.2-52.8 Gt CO₂e) between 2015 and 2100 under RCP 8.5, with the magnitude of SOC recovery depending heavily on the pre-existing ‘carbon debt’ from the corresponding historical IT scenarios (Fig. 2-1). SOC accumulation in NT scenarios increases asymptotically throughout the 21st century but never recovers to initial equilibrium levels of SOC prior to historical IT, though this may be partially attributable to the shorter time interval for recovery in future scenarios compared to historical scenarios (85 versus 165 years, respectively). The cumulative gains in SOC from NT for 2015 – 2100, even with the optimistic assumption that all cropland is converted to NT, are equivalent to approximately one year of current fossil fuel emissions (8.9 Gt C yr⁻¹; 32.6 Gt CO₂e) (Minasny et al., 2017).

SOC storage with NT increased at global rates of 0.08 and 0.17 Gt yr⁻¹ (0.28 and 0.62 Gt CO₂e yr⁻¹) for the ‘moderate’ and ‘high’ scenarios, respectively, and the annual quantity of C stored via NT was 0.8 – 1.0% of annual emissions from fossil fuels (Le Quéré et al., 2019). The highest global SOC sequestration rate simulated here (0.17 Gt C yr⁻¹) is an order of magnitude lower than the target of 8.9 Gt C yr⁻¹ set by the ‘4 per 1000’ initiative, implying that offsetting current fossil fuel emissions through SOC increases is unlikely to be achieved through NT practices alone, and will require major investments in additional management practices (Baveye et al., 2018). Annual global increases in SOC from NT were on the low end of values in the literature, but agree well with a comprehensive review on the global potential for SOC sequestration using NT (Powlson et al., 2014), which estimated global SOC storage rates of 0.11 – 0.17 Gt C yr⁻¹ (0.4-0.6 Gt CO₂e yr⁻¹).

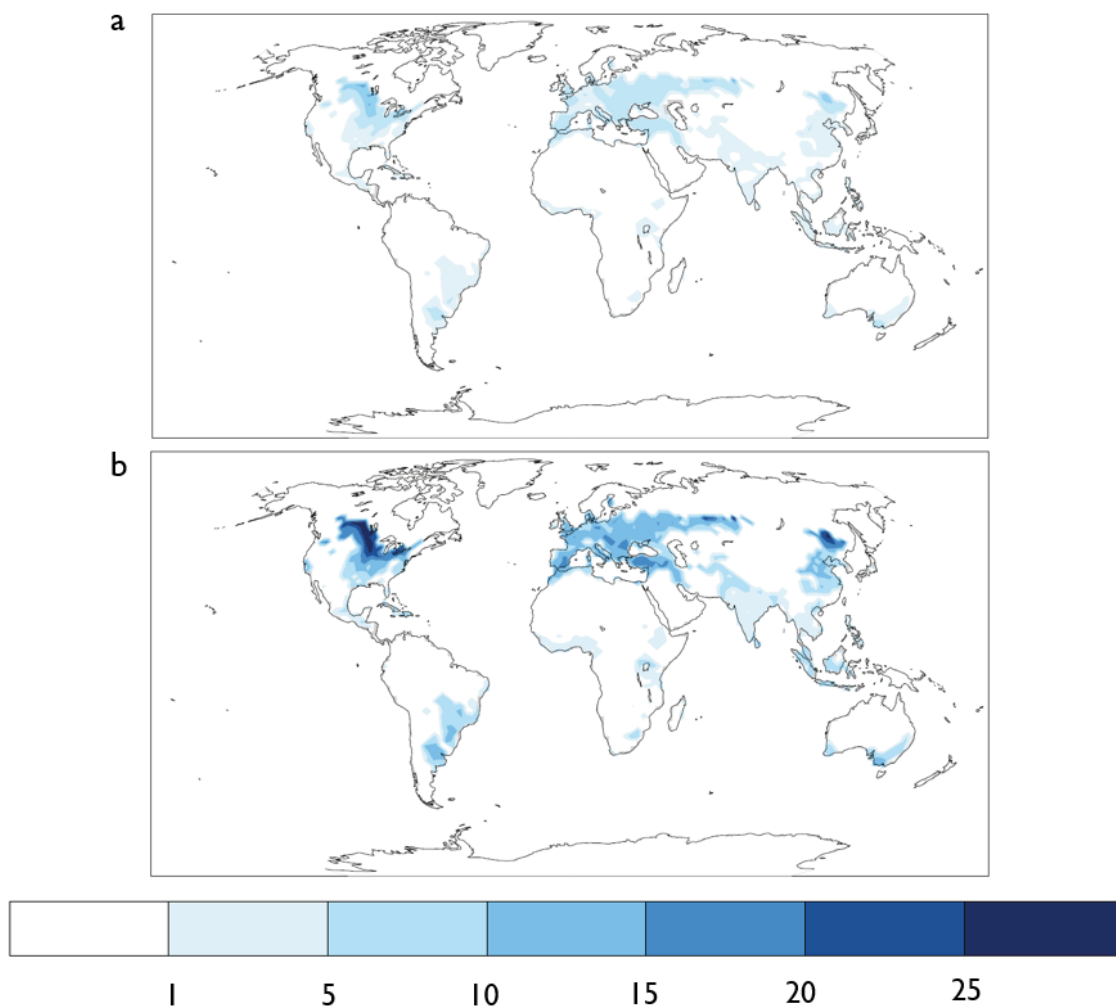
Global average rates of SOC sequestration per hectare under NT in our simulations ranged from 0.04 Mg ha⁻¹ yr⁻¹ to 0.11 Mg ha⁻¹ yr⁻¹ for ‘moderate’ and ‘high’ scenarios, respectively (Supplementary Fig. S-5). Reported rates of SOC storage from NT practices vary widely (Angers and Eriksen-Hamel, 2007; Luo et al., 2010; Corbeels et al., 2019), but literature reviews suggest an operational rate of 0.04 – 0.19 Mg C ha⁻¹ yr⁻¹ (Smith et al., 2008), a range which comports well with per hectare rates found here.

Cumulative SOC sequestration per hectare exhibited considerable variability in its geographical distribution and roughly mirrored losses under historical IT practices, since the highest absolute gains were concentrated in temperate regions of North America and Eurasia (Fig. 2-3). Cumulative SOC gains from these regions as a proportion of the global total closely paralleled those for the historical ‘carbon debt’ (Fig. 2-2c; Supplementary Fig. S-6). The largest simulated gains with NT were in locations with high initial levels of SOC prior to historical IT, suggesting that soils with more SOC to lose may also have the greatest capacity to regain lost SOC through improved management (Stewart et al., 2008; Castellano et al., 2015).

Cumulative SOC increases per hectare were largely on par with those achieved in field and modeling studies of NT for most locations. DayCent simulations of NT practices in Europe for the 21st century simulated an average cumulative gain of 2.9 Mg C ha⁻¹ (10.8 Mg CO₂e ha⁻¹), which closely approximates gains in the ‘moderate’ NT scenario for locations in Europe (Fig. 2-3a). Cumulative gains for locations with extreme SOC

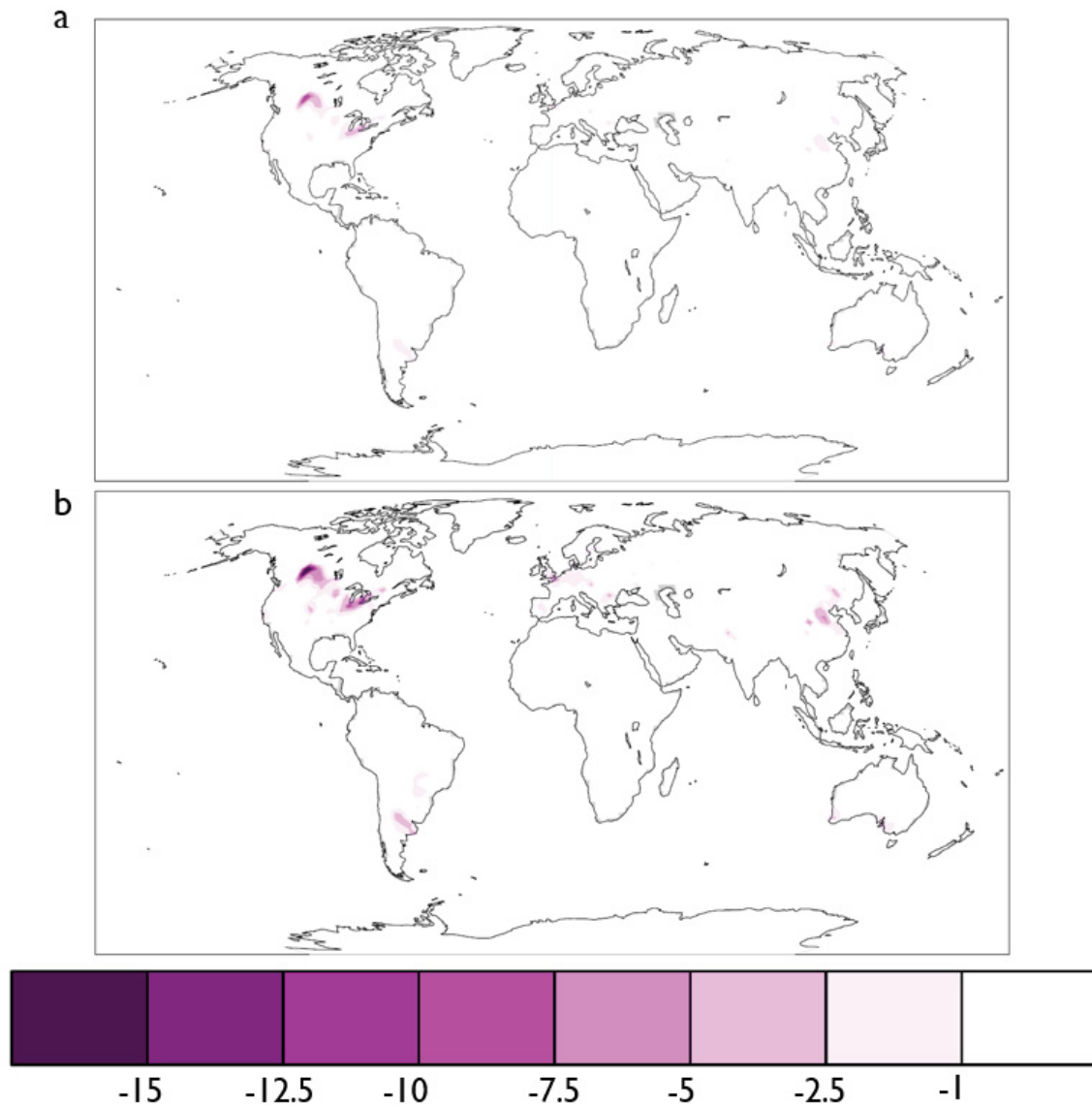
increases in the ‘high’ scenario (Fig. 2-3b), particularly in North America, surpass the most optimistic observations of attainable increases in SOC stocks using NT practices in this region (i.e., 0-10 Mg ha⁻¹) (Lal et al., 2015; Syswerda et al., 2011; Hollinger et al., 2005). Although SOC sequestration rates per hectare are reasonable for this region on an annual basis (Supplementary Fig. S-5), cumulative SOC increases constantly at these rates over the 21st century and never approaches equilibrium (Supplementary Fig. S-7). Possibly unrealistic cumulative SOC gains for North America indicate that, though we simulate tillage in an idealized manner, the magnitude of historical losses and the associated increase in decomposition rates for the ‘high’ IT scenario may be unrealistic, and that subsequent cumulative gains in SOC from NT adoption may also be optimistic.

Figure 2-3 Maps showing the distribution of increases in soil organic carbon (SOC) for ‘no-till’ (NT) relative to intensive tillage (IT) scenarios over the 2015-2100 time period. Maps displays average absolute differences in SOC (Mg C ha⁻¹) per hectare of cropland between ‘high (A) and ‘moderate’ (B) NT scenarios and the corresponding IT scenarios. Areas with less than 15% crops are masked out. Increases in the annual rate of SOC storage on a per hectare basis are shown in Supplementary Fig. S-5.



The geographical distribution of large absolute increases in SOC stocks coincides with some areas where NT is already widely practiced (Supplementary Fig. S-8), suggesting that NT might have a lower impact on SOC than our idealized scenarios estimate. We applied a post-hoc mask based on the proportion of cropland currently under NT at a given location using a globally gridded data product to account for the possibility of diminished SOC storage potential in areas where NT has been already adopted (Prestele et al., 2018). Adjustments for extant NT practices were performed by reducing SOC gains as a proportion of the fractional area in NT at each location as of 2012. The proportion of croplands in NT globally as of 2012 was 6.3%. After adjusting for present-day NT practices, locations with the largest reductions in SOC sequestration per hectare tended to be areas with both a high fraction of cropland currently in NT and relatively large simulated increases in SOC under NT (Fig. 2-4). Globally, masking areas currently in NT reduced cumulative SOC storage by 6.1% from 6.6 to 6.2 Gt C in the ‘moderate’ scenario, and by 6.3% from 14.4 to 13.5 Gt C in the ‘high’ scenario. The small reductions in SOC storage are proportional to the limited area currently in NT, portending that there is still potential to realize SOC gains through NT adoption in many areas based on our idealized estimates.

Figure 2-4 Maps showing the geographic distribution of reductions in soil organic carbon (SOC) sequestration after accounting for areas where ‘no-till’ (NT) is already practiced as of 2012. Reductions in SOC sequestration are displayed on a per hectare of cropland basis (Mg C ha^{-1}) for the ‘moderate’ NT (A) and ‘high’ NT (B) scenarios over the entire 2015 – 2100 time period. Areas with less than 15% crops are masked out. A map showing the mask as a proportion of the total cropped area in ‘no-till’ practices as of 2012 for each location can be found in Supplementary Fig. 8. Global changes in SOC storage due the mask can be found in Supplementary Fig. S-9.



Overall, these results demonstrate that the capacity of NT practices to offset current emissions through SOC sequestration is more limited than has been previously anticipated (Lal, 2004; Elzen et al., 2013; Smith et al., 2014; Minasny et al., 2017), and that NT is unlikely to represent a “silver bullet” policy tool for increasing SOC on agricultural land. Annual rates of SOC sequestration, which we consider to be optimistic for the ‘high’ scenario due to unrealistic gains in North America, are an order of

magnitude lower than ‘4 per 1000’ program objectives, implying that major investments in additional management practices will be required. Croplands with high initial SOC contents in mid-latitude regions had the highest simulated potential to lose SOC through intensive tillage, but also greater capacity for SOC sequestration following NT adoption. Making our idealized scenarios more realistic by adjusting for reduced SOC sequestration potential in regions where NT systems are already in place had a minor impact on SOC storage potential, due to the relatively small proportion of cropland on which NT has been adopted globally.

We used an idealized approach to modeling tillage practices by considering only changes in decomposition rates, whereas other work has emphasized that the dynamics of SOC storage with NT are more complex (Angers and Eriksen-Hamel, 2008; Virto et al., 2012; Stockmann et al., 2013; Powlson et al., 2014). Future work aimed at improving understanding and implementation of additional NT processes into LSMs, such as the effect of crop residue cover on albedo and soil moisture, should further refine these results (Davin et al., 2014; Bagley et al., 2015; Erb et al., 2017). Our idealized scenarios also assumed that NT was implemented on all croplands globally and did not account for practical and economic constraints to NT adoption, so our estimates may be higher than the actual economic potential for SOC gains from NT (Derpsch et al., 2010; Corbeels et al., 2014). Nonetheless, our results agree with observational estimates for many locations and provide the first global estimate of how tillage practices may contribute to climate mitigation efforts in an Earth system model.

From a policy perspective, the ‘carbon debt’ and potential for offsetting emissions via SOC sequestration from NT appears to be concentrated in temperate regions of developed countries and other major emitters under the United Nations Framework Convention on Climate Change. NT is already practiced in some of these regions, but adjusting for reduced potential SOC storage in these areas had minor impacts. This broadly suggests that any international policies aimed at meeting National Determined Contributions under the Paris Agreement can most efficiently offset emissions through NT by targeting adoption in the foregoing regions. By contrast, returns to SOC from NT adoption in the tropics are low and unlikely to represent an efficient means of offsetting fossil fuel emissions.

Acknowledgements

Melannie Hartman and Sam Levis provided background information and interpretation of code related to implementing DayCent tillage parameters into CLM 5.0. This research benefited from feedback and guidance from Gordon Bonan, Dave Lawrence, and other members of the Land Model Working Group within the Terrestrial Sciences Section of the Climate & Global Dynamics Lab at the National Center for Atmospheric Research in Boulder, CO, USA. Ben Ahlswede, Joshua Rady, Wyatt McCurdy, and Laura Puckett provided feedback and additions to the first draft of this manuscript. Financial support for this research was provided in part by U.S. Dept. of Agriculture – National Institute of Food and Agriculture Project #2015-67003-23485, EASM-3: Decadal Prediction of Sustainable Agricultural and Forest Management.

Supplementary Information

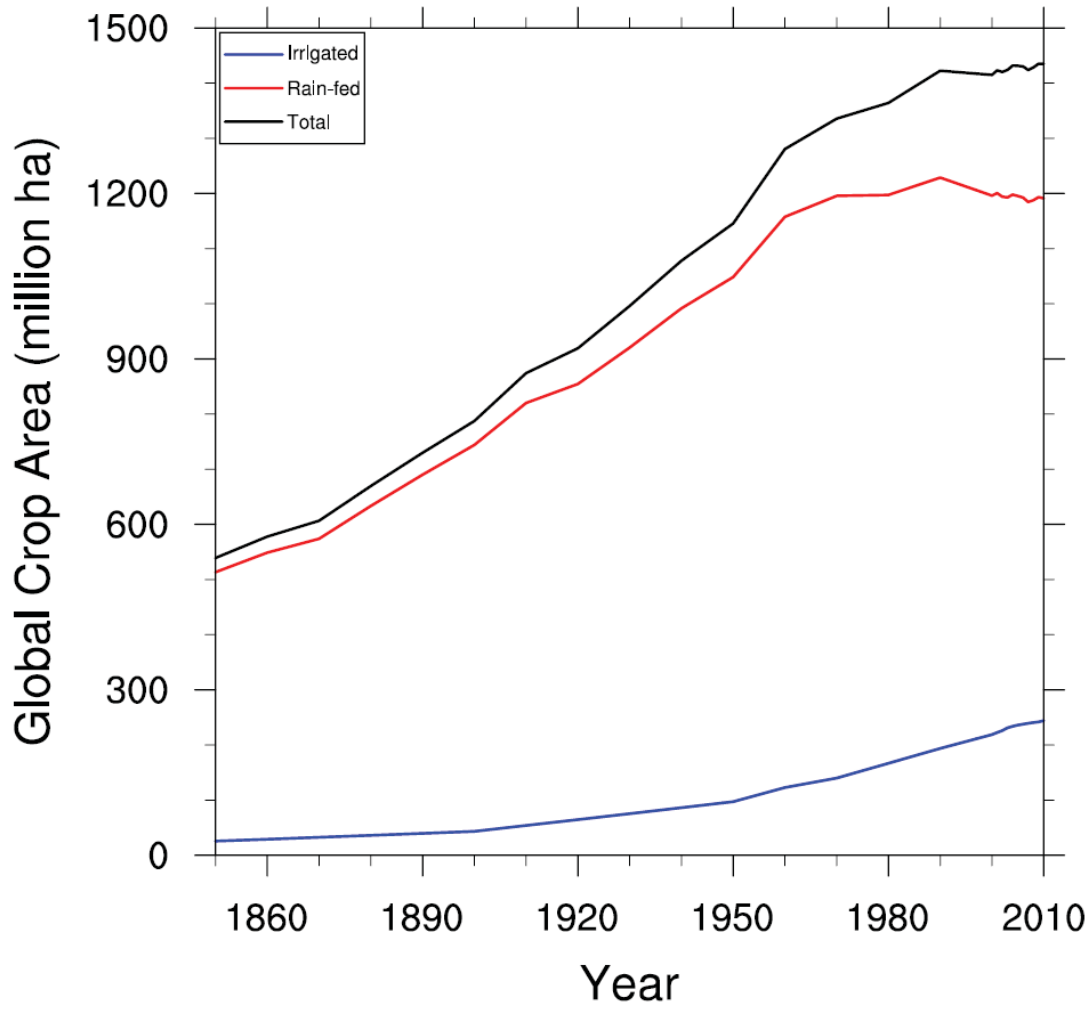
Supplementary Table S-1. Decomposition rate multipliers for various soil carbon pools based on DayCent tillage implements for ‘high’ and ‘low’ intensive tillage treatments. DAP= Days after planting; Litter2 = CLM Litter Pool 2; Litter3 = CLM Litter Pool 3; SOM1= CLM Soil Organic Matter Pool 1; SOM2= CLM Soil Organic Matter Pool 2; SOM3= CLM Soil Organic Matter Pool 3

DAP	Description	Litter2	Litter3	SOM1	SOM2	SOM3
High intensity scenario						
0-15	Point Chisel Tandem Disk multipliers	1.8	1.8	1.2	4.8	4.8
15-45	Field and Row Cultivator multipliers	1.5	1.5	1	3.5	3.5
45-75	Rod Weed Row Planter multipliers	1.1	1.1	1	2.5	2.5
Moderate intensity scenario						
0-15	Point Chisel Tandem Disk multipliers	1.5	1.5	1	3	3
15-45	Field and Row Cultivator multipliers	1.5	1.5	1	1.6	1.6
45-75	Rod Weed Row Planter multipliers	1.1	1.1	1	1.3	1.3

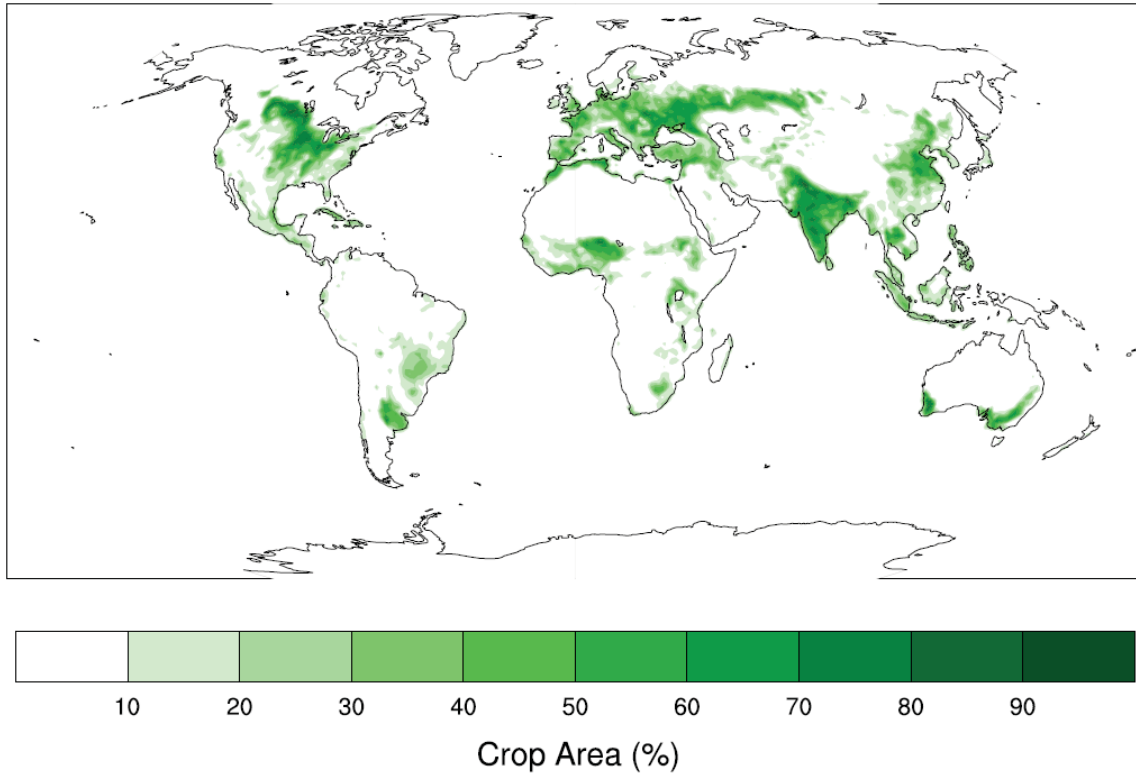
Supplementary Table S-2. List of simulations run for various tillage scenarios, plus associated treatments and time intervals.

Number	Scenario name	Treatment	Time interval
1	Control	CLM 5.0 default settings	1850 - 2100
2	'High' intensive tillage (IT)	'High' soil decomposition mutlipliers (Supplementary Table S-1)	1850 - 2100
3	'Moderate' intensive tillage (IT)	'Moderate' soil decomposition mutlipliers (Supplementary Table S-1)	1850 - 2100
4	'High' no-till (NT)	'High' soil decomposition mutlipliers = 1	2015 -2100
5	'Moderate' no-till (NT)	'Moderate' soil decomposition mutlipliers = 1	2015 -2100

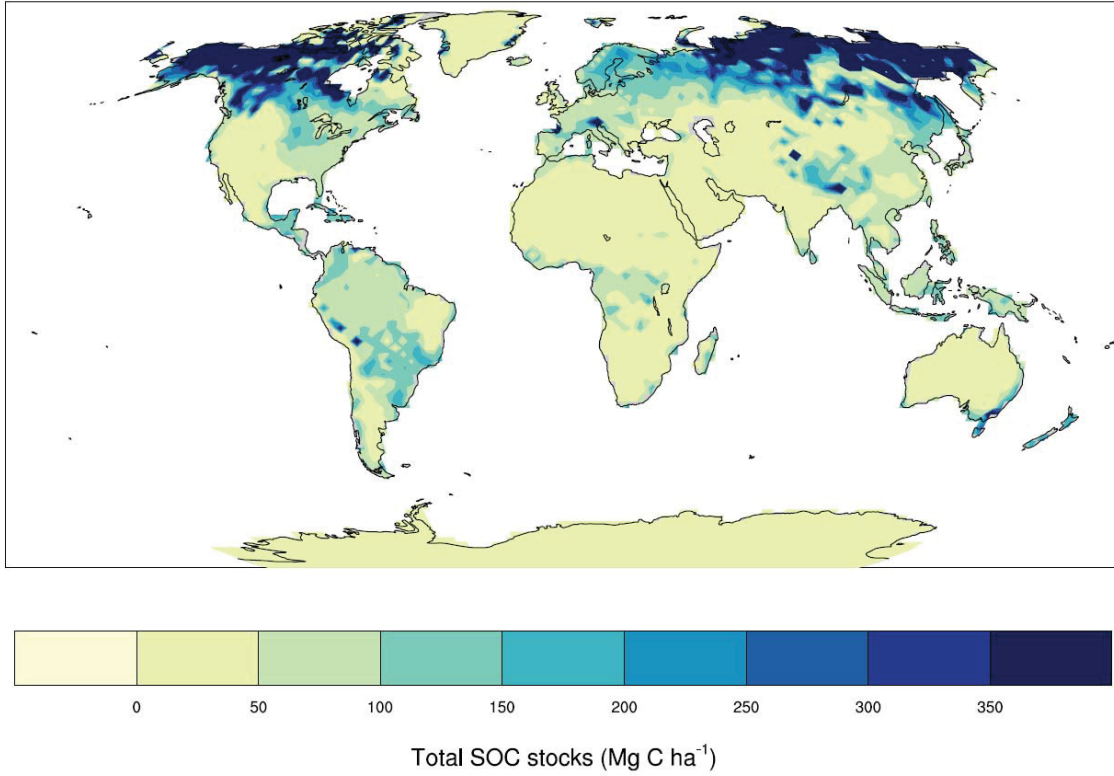
Supplementary Figure S-1. Time-series plot showing changes in irrigated, rain-fed, and total area in crops in millions of hectares (million ha) globally in the Community Land Model for the 1850 – 2015 historical time period. Land use change is based on Land Use Harmonized, version 2 (LUH2) data (<http://luh.umd.edu/data.shtml>)



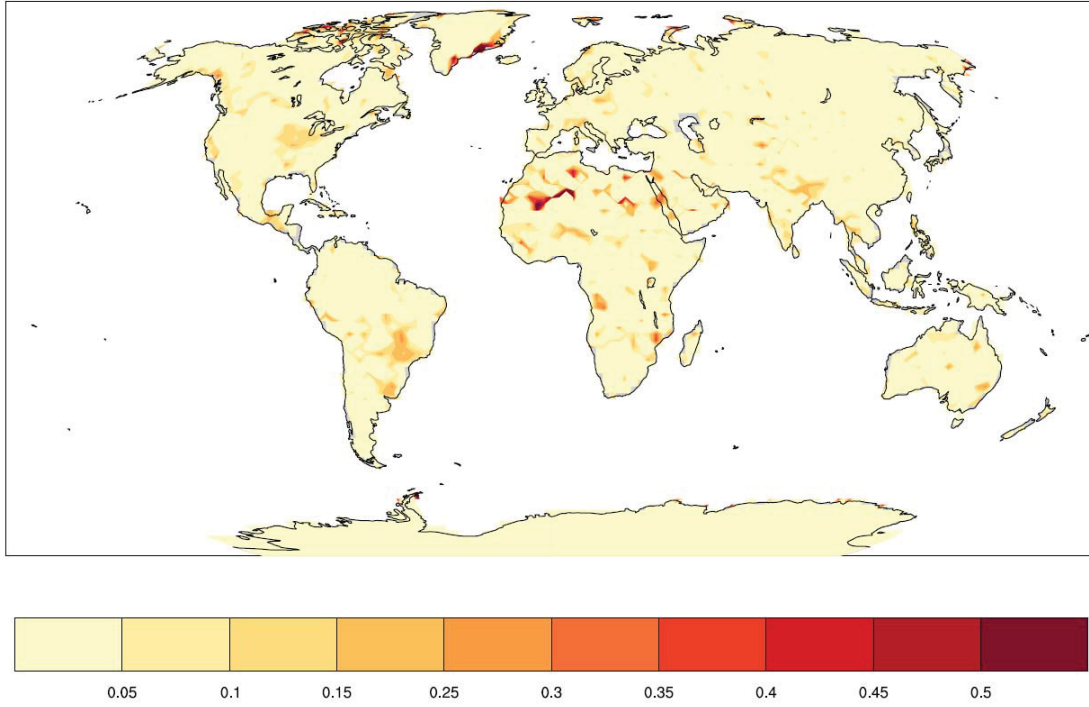
Supplementary Figure S-2. Map showing the total area in crops as a proportion of each individual grid cell in the Community Land Model. Proportional crop area is averaged for the 1990 to 2010 time period. Land use distribution is based on Land Use Harmonized, version 2 (LUH2) data (<http://luh.umd.edu/data.shtml>)



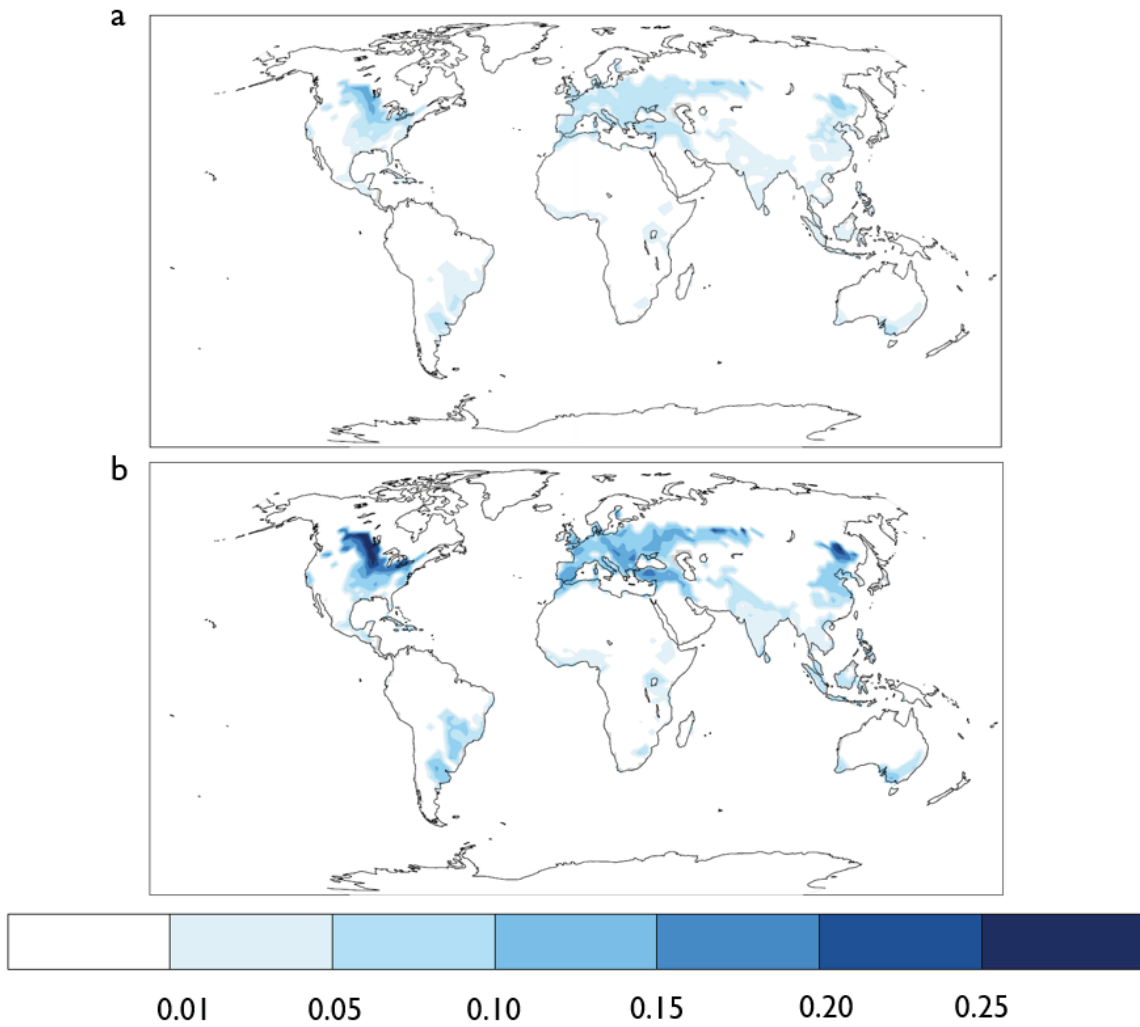
Supplementary Figure S-3. Map showing the initial distribution of average soil organic carbon stocks in 1850 (i.e. prior to implementation of intensive tillage practices) for each individual grid cell in the Community Land Model.



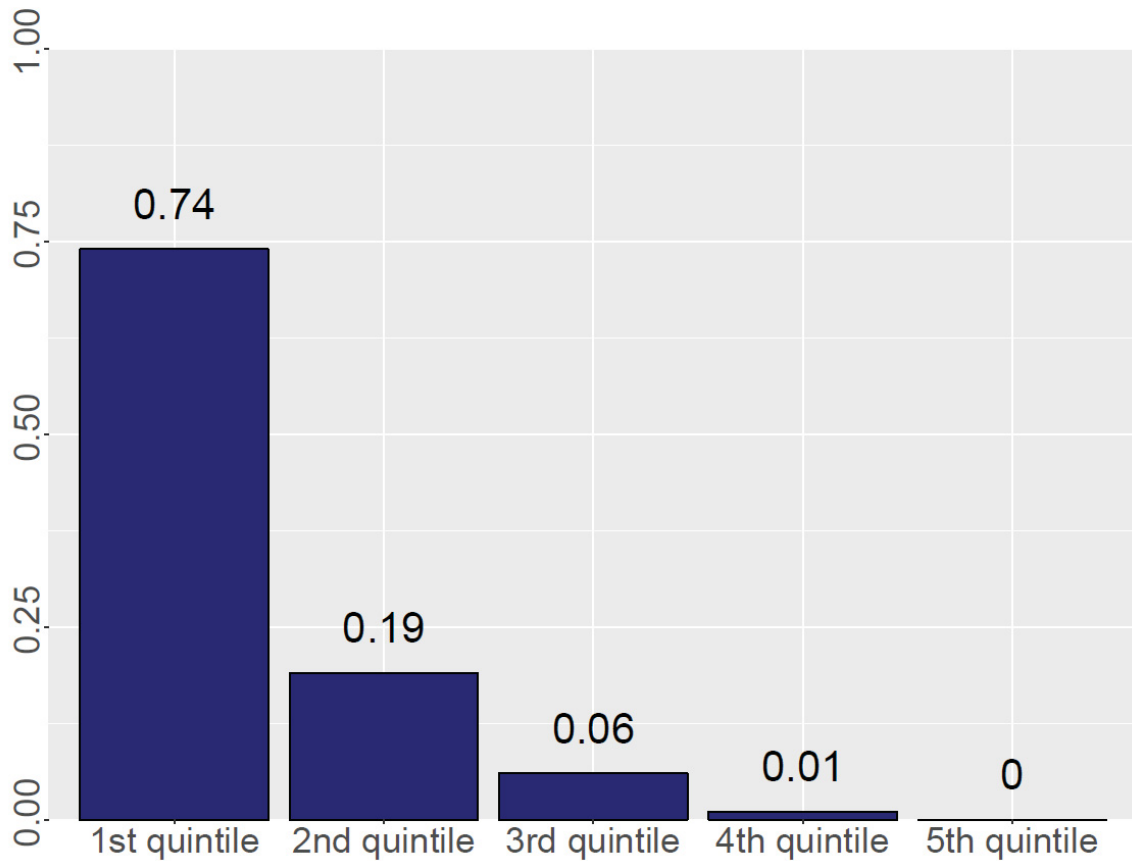
Supplementary Figure S-4. Maps showing the distribution of losses in soil organic carbon (SOC) as a percentage of initial SOC stocks for each individual grid cell in the ‘high’ intensive tillage scenario over the 1850 -2014 time period.



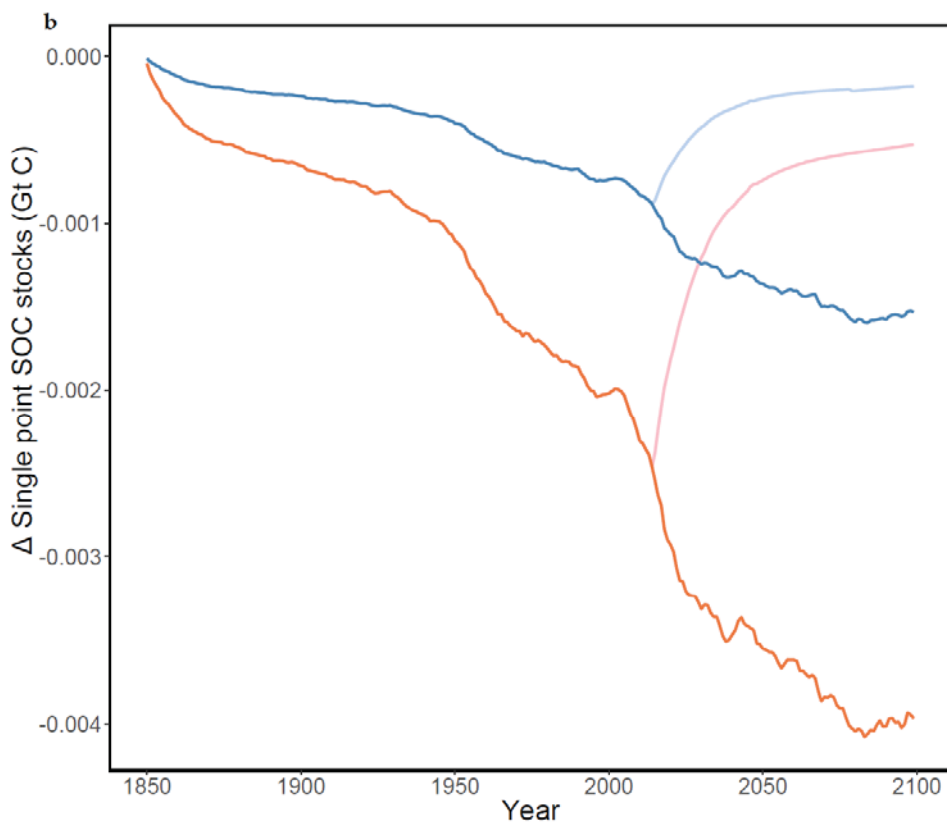
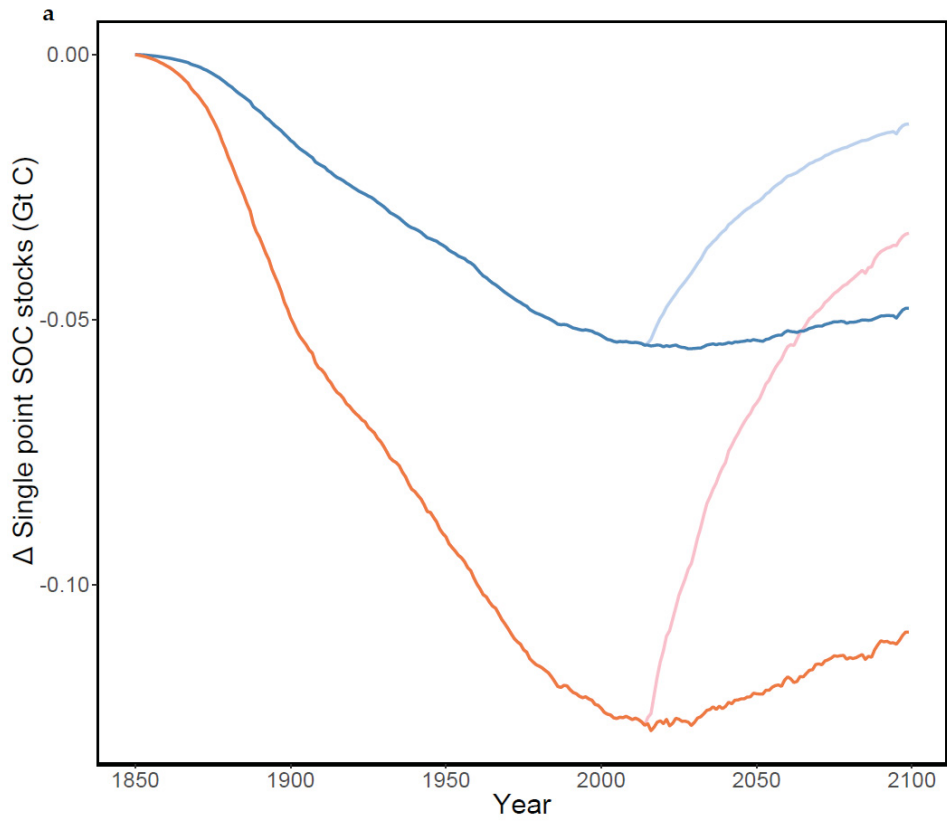
Supplementary Figure S-5. Maps showing the distribution of the annual rate of increase in soil organic carbon (SOC) for ‘no-till’ (NT) relative to intensive tillage (IT) scenarios over the 2015-2100 time period. Maps displays differences in the annual rate of SOC accumulation per hectare of cropland per year ($\text{Mg C ha}^{-1} \text{ yr}^{-1}$) for ‘high (A) and ‘moderate (B) scenarios compared to corresponding IT scenarios. Areas with less than 15% crops are masked out.



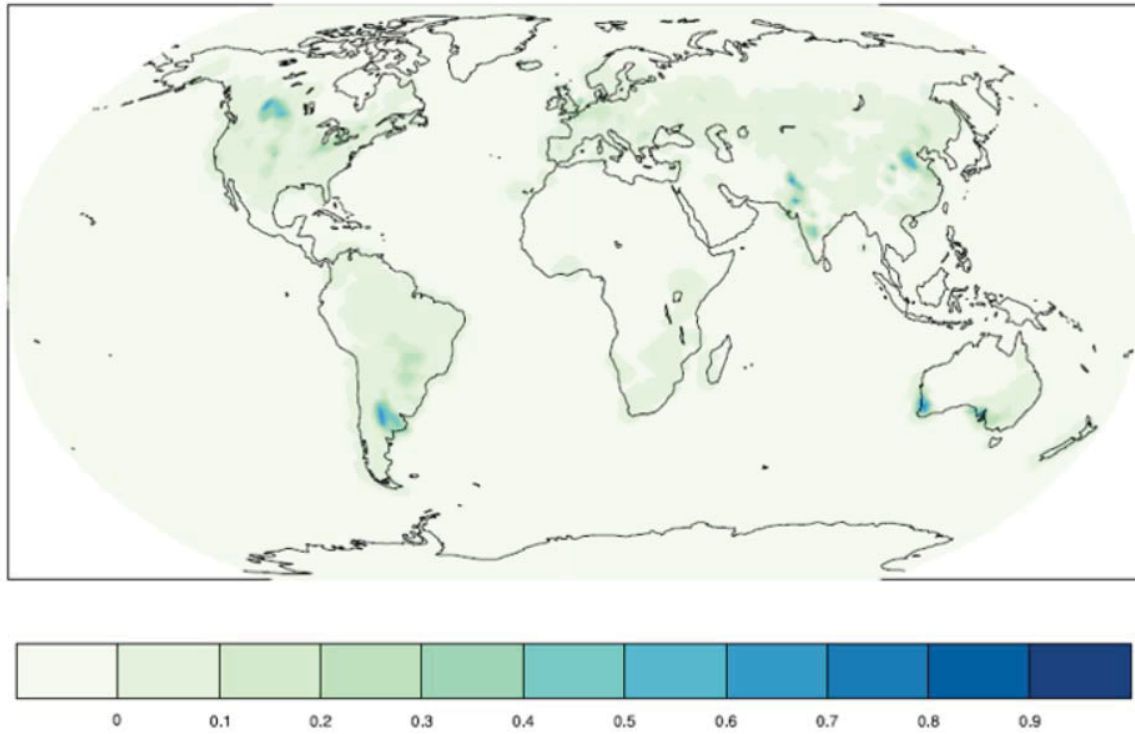
Supplementary Figure S-6. Bar plots showing the proportion of absolute change in SOC accounted for by each quintile of cropped area in the Community Land Model for ‘no-till’ simulations over the 2015-2100 time period. Cropped areas with high per hectare gains in Figure 2 (a) and (b) accounted for a large proportion of the cumulative global change in SOC by quintile over the RCP 8.5 time period (2015 -2100).



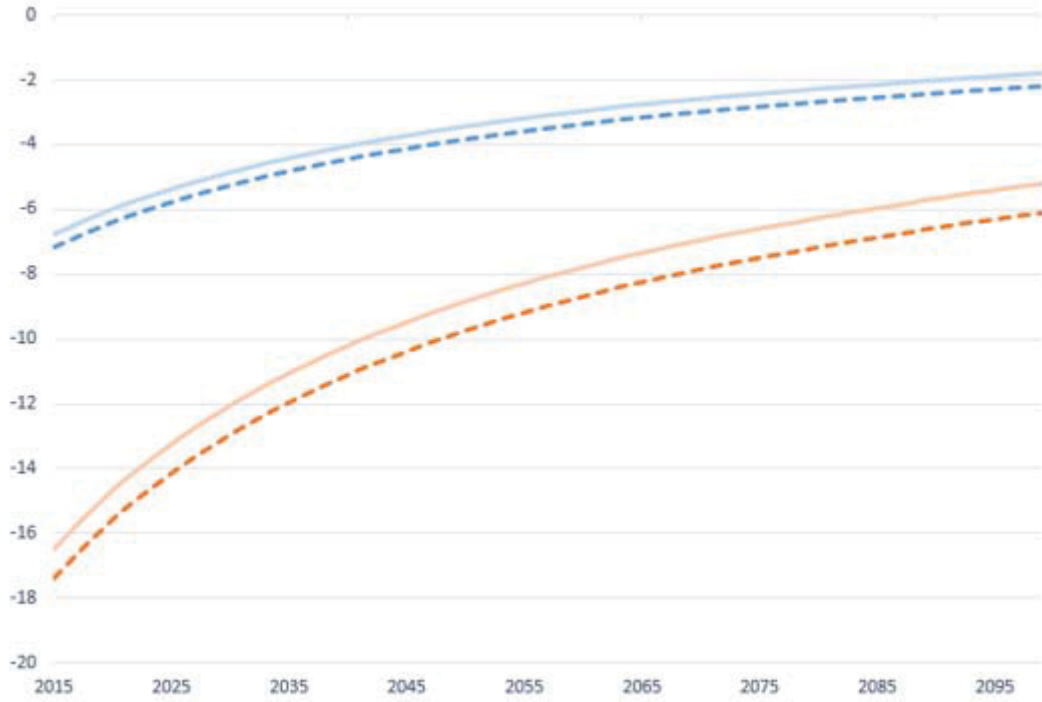
Supplementary Figure S-7. Time-series of changes in soil organic carbon stocks subtracted from the control scenario for two grid cells with high proportional crop area over the entire 1850 - 2100 time frame. Dark red lines denote intensive tillage (IT) scenarios with ‘high’ decomposition rates for the historical (1850-2014) and future (2015-2100) time periods. Dark blue lines denote intensive tillage (IT) scenarios with ‘low’ decomposition rates for the historical (1850-2014) and future (2015-2100) time periods. Light red lines denote changes in soil carbon stocks for ‘no-till’ (NT) scenarios following the ‘high’ historical IT scenarios. Light blue lines denote changes in soil carbon stocks for NT scenarios following the ‘low’ historical IT scenarios. The two locations in central United States (A) and northern Nigeria (B) demonstrate contrasting behavior with respect to equilibria of soil carbon stocks following for implementation of ‘no-till’ practices after 2015. Soil carbon stocks in the ‘high’ scenario for location A continuously increase over the 2015 – 2100 and do not reach equilibrium, whereas soil carbon at location B approaches equilibrium in both scenarios.



Supplementary Figure S-8. Global map showing the mask for ‘no-till’ practices as a proportion of total cropped area for each grid cell in CLM5 as of 2012. The mask and areal extent of ‘no-till’ practices are based a globally gridded data product of ‘no-till’ practices from Prestele et al. (2018).



Supplementary Figure S-9. Plot showing the cumulative soil carbon gains over the 2015- 2100 time period for the low (blue lines) and high (red lines) scenarios. Dotted lines show reductions in SOC due to the tillage mask for each scenario.



CHAPTER 4. ADDING FULL RANGE OF CROP MANAGEMENT PRACTICES INCREASES LAND USE CHANGE EMISSIONS AND REDUCES SOIL CARBON IN THE COMMUNITY LAND MODEL

Graham, M.W., R.Q. Thomas, D.L. Lombardozzi, M.E. O'Rourke

Abstract

Emissions from land use and land cover change (LULCC) represent a major source of uncertainty in the global carbon budget. Earth System models used in climate projections may underestimate LULCC emissions and associated declines in soil organic carbon (SOC) by excluding the full range of global management activities on croplands. Here, we used the Community Land Model (CLM) to assess 1) the impact of the full range of crop management practices (residue harvest, grain harvest, soil tillage, irrigation, fertilization) on the cumulative LULCC emissions and SOC stocks over the historical time period (1850 – 2015), and 2) the impact of individual crop management practices on the historical LULCC emissions and SOC stocks over the historical time period. Including the full range of crop management practices increased the cumulative historical Net LULCC emissions by 29.2 – 38.3 Pg C. Crop residue harvest was the most important crop management practice (17.6 Pg C), followed by grain harvest (9.4 Pg C), and soil tillage (5.3 Pg). Including the full range of management practices reduced SOC stocks by 33.4 – 38.8 Pg C, and adding more crop management practices to the CLM resulted in net cumulative decreases in SOC for virtually all locations globally. Continued exclusion of critical crop management practices may result in underestimation of changes in LULCC emissions and SOC stocks for ESMs in CMIP6, with implications for climate change mitigation and adaptation on croplands.

Introduction

Anthropogenic impacts on ecosystems have increased substantially over last several centuries, with three-quarters of Earth's ice-free land surface now in some form of management dedicated to meeting human needs for food, fuel, and fiber (Luyssaert et al., 2014). Broad-scale conversion of natural ecosystems to agricultural and other management activities has been an important driver of historical anthropogenic CO₂ emissions, and emissions from land use and land cover change (LULCC) account for approximately one-third of all historical anthropogenic CO₂ emissions (Ciais et al., 2013; Houghton and Nassikas, 2017). Historical emissions from LULCC also represent a major source of uncertainty in the global carbon budget – based on multiple climate models, the mean estimate for cumulative historical CO₂ emissions due to LULCC is 195 Pg C over the 1850 - 2014 time period, but there is considerable variability in estimates of the

historical LULCC flux among models (± 75 Pg C; ± 0.7 Pg C/yr) (Le Quéré et al., 2018). Uncertainty in estimates of LULCC between models likely arises from a combination of differences in representation and inclusion of land management activities (Erb et al., 2017), disparities in methodologies and terminology, and uncertainty with respect to extant and historical soil and vegetation C stocks (Le Quéré et al., 2018). Moreover, it has been suggested that LULCC emissions and the corresponding size of the residual land sink of carbon may be underestimated due to the exclusion of many prominent land management activities in the current generation of ESMs (Arneeth et al., 2017).

Management practices on croplands are one set of land management activities that have not been comprehensively represented in many ESMs, and process-level understanding of the impacts of crop management on the historical and future LULCC flux is poor (Erb et al., 2017). The majority of ESMs that will form the basis of Coupled Model Intercomparison Project 6 (CMIP6) and future Inter-Governmental Panel on Climate Change reports do not include many important crop management practices. Several of the highest priority crop management practices - replacing generic crop parameterizations with crop-specific plant functional types (CFTs), harvesting and removing grain, harvesting residue, transferring harvested crops to crop product pools, fertilizing, irrigating – are present in less than half of the ESMs submitted to CMIP6 (Pongratz et al., 2018).

However, since permanent cropped area accounts for 12 percent of Earth's ice-free land surface, the management of these ecosystems on the LULCC flux could be substantial (Luyssaert et al., 2014). The exclusion and uneven representation of crop management practices in ESMs could therefore partially explain variability in estimates of historical LULCC emissions between models. This could also potentially lead to underestimation of LULCC historical emissions because agricultural practices typically reduce the quantity of C entering crop ecosystems due to biomass removal by harvest, as well as accelerating decomposition of SOC via intensive tillage practices (Pugh et al., 2015). Cropland management activities are a key pillar of many strategies aimed at climate change mitigation and adaptation, so inadequate representation of crop management in ESMs could have major policy implications for future assessments of carbon cycling and land management decisions (Soussana et al., 2017; Baveye et al., 2018). Although most important crop management practices are implicitly included in bookkeeping models of carbon accounting, which calculate LULCC emissions based on empirically derived estimates of changes in carbon density following LULCC, assessments of crop management in ESMs used for climate change projections have been limited (Hansis et al., 2015; Houghton and Nassikas, 2017). Yet, inclusion of crop management practices in ESMs is a key requirement for evaluating the overall effects of different crop management practices on C cycling and their potential interactions with climate. While some studies have reviewed how different crop management activities might influence the LULCC flux (Pongratz et al., 2018), no studies have examined the aggregate effects of the full range of high priority crop management practices (i.e., residue harvest, grain harvest, soil tillage, irrigation, fertilizer) on LULCC emissions in an ESM. The uncertainty and potential underestimation of the cumulative historical LULCC flux among ESMs could be partially attributable to the absence of a soil 'legacy flux', which

refers to alterations in emissions and sink capacity due to crop management practices on existing cropland following LULCC transitions (Pongratz et al., 2014; Pugh et al., 2015). The legacy flux on croplands in general is likely to result in increased emissions and reductions in sink capacity due to practices such as soil tillage and crop harvest, which accelerate decomposition and losses of soil organic carbon (SOC) to the atmosphere while also reducing the potential productivity of crop vegetation over time (Levis et al., 2014). The absence of many critical crop management practices in the current generation of CMIP6 models may therefore underestimate the soil legacy flux.

The soil legacy flux typically manifests itself as decline in SOC on cropland, and field studies indicate that conversion of natural vegetation to crops typically results in a decrease in SOC of 20-40 Mg/ha (10 – 50%) depending on environmental and edaphic factors (Guo and Gifford, 2002; Don et al., 2011; Poeplau et al., 2011). Yet, the current generation of ESMs that comprise CMIP6 show unrealistic increases in SOC rather than losses following LULCC to crops globally (Lombardozzi et al., 2019). Further, most field studies that evaluate declines in SOC over time following conversion of natural vegetation to crops examine the impact of all changes in crop management in aggregate, and do not differentiate between individual management practices. Crop management practices are likely to vary not only in magnitude, but whose impact on SOC is likely differ in direction as either positive (e.g., fertilization, irrigation) or negative (e.g., grain harvest, tillage) depending on the specific practice (Fujisaki et al., 2018). Identifying the contribution of individual land management practices is crucial to understanding historical changes in SOC and which management practices are likely to have the greatest potential impact for climate change mitigation and adaptation, and is thus relevant to identifying policy options within the CMIP6 framework (Bonan and Doney, 2018). Adding or refining crop management practices in current generation ESMs may not only provide more realistic estimates of changes in SOC stocks and the historical LULCC flux, but should also be useful in assessing model sensitivity to specific crop management practices and evaluating the relative importance of these practices to changes in SOC and the LULCC flux.

Here we investigate the combined, historical effects on LULCC emissions and SOC stocks of including the full range of practices prioritized by Pongratz et al. (2018) in an Earth System model – the Community Land Model (CLM) within the Community Earth System Model. In addition, we partition the effects on historical LULCC emissions and changes in SOC stocks attributable to individual crop management practices in the CLM. We also examine whether adding crop management practices to the CLM results in more realistic model outputs in terms of the magnitude and spatial distribution of changes in SOC.

We focus on the CLM because it is relatively well-developed with respect to crop management and includes crop-specific plant functional types (CFTs), grain harvest, crop product pools, irrigation, and fertilization (Levis et al., 2012). Somewhat surprisingly, the difference in cumulative historical LULCC flux between CLM simulations with active crops, in which the preceding management practices are implemented, and generic crops (i.e. no crop-specific PFTs or management practices) is relatively small (Lawrence et al.,

2019). Both active and generic crop simulations in the CLM display an overall increase in global SOC stocks over the historical time period, despite large simulated increases in crop area due to LULCC, and cropped areas in several mid-latitude regions show increases in SOC with active crops (Lombardozzi et al., 2019). Although preliminary analysis of aggregate changes in SOC due to management in the CLM has been conducted, the effects of existing, individual crop management practices present in the CLM have not been investigated in terms of the historical LULCC flux and SOC stocks over the historical time period, and we add soil tillage and crop residue harvest to the foregoing list of practices in order to obtain the full range of management practices in the CLM.

Materials & Methods

Model Description

All simulations were run with Community Earth System Model (version 2.0) land and atmosphere components using coupled Community Land Model (CLM, version 5.0; Oleson et al., 2013; Lawrence et al., 2019) and Community Atmosphere Model (CAM, version 5; Neale et al., 2012). CLM5.0 simulations were performed with active carbon and nitrogen biogeochemistry and prognostic crops (CLM5.0-BGC-CROP) at 1.9° x 2.5° resolution. Simulations were run with 1850 initial conditions and uncoupled from ocean and ice model components using prescribed atmospheric forcings for radiative gases and repeated 20th century climate from Global Soil Wetness Project data (GSWP; Dirmeyer et al., 1999) for the 1850 to 2014 historical time period, in agreement with the Land Use Model Intercomparison Project (LUMIP) and CMIP6 (Lawrence et al., 2016). Historical changes in LULCC in CLM5.0 were prescribed using Land Use Harmonized version 2 data (LUH2; Hurtt et al., 2011; <http://luh.umd.edu/data.shtml>) in accordance with LUMIP protocols.

The CLM5.0 crop sub-model (CLM5.0-CROP) has crop species and phenology based on the Agro-IBIS land surface model. CLM5.0-CROP maintains crop with four distinct phenological growth phases (planting, leaf emergence, grain fill, and harvest) that are individualized for each species, as described by Levis et al. (2012). CLM5.0-CROP has numerous crop species, which are represented as CFTs. Each CFT is assigned a separate, individual soil column from that for natural vegetation, which prevents crop management practices from affecting natural vegetation.

For existing CLM management practices, crop yields and grain entering product pools in CLM are determined dynamically, while irrigation and fertilization are prescribed using external data. Crop yields and quantity of grain harvested depend on dynamically modelled annual crop productivity; grain enters the one-year crop product pool following harvest annually. Nitrogen fertilization is prescribed by CFT and by region in a geographically explicit manner based on transient LUH2 data on fertilizer use. Transient fertilizer is prescribed for CFTs according to crop N needs, with N being added directly to the soil mineral N pool (Lawrence et al., 2016). For irrigation, CFTs are divided between an irrigated and non-irrigated column in each grid cell to ensure irrigation is applied only to irrigated crops. The proportion of irrigated versus non-irrigated columns

for a CFT is prescribed based on a geographically explicit, transient dataset of areas equipped for irrigation (Portmann et al., 2010).

Along with existing CLM management practices, soil tillage and residue harvest were added in a simplified manner in this study to obtain a full range of crop management practices. CLM biogeochemistry is based on the DayCent/CENTURY model, and intensive soil tillage was added to the model by increasing the rate of SOC decomposition for multiple SOC pools based on previously tested rates derived from DayCent decomposition multipliers for tillage (Chapter 2, this document). DayCent decomposition multipliers were obtained from the high end of values found in the literature. Increased SOC decomposition rates were restricted to crop columns and prescribed based on crop phenology to occur over 75 days after planting for each CFT annually (Levis et al., 2014). Crop residue harvest was modelled in a simple manner by harvesting 100% of the aboveground crop biomass (i.e., stems and leaves) remaining in all crop columns at the time of grain harvest, with harvested leaves and stems subsequently entering the crop product pool, as per grain harvest. Although the intensity of management for soil tillage and crop residue harvest is extreme, this approach is useful for assessing model sensitivity to changes in these practices and their underlying biophysical processes.

Experimental Design

Each treatment run consists of paired simulations with transient LULCC on (LU) and an analogous simulation with no LULCC (NOLU). These simulations are in accordance with Pongratz et al. (2014) to reduce terminological uncertainty and ensure valid comparisons of changes in the historical LULCC flux and SOC across models. Treatment runs consisted of three main simulations: generic crops, CLM 5.0 default, and all management practices (Table 1). In the generic crops (GC) simulation, active crops are turned off and there are no crop-specific CFTs; crops are treated as generic grasses with no management. Generic crops were used to simulate crops in previous versions of the CLM and many of the ESMS contributing to CMIP6 continue to simulate crops in this manner. GC simulations are therefore included to represent the range of complexity in simulating crops across ESMS in CMIP6, and to assess the potential effects of excluding crop management practices on the LULCC flux and SOC stocks in CMIP6.

Table 4-1. List of all simulations in this study with number, name, and description. Simulations are divided into three ‘main’ and five ‘individual crop management’ simulations.

Main simulations		
Number	Simulation name	Description
1	Generic crops (GC)	All crops modelled as generic C3 grasses, with active crops turned off and no management practices applied
2	CLM 5.0 default (CLM5)	Active crops with existing crop management practices in CLM, version 5.0 applied (i.e., grain harvest, irrigation, fertilization)
3	All management (AM)	Active crops with existing CLM 5.0 and novel management practices applied (i.e., grain harvest, irrigation, fertilization, soil tillage, residue harvest)
Individual crop management simulations		
Number	Simulation name	Description
4	AM - Residue Harvest	Active crops and all crop management practices applied, with the exception of residue harvest
5	AM - Grain Harvest	Active crops and all crop management practices applied, with the exception of grain harvest
6	AM - Tillage	Active crops and all crop management practices applied, with the exception of soil tillage
7	AM - Irrigation	Active crops and all crop management practices applied, with the exception of irrigation
8	AM - Fertilizer	Active crops and all crop management practices applied, with the exception of fertilizer

In the CLM 5.0 default simulation (CLM5), crops were simulated with CLM 5.0 default settings using active crops and standard management practices, which included grain harvest, crop product pools, irrigation, and fertilization. CLM5 serves as a baseline to compare indirectly the current state of the CLM-CROP model with less developed ESMs in CMIP6, as represented by the GC simulations, and to determine the impact of additional management practices.

In the all management (AM) simulation, crops were simulated using active crops and existing management practices as per the CLM5 simulations, but also included soil tillage and residue harvest as additional management practices. AM simulations were conducted in order to determine the aggregate impact of the full range of high priority crop management practices in the CLM.

In addition to the three main sets of paired simulations (GC, CLM5, AM), scenarios were run to isolate the effects of individual crop management practices on the historical LULCC flux and SOC stocks globally. This was accomplished through five simulations, corresponding to each management practice, and running simulations with all management practices in place, but with the management practice of interest removed from the full set.

Framework for Partitioning and Analysis of LULCC Flux

In order to determine which processes contribute to changes in LULCC flux for simulations with varying levels of crop management implementation, the following framework for partitioning the LULCC flux is adopted from previous work by Lawrence et al. (2018) on historical and future LULCC fluxes in CLM (version 4.0), and adheres to definitions set out by Pongratz et al. (2014). The framework presented here is modified from Lawrence et al. (2018) to include fluxes associated with the creation of crop product pools and losses thereof in CLM 5.0. The framework partitions the LULCC Flux into Net, Direct, and Indirect Fluxes. Prior and Feedback Fluxes that are defined in Pongratz et al. (2014) are excluded from this analysis due to limitations of the experimental design in this study. Prior Fluxes were excluded because a suitable LULCC dataset of potential natural vegetation, which is required for calculating the Prior Flux, was not available for the CLM. Calculating the Feedback Flux was not possible because this would require running fully coupled simulations with ocean and ice components activated, and this was deemed to be too computationally intensive for the purposes of this study.

It should be noted that all simulations in this study involved only changes to management practices for crops. Non-crop management practices, such as wood harvest from forests, are included in all simulations, but are identical and constant across all simulations since no changes have been made with respect to these non-crop management practices. All differences in LULCC fluxes and SOC stocks between simulations are therefore attributable to alterations in crop management practices alone.

The Direct LULCC flux (LULCCDirect) refers to the losses in C associated with direct actions from land cover change and harvest of wood products, and is analogous to the

"instantaneous flux" from Pongratz et al. (2014). The Direct Flux is computed in CLM5.0 as:

$$\text{LULCCDirect} = \text{ConversionATM} + \text{ConversionPROD} + \text{Wood Harvest (Equation 1)}$$

The Direct Flux consists of C released to the atmosphere through fires and accelerated turnover during land cover change (ConversionATM), along with wood harvested during conversion that subsequently enters the wood product pool (ConversionPROD). Wood Harvest refers to harvest of wood products from natural ecosystems without a concomitant change in land cover. The Direct Flux has been extensively treated by Lawrence et al. (2018) and is identical across all simulations in this study, since all treatment simulations involve only changes to crop management following land cover transitions.

Differences in LULCC flux between simulations in this study therefore occur primarily due to changes in the Indirect Flux, which is effectively the "legacy flux" (the L variable in equation 3 from Pongratz et al., 2014). The Indirect Flux accounts for changes in sink capacity due to both management practices on existing cropland and due to changes in land cover back to natural vegetation (i.e., afforestation of previously cropped areas), as well as recovery from disturbance in natural vegetation. The Indirect Flux is modified from Lawrence et al. (2018) to account for losses from crop product pools as follows:

$$\text{LULCCIndirect} = \text{CropProdLoss}_{\text{LU-NOLU}} + \Delta\text{HR}_{\text{LU-NOLU}} + \Delta\text{Fire}_{\text{LU-NOLU}} - \Delta\text{NPP}_{\text{LU-NOLU}}$$

(Equation 2)

Since calculating changes in carbon uptake by ecosystems requires comparing simulations with full transient LULCC (LU) and no LULCC (NOLU), the Indirect Flux is computed based on the difference between variables in Equation 2. Losses from the one-year crop product pool are accounted for by the CropProdLoss variable and represent losses to the atmosphere of harvested C from cropland ecosystems. HR refers to Heterotrophic Respiration and NPP is the net primary production of ecosystems. Fire is the loss in C due to the presence of wildfires in CLM.

From the Direct and Indirect Fluxes, the overall Net Flux due to LULCC (LULCCNet) can then be calculated to ways, as follows:

$$\text{LULCCNet} = \text{LULCCDirect} + \Delta\text{CropProdLoss}_{\text{LU-NOLU}} + \Delta\text{HR}_{\text{LU-NOLU}} + \Delta\text{Fire}_{\text{LU-NOLU}} - \Delta\text{NPP}_{\text{LU-NOLU}} - \text{GrowthProdC (Equation 3)}$$

$$\text{LULCCNet} = \text{LULCCDirect} + \text{LULCCIndirect} - \text{GrowthProdC (Equation 4)}$$

The CLM diverges from equations in Pongratz et al. (2014) again by adding a slowly decaying wood product pool that contains C from harvest of wood products in Equation 4 and 5. GrowthProdC refers to the growth in product pool C over time and is computed as follows:

$$\text{GrowthProdC} = \text{ConversionProd} + \text{Wood Harvest} + \text{DecayProd} \text{ (Equation 5)}$$

The DecayProdC variable in Equation 5 refers to the slow loss of C from the overall wood product pool over time. The GrowthProdC is constant across all simulations and has been treated extensively in the CLM by Lawrence et al. (2018).

Results

Analysis of Net LULCC Flux for Three Main Simulations

Adding the full range of crop management practices to the CLM increased the Net LULCC Flux compared to simulations with generic crops and CLM 5.0 default settings. The cumulative historical Net LULCC Flux for the AM simulation was 225.0 Pg C over the 1850 to 2014 time period compared to 187.0 Pg C and 196.0 Pg C for the GC and CLM5 simulations, respectively (Figure 4-1a). This represents a cumulative increase in historical Net LULCC Flux for AM relative to GC of 38.3 Pg C (20.4%) and 29.2 Pg C (14.9%) for the CLM5 simulation. Changes in annual Net LULCC Flux over time followed roughly similar patterns for all three simulations, but at higher annual rates for AM (1.36 Pg C/yr) versus both GC (1.13 Pg C/yr) and CLM5 (1.18 Pg C/yr) (Figure 4-1b). Geographically, the Net LULCC Flux tended to be greatest in areas where a large fraction of natural vegetation has been cleared for crops via LULCC, with larger Net Fluxes in these areas in the AM simulations (Supplementary Figure S-10).

Attributing Changes in Net LULCC Flux to Individual Crop Management Practices

Impacts of individual management practices were assessed by removing each individual practice from the full suite of practices in the AM simulation, as described in the Section 2.2. Decreases in Net LULCC Flux relative to AM when individual practices are removed therefore represent a positive impact on the cumulative Net LULCC Flux for AM, and vice-versa.

The results of individual management simulations indicate that practices that remove crop products via harvest were the most important management practices in terms of changes in the Net LULCC Flux (Figure 4-2). Subtracting crop residue harvest from AM (AM – Residue) reduced the historical LULCC flux by 17.6 Pg C (-7.8%), followed by grain harvest (AM – Grain) at 9.4 Pg C (-4.1%) (Figure 4-2a).

Soil tillage was the third largest contributor to changes in the Net LULCC Flux, as its subtraction from the full suite of management practices (AM – Tillage) resulted in a cumulative decrease of 5.3 Pg C (-2.4%) in the historical Net Flux. Eliminating crop irrigation and fertilization from the full AM simulation had comparatively minor impacts on the historical LULCC flux. Removing irrigation (AM – Irrigation) resulted in minimal changes, as irrigation appears to cause a slight decrease in the cumulative Net LULCC Flux of 0.18 Pg C (<0.01%). The impact of crop fertilization (AM – Fertilizer) was also small, but its subtraction from the AM simulation increased the Net LULCC Flux by 2.6 Pg C (-1.1%).

Figure 4-1. Plot (A) showing cumulative change in Net LULCC Flux between the three main simulations over the historical time period (1850–2014). Plot (B) shows the annual change in Net LULCC Flux for the three main simulations over the historical time period, as well as the mean estimate and range of uncertainty for Net LULCC Flux from Global Carbon Project data (Le Quéré et al., 2018).

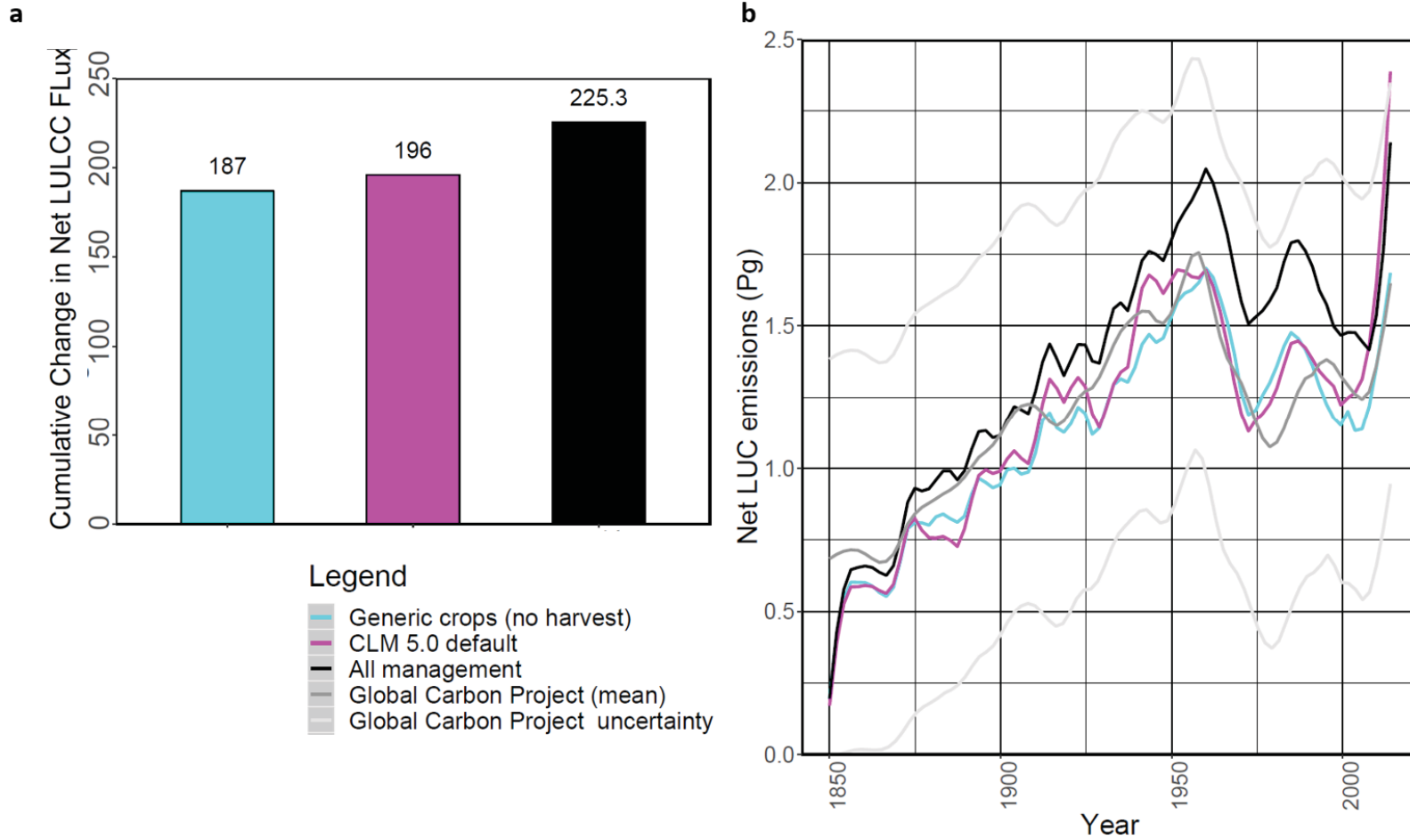
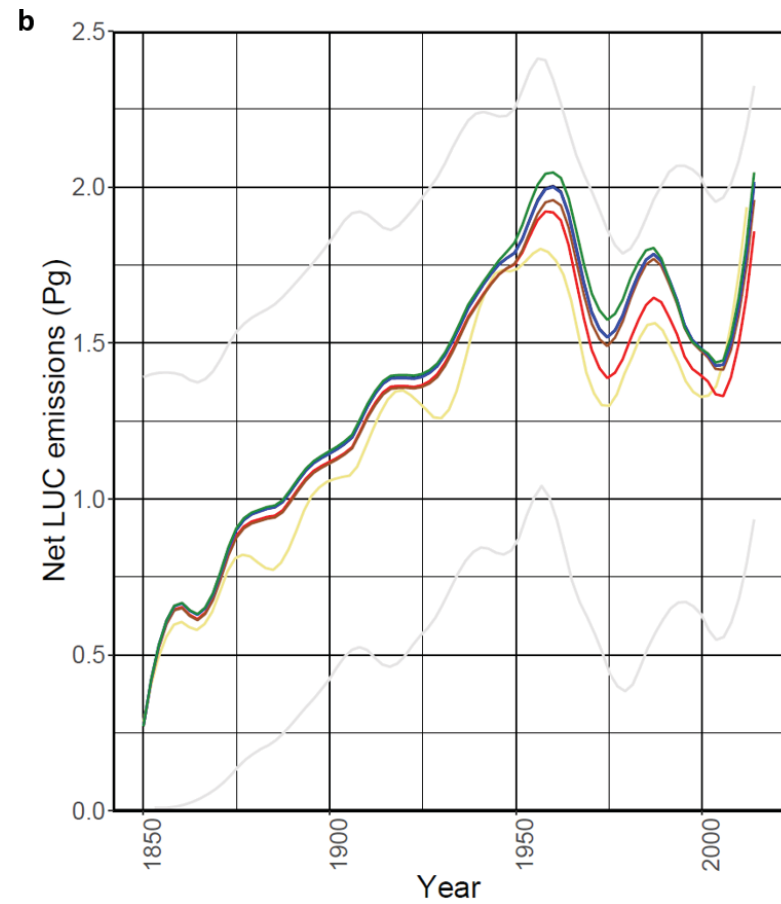
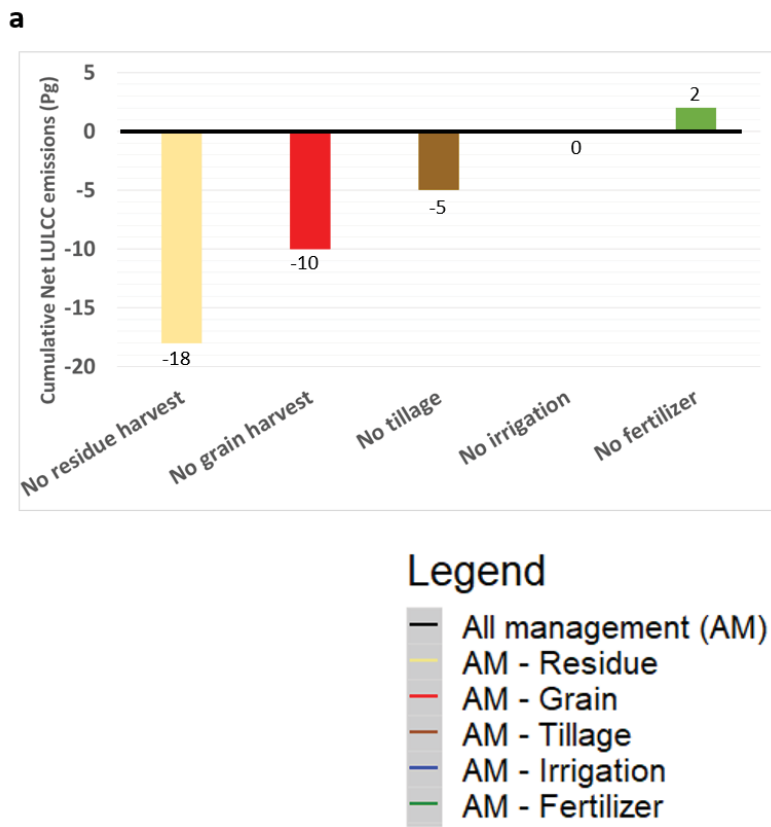


Figure 4-2. Plot (A) showing cumulative change in Net LULCC Flux for the five subtractive simulations of individual crop management practices relative to the full AM simulation over the historical time period (1850 – 2014). Plot (B) showing annual change in Net LULCC Flux for the full AM and five subtractive simulations of individual crop management practices over the historical time period.



Partitioning of Net LULCC Flux into Component Fluxes

The Net LULCC Flux can effectively be broken into components as the sum of Direct Flux and Indirect Flux minus growth in wood product C pools (GrowthProdC), as per Equation 4. The Direct LULCC Flux represents loss of carbon from ecosystems due to direct or instantaneous emissions during LULCC-induced deforestation, degradation, and harvest of wood products.

The quantity for the Direct Flux was constant across all simulations, and accounted for a cumulative total of 138.9 Pg C (0.84 Pg C/yr) of the total Net LULCC Flux (Figure 4-3). The proportion of the historical Net LULCC Flux attributable to the cumulative Direct LULCC Flux varied between simulations, and accounted for 74.3%, 70.9%, and 61.7% of the cumulative Net LULCC Flux for the GC, CLM5, and AM runs, respectively. Similarly, growth in the wood product pool (GrowthProdC) was constant across all simulations and represented a cumulative decrease in the Net LULCC Flux of 5.9 Pg C over the historical time period. Increases in the GrowthProdC are considered a decrease in emissions due to the fact that harvested wood products tend to decay relatively slowly over time and thus do not necessarily result in an instantaneous loss of C to the atmosphere. Geographically, the magnitude of the Direct Flux was highest in regions with high historical rates of land cover conversion from natural ecosystems, especially forests, to crops and pasture (Supplementary Figure S-11).

Differences in Net LULCC Flux between simulations were exclusively attributable and identical to changes in the Indirect LULCC Flux or “legacy flux” (i.e., changes in biospheric capacity to uptake carbon) among simulations, as demonstrated in Figure 4-3. The Indirect Flux was highest in the AM simulation, corresponding to a cumulative loss of C from ecosystems of 92.6 Pg C (41.1% of the Net LULCC Flux in the AM simulation) over the historical time period. Indirect LULCC Flux was lower and accounted for a smaller proportion of the Net LULCC Flux in each of the other primary simulations, which recorded losses of 53.0 Pg C (28.3% of Net LULCC Flux) for GC and 63.0 Pg C (32.1%) for CLM5. The geographic distribution of the Indirect Flux was similar to the Direct Flux, but the magnitude of localized differences between the three main simulations was more pronounced (Supplementary Figure S-12). In particular, the magnitude and areal extent of positive fluxes was higher in regions with larger proportional crop area for AM relative to the corresponding GC and CLM simulations.

Figure 4-3. Time-series plots of cumulative change in Net LULCC Flux and components fluxes (Direct, Indirect, GrowthProdC) over the historical time period (1850 – 2015) for the three main simulations: generic crops (GC) (A), CLM 5.0 default (CLM5) (B), and all management practices (AM) (C).

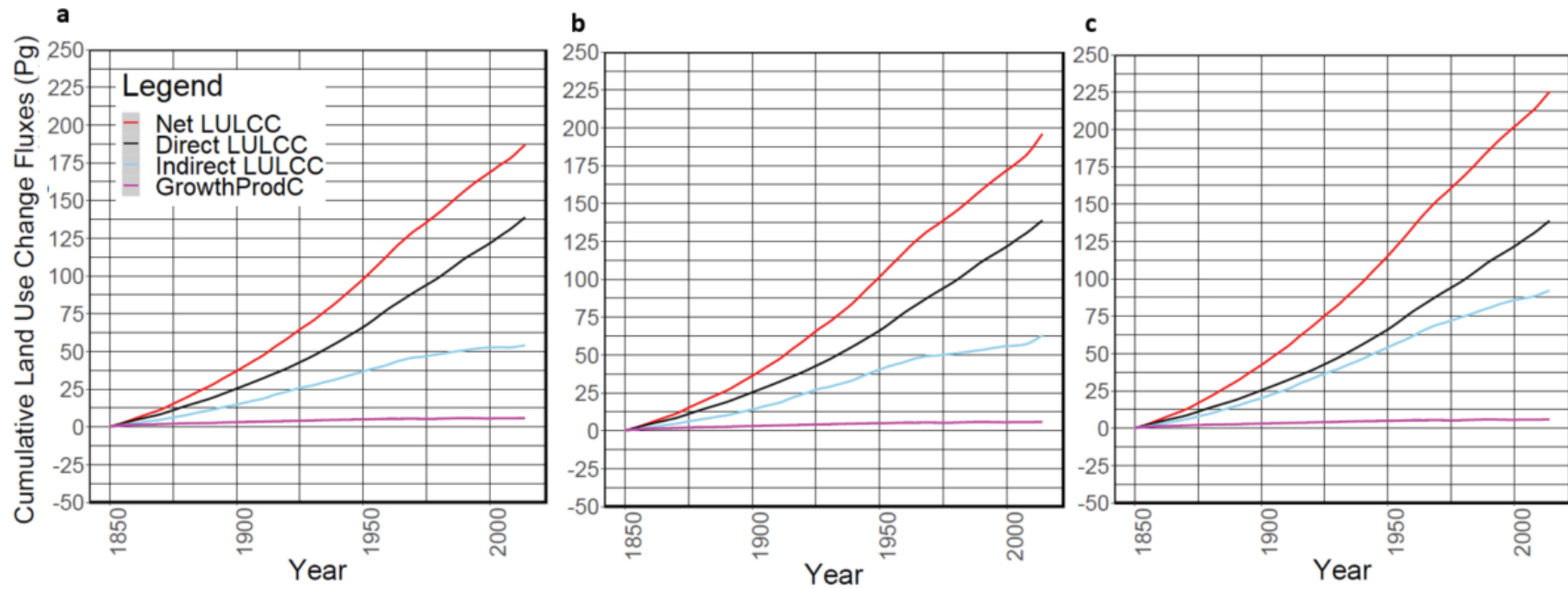
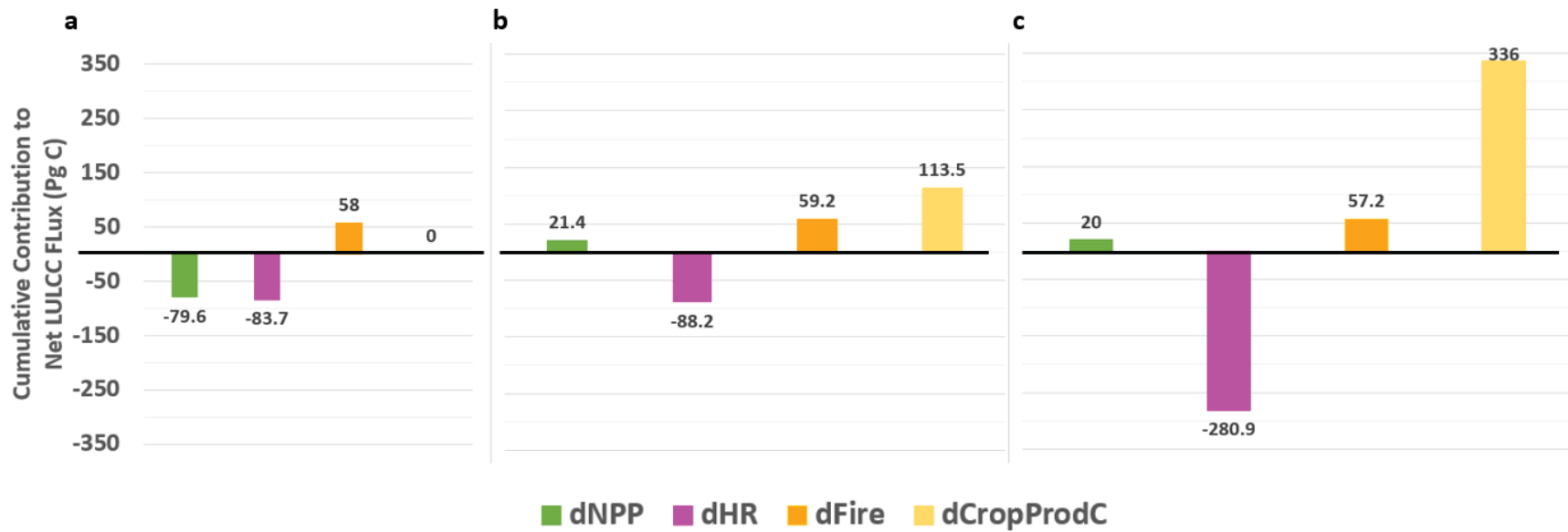


Figure 4-4. Bar plots showing the cumulative difference over the historical time period (1850 – 2015) for components of the Indirect Flux (Δ NPP, Δ HR, Δ Fire, Δ CropProdC) between LULCC on (LU) and LUC off (NOLU) runs of the three main simulations: generic crops (GC) (a), CLM 5.0 default (CLM5) (b), and all management practices (AM) (c).



Further partitioning of the Indirect Flux into its constituent parts (Equation 3) demonstrates that the net positive direction of the Indirect Flux in the two simulations with active crops (i.e., CLM 5 and AM) was mainly due to the removal of C from cropland ecosystems via harvest of grain and crop residues (Figure 4-4), which corroborates the importance of these individual management practices, as discussed in Section 3.2. The change in harvest losses ($\Delta\text{CropProdLoss}_{\text{LU-NOLU}}$) was 113.5 Pg C and 336 Pg C for the CLM5 and AM runs, respectively. By contrast, in the GC simulations the positive flux to the atmosphere was caused by differences in NPP (79.6 Pg C) between LU and NOLU runs ($\Delta\text{NPP}_{\text{LU-NOLU}}$).

Across all three main simulations, large positive fluxes to the atmosphere were partially counteracted by decreases in HR between LU and NOLU simulations ($\Delta\text{HR}_{\text{LU-NOLU}}$), though the magnitude of the $\Delta\text{HR}_{\text{LU-NOLU}}$ term varied substantially between GC (-83.7 Pg C), CLM5 (-88.2 Pg C), and AM (-280.9) simulations. Negative values for $\Delta\text{HR}_{\text{LU-NOLU}}$ in the AM simulations occurred despite increases in HR through accelerated decomposition of SOC due to intensive soil tillage. Comparison of AM with the AM-Tillage simulation shows that the magnitude of the negative cumulative flux for $\Delta\text{HR}_{\text{LU-NOLU}}$ would be larger by 3.4 Pg C if tillage were removed from the simulation (Supplementary Figure S-13), which was slightly less than the 5.3 Pg C reduction in the historical Net LULCC Flux obtained by subtracting tillage from the full AM simulation in Section 2.2. The additional difference between AM and AM-Tillage with respect to the Net LULCC Flux was due to reductions in NPP and in AM-Tillage simulation.

Analysis and Attribution of Changes in Soil Carbon Stocks

Cumulative losses in SOC were substantially higher for the AM simulation at -51.5 Pg C compared to losses of -12.7 and -18.2 Pg C for GC and CLM5 simulations, respectively (Figure 4-5). Losses in SOC stocks in all three simulations accelerated over time, but AM simulations had a much sharper decrease than the other simulations beginning in the 20th century.

The difference in SOC losses between simulations closely approximated changes in the Net LULCC Flux and Indirect Flux – declines in AM simulations were 38.8 Pg C higher than in GC, and 33.4 Pg C higher than CLM5. This was roughly equivalent to analogous disparities in Net Flux and Indirect Flux of 38.3 and 29.2 Pg C for the GC and CLM5 simulations, respectively.

Adding the full range of crop management practices altered the geographical distribution and local magnitude of SOC losses relative to simulations with CLM 5.0 defaults and generic crops (Figure 4-6). Previous work in CLM 5.0 has shown that some mid-latitude regions display net gains in SOC following LULCC to crops under CLM 5.0 defaults compared to GC simulations (Supplementary Figure S-14) (Lombardozzi et al., 2019). However, the implementation of crop management practices in the AM simulation largely eliminated this phenomenon, since virtually all cropped areas demonstrate losses in SOC following LULCC in the AM relative to CLM5 and GC simulations. Further, the difference in the magnitude of losses by location was higher in AM relative to both GC and CLM5 simulations, with some major crop production regions experiencing declines

of >75 Pg C per hectare, though the spatial distribution of this difference varied between GC and CLM5 simulations.

The impact of individual crop management practices on SOC stocks was similar to those on Net LULCC and Indirect Fluxes (Figure 4-7). Removing crop residue harvest from the AM simulation (AM – Residue) had the largest impact of changes in SOC stocks, reducing cumulative losses by 21.3 Pg C from -51.5 Pg C in AM to -30.2 Pg C in the AM – Residue simulation. This was followed by grain harvest (AM – Grain), which saw cumulative declines in SOC of -41.3 Pg C –10.2 Pg C less than the full AM simulation. Soil tillage moderated the SOC decrease by 4.8 Pg C (AM – Tillage = 46.7 Pg C), whereas the SOC changes attributable irrigation (AM – Irrigation) and fertilization (AM – Fertilizer) differed little from the full AM total of -51.5 Pg C at -51.4 and 53.3 Pg C, respectively. As with the three main simulations, variation in the magnitude of SOC losses for the subtractive simulations closely paralleled the corresponding changes in Net and Indirect LULCC Fluxes discussed in Section 3.2.

The geographical distribution of SOC decreases followed similar patterns for most individual management practices – the distribution of gains and losses associated with grain and residue harvest, tillage, and fertilizer was similar (Figure 4-8a-c,f), whereas irrigation demonstrated gains and losses depending on location (Figure 4-8d). The magnitude of localized declines in SOC largely followed the patterns described in the preceding paragraph, with more impactful practices showing higher losses at a given location.

Figure 4-5. Bar plot (A) showing cumulative change in soil organic carbon (SOC) between LULCC on (LU) and LUC off (NOLU) runs of the three main simulations over the historical time period (1850 – 2014). Line plot (B) shows the annual change in cumulative global SOC stocks between LU and NOLU runs of the three main simulations over the historical time period.

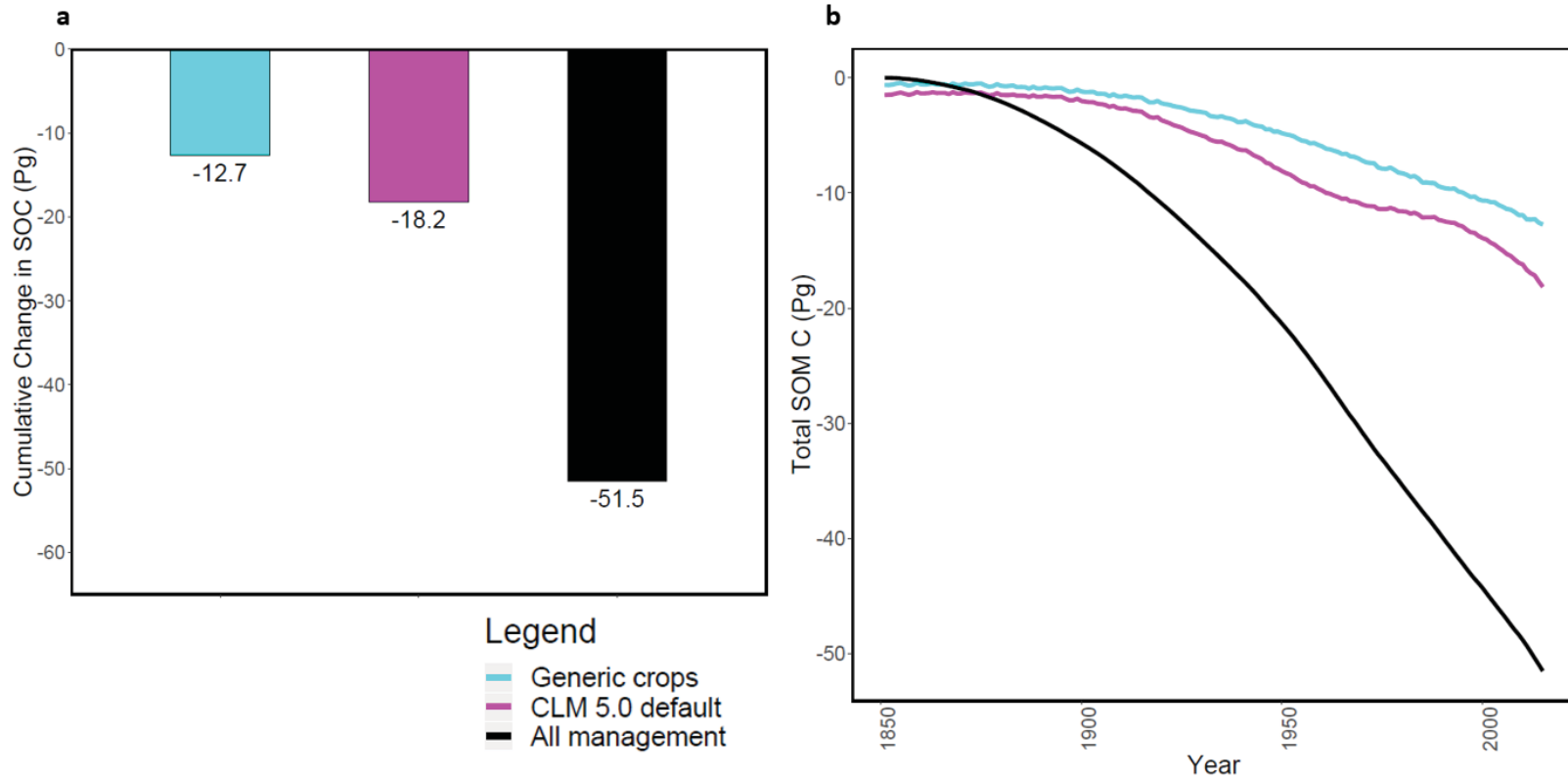


Figure 4-6. Geographical distribution of the cumulative difference in soil organic carbon (SOC) per hectare of cropland (Mg C/ha) over the historical time period (1850 – 2015) for all management minus generic crops (AM – GC) (A) and all management minus CLM 5.0 default (AM – CLM5) (B) simulations.

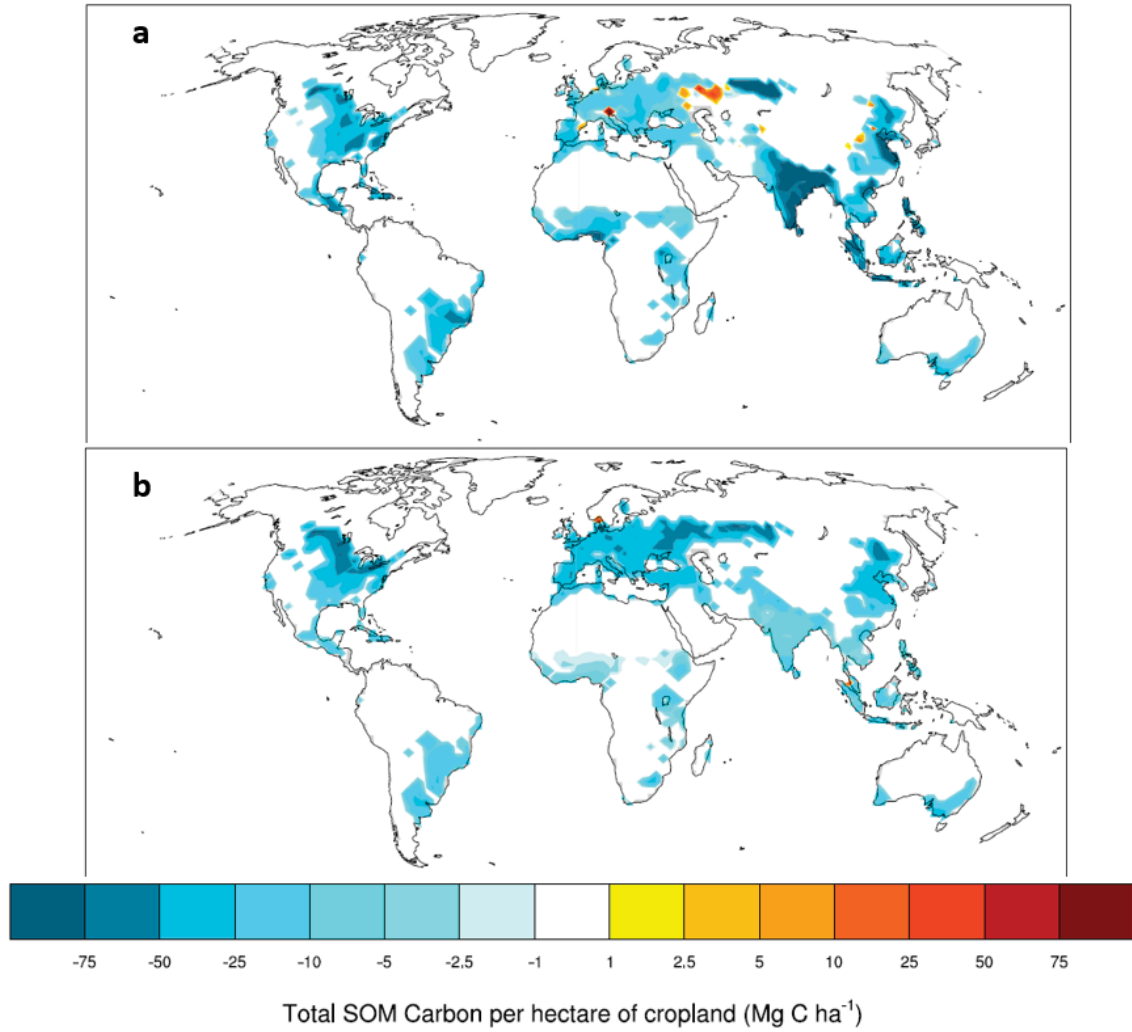


Figure 4-7. Plot (A) shows cumulative change in soil organic carbon (SOC) between LULCC on (LU) and LUC off (NOLU) runs of the AM simulation and five subtractive simulations over the historical time period (1850 – 2014). Plot (B) shows the associated annual change in cumulative global SOC stocks between LU and NOLU runs over the historical time period.

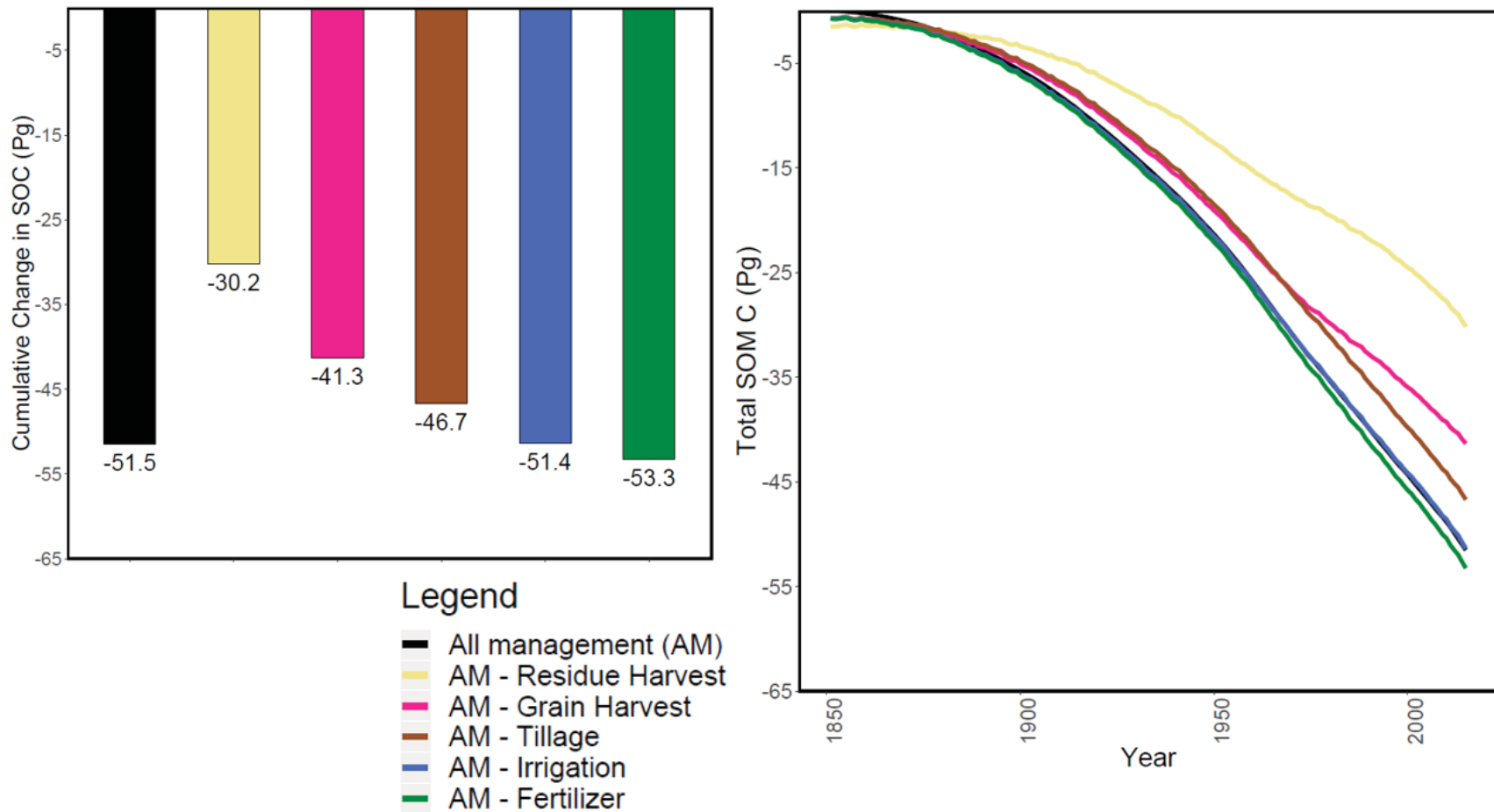
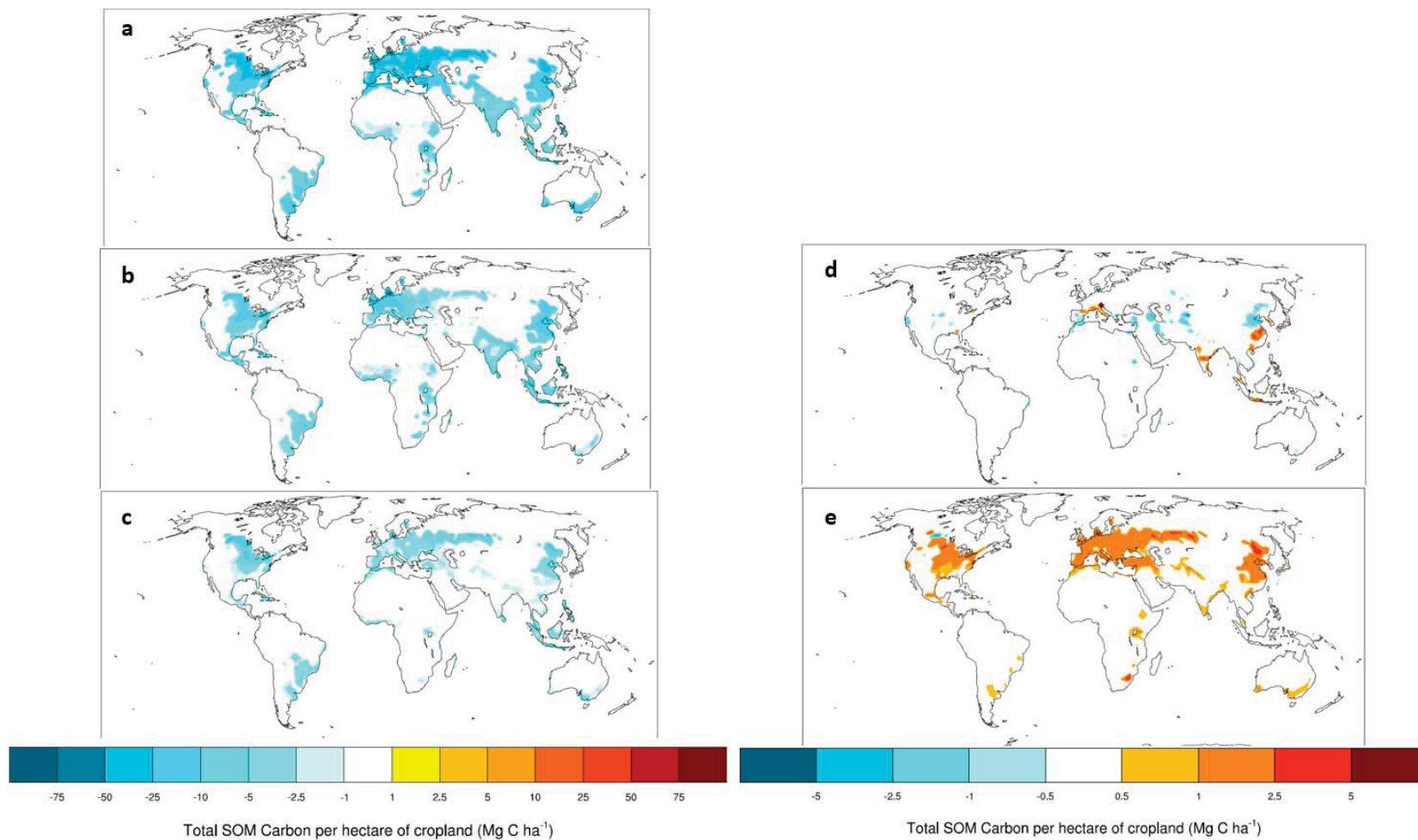


Figure 4-8. Geographical distribution of the cumulative difference in soil organic carbon (SOC) per hectare of cropland (Mg C/ha) over the historical time period (1850 – 2015) for all management (AM) simulations minus AM – Residue (A), AM – Grain Harvest (B), AM – Tillage (C), AM – Irrigation (D), and AM – Fertilizer (E). Note the different scale for AM – Irrigation and AM – Fertilizer plots.



Discussion

Analysis of Net LULCC Flux for Three Main Simulations

The magnitude of the cumulative historical Net LULCC Flux for simulations with the full range of crop management practices was higher by 29 – 38 Pg C (14 – 20%) compared to both simulations with generic crops and current CLM 5.0 default crop management practices (Figure 4-1a). Cumulative historical Net LULCC Flux for GC and CLM 5 simulations closely approximates the multi-model mean of 196 Pg C for 1850 – 2014 reported by Le Quéré et al. (2018), whereas the Net Flux for the AM simulations is higher but within the stated bounds of uncertainty for Net LULCC emissions (± 75 Pg C; ± 0.7 Pg C/yr) (Figure 4-1b). Although we simulate crop residue harvest and soil tillage in an idealized manner in this study, these results imply that the current version of CLM 5.0, as well as other ESMs in CMIP6 with limited crop management implementation, may be underestimating the cumulative historical Net LULCC Flux. Consequently, outputs of the forthcoming CMIP6 simulations and the associated Inter-governmental Panel on Climate Change reports on climate change may discount the role of land management activities and crop management in particular with respect to contributions to current emissions and options for climate change mitigation and adaptation. From a policy perspective, this could lead to inappropriate actions on climate change mitigation on agricultural land, as well as possibly underestimating the size of the residual land sink (Pugh et al., 2015; Arneeth et al., 2017).

Cumulative Net LULCC Flux in this study was higher in all simulations compared to results from an earlier version of the CLM (CLM 4-CN; CESM1.0), which found a Net Flux of 127 Pg C over the 1850 – 2005 period for simulations analogous to the GC simulations found here (Lawrence et al., 2018). The cumulative Net LULCC Flux was 174.7 Pg C (1.12 Pg C/yr) when computed over the same interval for the GC simulation in this study. Differences between results may be due in part to changes in model structure between CLM4-CN (CESM 1.0) and CLM5.0 (CESM 2.0), but may also be due to differences in climate forcing data, as recent work has shown that uncertainty among fluxes due to differences in forcing datasets may be substantial (Bonan et al., 2019).

The cumulative Net LULCC Flux in AM simulations matches closely with previous work using a similar analytical approach for crop and grazing management practices in the LPJ-GUESS ESM (Pugh et al., 2015). The foregoing research found a cumulative LULCC flux of 225 Pg C over the historical time period for simulations with multiple crop and grazing management practices activated over the 1850 - 2012 time period. Given the difference in models between CLM and LPJ-GUESS, the result of the LPJ-GUESS study is surprisingly close to the cumulative flux of 225.2 Pg C for the AM simulation reported in the present study. These results should be compared with caution, however, since the LPJ-GUESS study included grazing harvest, in addition to all crop management practices included in AM simulations for this study with the exception of fertilizer.

On an annual basis the Net LULCC Flux for all simulations stayed within the range of uncertainty reported by Le Quéré et al (2018) , with the exception of the 2010 – 2015 interval at the end of the CLM5 simulation, when LULCC emissions exceeded the

bounds of uncertainty due to large increases in Net LULCC Flux in 2010 and 2013 (Figure 1b). Increases in Net LULCC Flux in all three main simulation appear to be driven in part by increases in the Direct Flux (Supplementary Figure S-15) due to broad-scale deforestation in multiple regions (primarily in Southeast Asia, and Amazon and Congo Basins). Concomitant increases in wildfires and reductions in these regions (Supplementary Figure S-16) contributed to increases in the Indirect Flux and further increases in Net LULCC Flux for these years. Surprisingly, wildfires had a larger impact in the CLM5 simulation and also caused a reduction in NPP on croplands in the CLM5 (Supplementary Figure S-17), presumably because unharvested crop residue left in fields and previously higher crop productivity compared to AM simulations provided more fuel. An additional sharp increase in Net LULCC Flux at beginning of the simulation was likely due to the absence of crops being planted in the first year of the simulation (1850) due to model spinup conditions, and because not all crops complete their life cycle in the first year (1851) in which crops are planted in CLM. Two other major increases in Net LULCC Flux over the historical time period are attributable to widespread deforestation in India and Russia in mid-20th century, and in China during the 1980s (Lawrence et al., 2018).

Attributing Changes in Net LULCC Flux to Individual Crop Management Practices

Results of this study suggest that practices which remove biomass C from cropland ecosystems via harvest are the most important crop management practices in terms of driving changes in the historical LULCC flux. These results are largely in agreement with global studies regarding the effects of management activities on carbon cycling across multiple ecosystems, which attribute the majority of losses in carbon on croplands to harvest of crop products, as well as replacement of natural vegetation with lower productivity crop species (Haberl et al., 2007).

Although harvesting all aboveground biomass from crops globally, as implemented in the AM simulations, is extreme in intensity, multiple lines of evidence indicate that the amount of aboveground biomass removed from cropped areas in CLM 5.0 using default practices (i.e., CLM5 in this study) may be low relative to other estimates. Firstly, grain yields in the CLM tend to be low relative to those reported elsewhere, suggesting that the corresponding removal of grain C may also be underestimated (Lombardozi et al., 2019). Implementing the full range of crop management practices in this study reduced grain yields by 17% compared to the CLM 5.0 default simulations, with wheat and rice experiencing the largest yield decreases (Supplementary Figure S-18), but this effect was more than compensated for by residue harvest in the AM simulations. Presumably, grain yield reductions obtained in this study are attributable to decreases in N mineralization and availability associated with removal of litter and cumulative declines in SOC. Secondly, the implied harvest index (HI), which measures the proportion of grain product as a proportion of total aboveground crop biomass, is 28% according to calculations from the AM simulations. This value is low compared to HI values found in the literature for major crops, which typically fall in the 40-60% range (Wirsenius, 2000; Peng et al., 2018), and is well-below the HI of >70% implied by Haberl et al. (2007). Finally, CLM 5.0 default practices do not include any residue harvest which, though extreme in the AM simulations, is widely practiced in some regions, and is particularly intensive in

smallholder cropping systems in developing countries (Tittonell et al., 2015). Intensive residue harvest is also likely to be more prevalent in biofuel crop systems, and the importance of residue harvest highlighted here implies that future climate change mitigation efforts based on broad-scale LULCC conversion to crops for biofuel production need to be carefully assessed for their impacts on LULCC fluxes over long time frames (Creutzig et al., 2015; Harris et al., 2015; Qin et al., 2016).

The AM simulations with intensive tillage applied a relatively high multiplier to decomposition rates for SOC pools based on previous work in the DayCent crop model, so the changes attributable to tillage here are driven primarily by relatively large increases in HR due to accelerated decomposition of SOC and associated release of CO₂ on cropped areas. Increases in the Net LULCC Flux of 5.3 Pg C attributable to tillage found in the present study were lower than those found in the literature, despite simulating tillage as an increase in decomposition rates based on the high end of values found in the literature (Hartman et al., 2011). Levis et al. (2014) reported declines in SOC of 12 Pg C over 30 years and with constant crop area in CLM 4.5-BGC, while Pugh et al. (2015) found that tillage contributed to 18 Pg C of the cumulative historical Net LULCC Flux for the 1850 – 2012 time period. Computed over equivalent time intervals, changes in the LULCC flux due to tillage in this study are lower compared to the foregoing studies, indicating that the impact of tillage on LULCC flux may be overestimated elsewhere (Chapter 2, this document).

In contrast to the simplified, uniform representation of tillage and harvest practices in the AM simulations, crop irrigation and fertilization were simulated in detail using spatially explicit, transient data, and this research is among the first to assess the impacts of crop irrigation and fertilization on historical LULCC fluxes. Although these practices are an important driver of increases in crop grain yields over the historical time period (Lombardozzi et al., 2019), their impact on carbon cycling appears to be minimal, with irrigation in particular having close to net zero impact on historical fluxes. The relatively minor contribution of both irrigation and fertilization to changes in the LULCC flux is likely because these practices mainly influence crop productivity and biomass C, and all aboveground biomass from crops is harvested in the AM simulations. The negligible impact of irrigation may be due to variations in soil properties and changes in soil decomposition due to increased moisture, whereas the somewhat larger impact for fertilization may be related to unharvested gains in belowground crop productivity associated with fertilizer application.

Taken together these results imply that the true impact of crop management in terms of historical LULCC fluxes is likely to lie between the current state of the CLM, represented by the CLM5 simulation here, and the AM simulation, which is relatively extreme in terms of management intensity for multiple practices. This highlights the need for development of globally gridded datasets of multiple management practices, particularly residue management and tillage practices, which can be integrated into ESMs to more accurately capture spatial variability in residue management practices and their relative impact on historical LULCC fluxes and SOC stocks (Pongratz et al., 2018). Some progress has been made in this regard with respect to tillage intensity (Prestele et al.,

2018), but implementation of residue harvest in ESMs is likely to be hindered by lack of primary data from official statistics (Wirseniens et al., 2003; Pittelkow et al., 2015; FAOSTAT, 2015). Still, it may be possible to obtain national to regional scale estimates based on crude harvest factors (Erb et al., 2017).

Partitioning of Net LULCC Flux into Component Fluxes

Differences in the Net LULCC Flux between simulations were exclusively attributable to changes in the Indirect Flux or “legacy flux”, since the Direct Flux and growth in wood product pools were constant across simulations and did not contribute to differences reported here. Changes in the Indirect Flux were largely driven by losses from grain and residue harvest ($\Delta\text{CropProdC}_{\text{LU-NOLU}}$) that were somewhat compensated by reductions in $\Delta\text{HR}_{\text{LU-NOLU}}$, presumably due to replacement of high litterfall forests with crop systems where 100% of aboveground litter was removed via harvest. This outcome is somewhat expected given that 100% of aboveground biomass from crops is harvested in the AM simulation, leading to substantial reductions in the quantity of litter C entering cropland ecosystems, as well as a corresponding release of CO_2 to the atmosphere from harvested product pools. The importance of changes in litter inputs is supported by differences in $\Delta\text{HR}_{\text{LU-NOLU}}$ between simulations, since $\Delta\text{HR}_{\text{LU-NOLU}}$ was lowest for GC (-83.7 Pg C), where no harvest of grain or residue occurs. Removal of grain resulted in a further reduction of inputs to the litter pool in the CLM5 simulation ($\Delta\text{HR}_{\text{LU-NOLU}} = 88.2$ Pg C), while the removal of all potential aboveground inputs to the litter pool through residue harvest in the AM simulation resulted in a $\Delta\text{HR}_{\text{LU-NOLU}}$ of -280.9 Pg C.

The large decrease in $\Delta\text{HR}_{\text{LU-NOLU}}$ due to changes in litter inputs in the AM simulation occurred despite a simulated increase in HR due intensive tillage practices in the AM simulation, indicating that reductions in litter entering the soil pool are more important in terms of the aggregate impacts of components fluxes. However, simulations with intensive tillage removed from the full AM simulation (AM – Tillage) demonstrate that the decrease in $\Delta\text{HR}_{\text{LU-NOLU}}$ for AM simulations is slightly attenuated by increased HR on cropped areas due to intensive tillage, and that the magnitude of decreases in $\Delta\text{HR}_{\text{LU-NOLU}}$ would be larger in the absence of tillage practices (Supplementary Figure S-13).

A number of recent studies within the LULCC research community have emphasized the importance of the legacy flux (i.e., Indirect Flux) for estimating the LULCC flux and the global carbon budget, but few studies have explicitly examined the impact of the legacy flux within ESMs (Wesemael et al., 2010; Houghton et al., 2012; Pongratz and Caldeira, 2012; Pongratz et al., 2014). Although management practices implemented here are extreme for residue harvest and soil tillage, these findings are among the first to corroborate the importance of legacy fluxes in ESMs and their impact on the Net LULCC Flux, particularly on cropland, and portend that the legacy flux on cropped areas may be substantial (14 – 20% of cumulative LULCC flux, as discussed above).

Analysis and Attribution of Changes in Soil Carbon Stocks

Adding the full range of crop management practices in AM simulations increased cumulative SOC losses over the historical time period by 33.3 – 38.8 Pg C (Figure 4-5), and the magnitude of cumulative changes in SOC stocks between the three main

simulations emphasizes the importance of crop management practices to global SOC stocks, particularly given that SOC differences among simulations occur exclusively within cropped areas within the CLM. There was also a close connection between the legacy flux (i.e., Indirect Flux) and losses of SOC stocks, indicating that the legacy flux and losses of SOC in cropped areas may be an important and potentially underestimated term in the global carbon budget. Cumulative losses in the AM simulation over time showed a sharp decrease beginning at the end of the 19th century, presumably due to major increases in LULCC from natural vegetation to crops and concomitant changes in the quantity of carbon entering and leaving the SOC pools via crop management practices.

Implementation of the full range of crop management practices in AM simulations altered the geographical distribution and the magnitude of changes for specific locations relative to both the GC and CLM5 scenarios, and this effect depended on the scenario to which AM was compared. Including more crop management practices in AM also largely eliminated the uneven geographical distribution reported for previous work in CLM (Lombardozzi et al., 2019; Supplementary Figure S-14), since virtually all cropped areas showed declines in SOC per hectare compared to both GC and CLM5 simulations. Moreover, when examining LU simulations only over the historical time period, GC and CLM5 simulations showed a small decline in cumulative SOC stocks globally until approximately 1960 and then increased, resulting in a net accumulation of SOC for these simulations (Supplementary Figure S-19). By contrast, the AM scenario showed a steep decline in cumulative SOC stocks until the end of 20th century, then stabilized at a lower level for the remainder of the historical time period. This pattern suggests that SOC dynamics in the AM simulation may more closely match patterns of declines in cumulative SOC following LULCC to crops based on the literature (Guo and Gifford, 2002; Poeplau et al., 2011; Poeplau and Don, 2011), despite the extreme treatment of crop residue and tillage practices in AM simulation.

With some exceptions, the magnitude and distribution of associated changes in SOC per hectare agree reasonably well with a recent global analysis of SOC declines due to agricultural activity (Sanderman et al., 2017). However, Sanderman et al. (2017) did not distinguish between losses attributable to crop activities and those due to grazing, rendering direct comparisons with results from the current study difficult. The difference between the AM and GC simulation, however, was larger than the highest magnitude losses due to agricultural activities (>75 Mg/ha) in the preceding study for much of South Asia, as well portions of East Asia and the central Asian steppe region. The difference in SOC per hectare between AM and CLM5 simulations also exceeded these levels for some regions, but the overall distribution was more in line with those reported in the aforementioned study.

The geographical distribution of gains and losses in SOC was similar across multiple management practices, indicating that soils with high initial SOC contents tend lose more SOC (Supplementary Figure S-20), but may also have greater capacity to recoup these losses through changes in management (Stewart et al., 2008; Castellano et al., 2015). Indeed, gains and losses of SOC for subtractive simulations, where individual

management practices were removed from AM, follow nearly identical distributions for all management practices, with the exception of irrigation (Figure 4-8). Changes in SOC due to irrigation were concentrated in areas where the proportion of irrigated crops is relatively high, such as along the Nile River and parts of South and East Asia, but the direction of changes was mixed and appears to depend heavily on the specific location. This may result from differences in crop type, or variations in soil texture that affect decomposition rates through alterations in soil moisture. The mixed and geographically distinct distribution of irrigation may help explain why subtracting irrigation from the full AM simulation had minimal impact on cumulative fluxes and SOC stocks, since SOC increases in some irrigated areas are offset by decreases elsewhere.

As with the results for LULCC fluxes and cumulative global changes in SOC stocks, the magnitude of losses reported for many individual locations is likely to be at the extreme end of possible changes in SOC per hectare because of the simplistic and high intensity manner in which residue harvest and tillage were simulated. The true geographical distribution and associated magnitude of changes in SOC per hectare is likely to fall somewhere between those simulated in AM and CLM5 scenarios.

Conclusions

Continued exclusion of the full range of crop management practices from ESMs in CMIP6 is likely to lead to underestimation of the soil “legacy flux” and net LULCC flux, with broader consequences in relation to management activities on croplands for climate change mitigation and adaptation purposes. Grain and residue harvest were the individual management practices with the largest effect on LULCC fluxes and SOC stocks, while soil tillage also had a major impact, though neither tillage nor crop residue harvest are included as part of the Land Use Model Intercomparison Project. Inclusion of the full range of crop management resulted in a more realistic geographical distribution of SOC changes per hectare, and cumulative changes in SOC stocks over the historical time period. Crop residue harvest and soil tillage were simulated in a simplistic and high-intensity manner, so changes simulated here likely represent an extreme in terms of effects on LULCC fluxes and SOC stocks. The true extent of alterations in the global carbon budget due to crop management likely lies between those simulated with all crop management practices activated and those obtained from simulations using current CLM 5.0 defaults for crop management in this study. Inclusion and standardization of crop management practices across ESMs ought to lead to more accurate estimates of the overall Net LULCC Flux and reduce uncertainty in estimates thereof. Future work should focus on improving process-level understanding and inclusion of additional crop management practices into the land surface components of major ESMs to better capture the effects of crop management on global carbon cycles. To more accurately simulate the effects of crop residue harvest, future work should aim to develop globally gridded datasets for crop residue harvest, even if these are created at the national to regional scale using crude harvest factors (i.e., “simple implementation”, as described by Pongratz et al., 2018). Crop sub-models of ESMs should continue to focus on accurate simulation of grain yields as proportion of total biomass, not only from the perspective of crop production and global food security, but because harvested grain likely constitutes the largest removal of C from many cropland ecosystems. Soil tillage should be included in

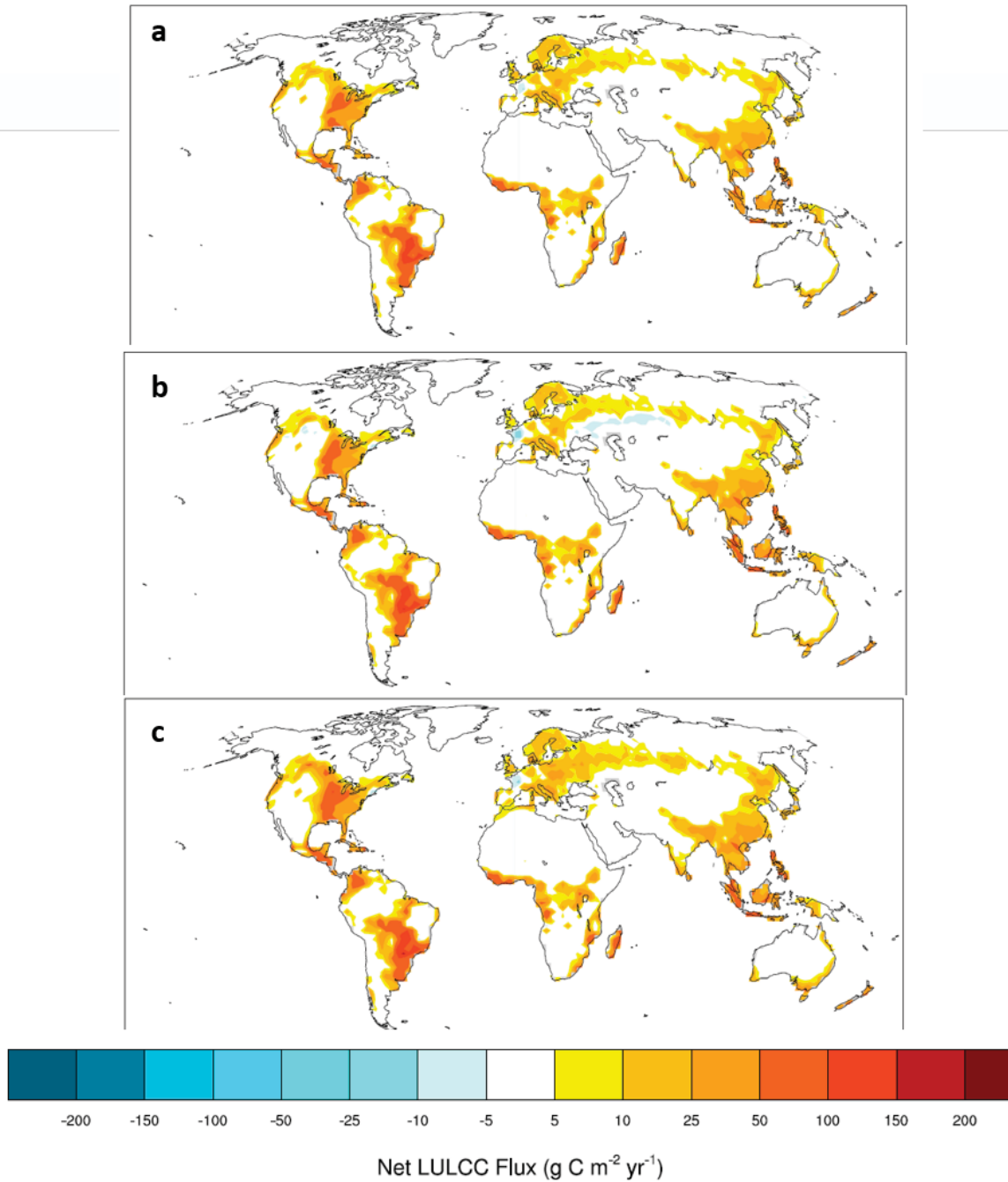
more ESMs, but future work ought to refine the simplistic representation of intensive tillage in this study, since the effects of tillage practices on SOC are more complex than mere changes in decomposition rates. Additionally, we did not assess the impact of replacing potential natural vegetation with crops, but productivity differences between natural vegetation and crop species may be another important source of LULCC-driven changes to LULCC fluxes and SOC.

Acknowledgments

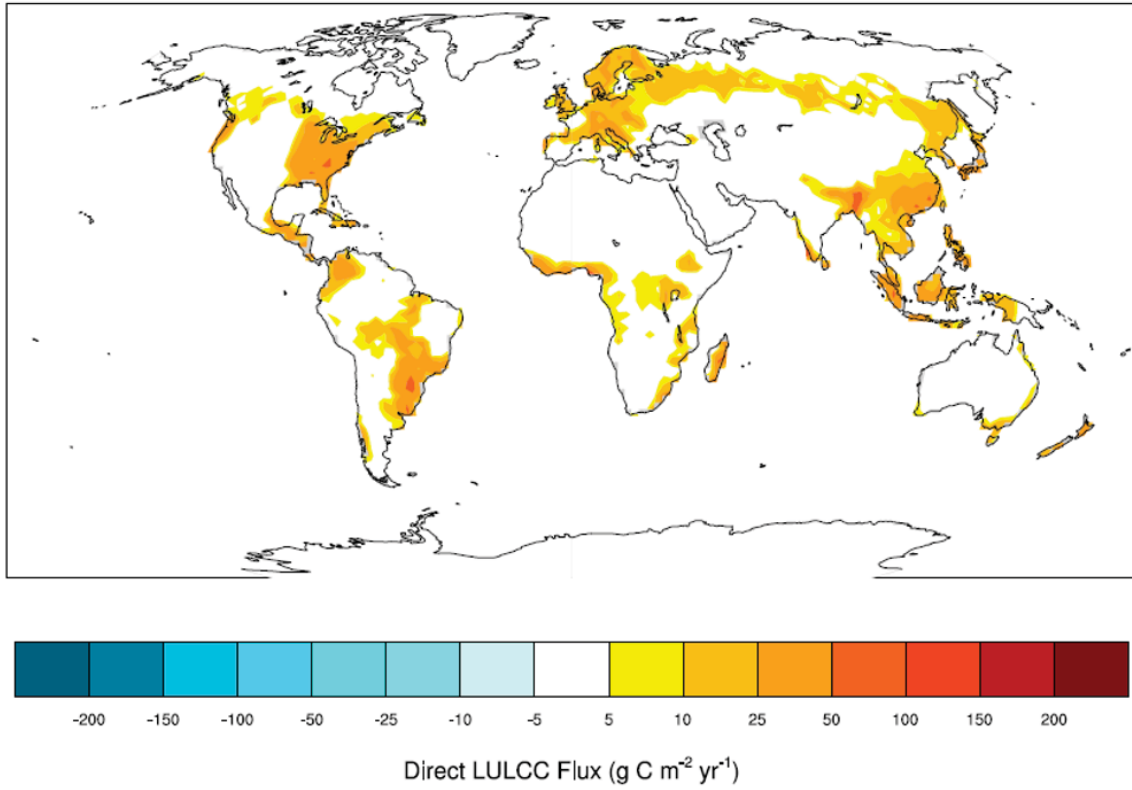
Joshua Rady provided feedback and assisted with implementation of code related to this research. Financial support for this research was provided in part by U.S. Dept. of Agriculture – National Institute of Food and Agriculture Project #2015-67003-23485, EASM-3: Decadal Prediction of Sustainable Agricultural and Forest Management.

Supplementary Information

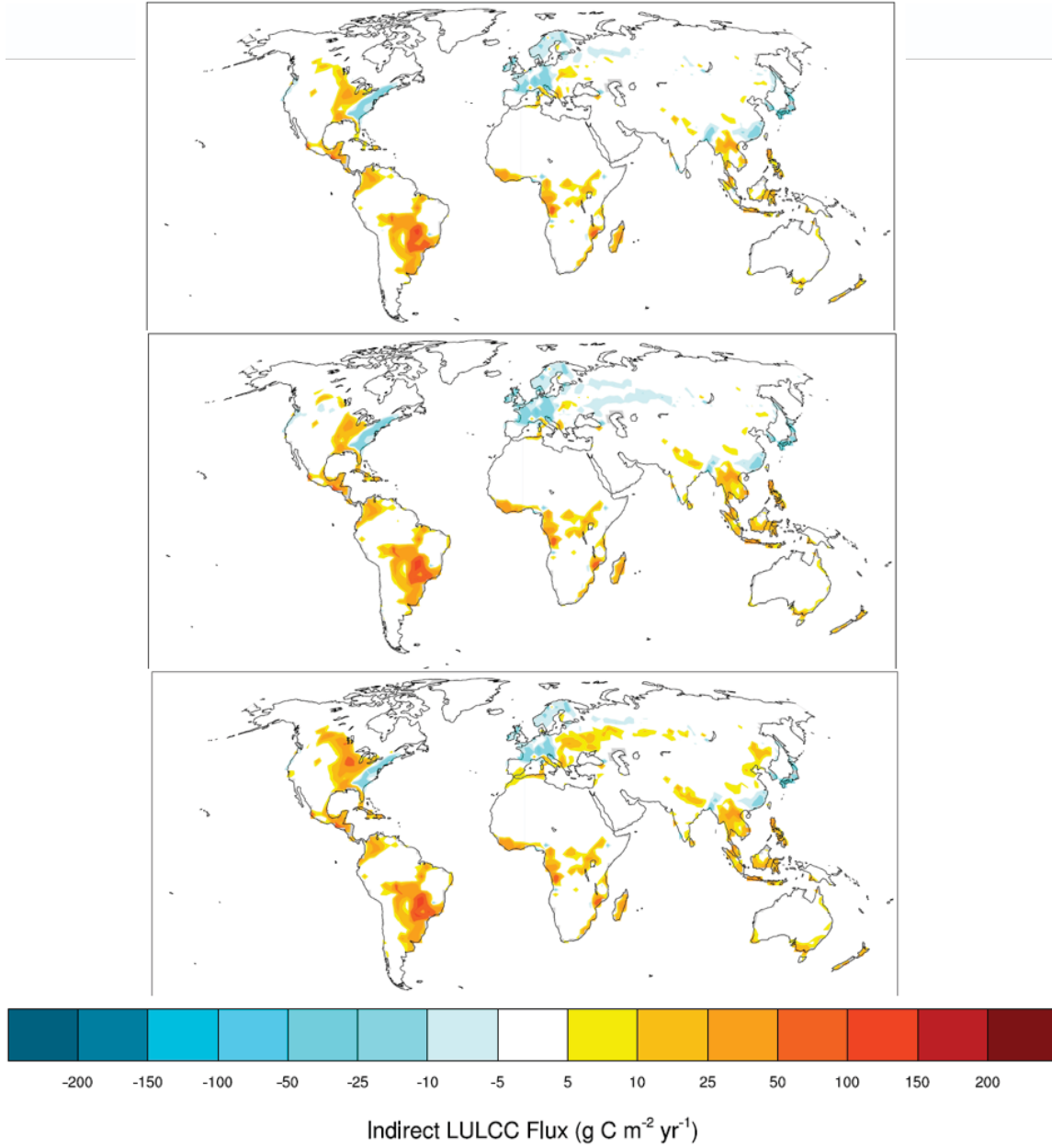
Supplementary Figure S-10. Spatial distribution of annual mean Net LULCC Flux ($\text{g C/m}^2/\text{yr}$) averaged over the historical time period (1850 – 2014) for the three main simulations: generic crops (GC) (A); CLM 5.0 default (CLM5) (B); all management practices (AM) (C).



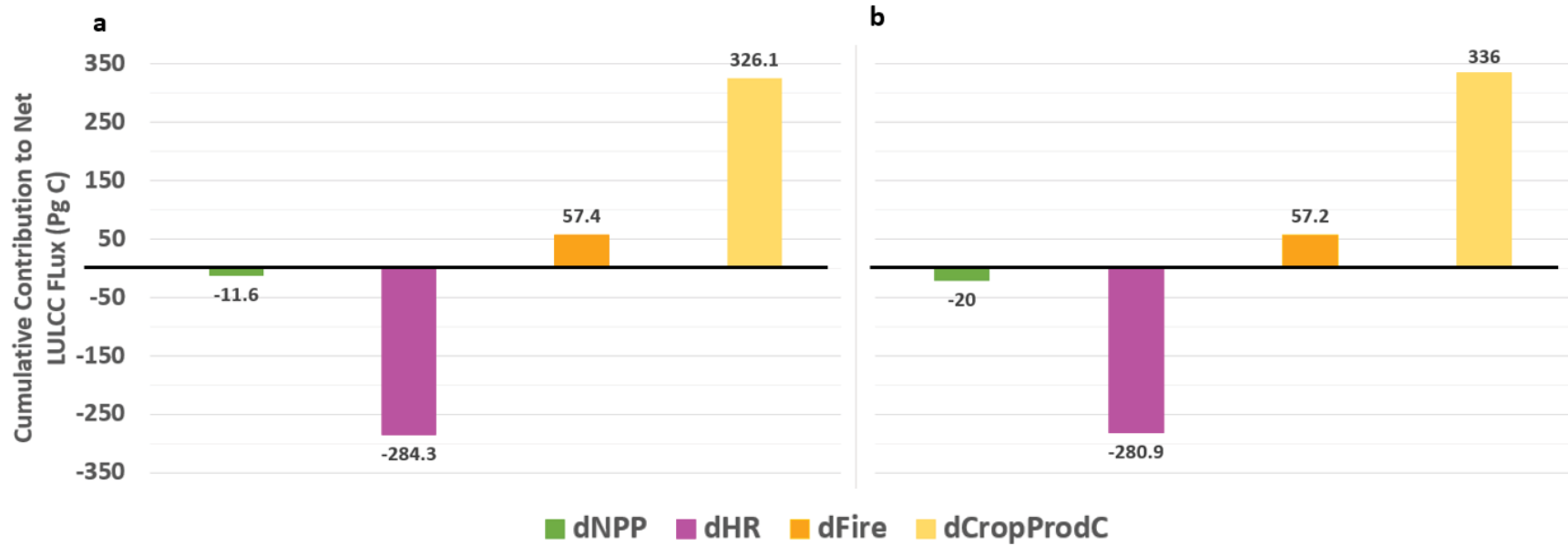
Supplementary Figure S-11. Spatial distribution of annual mean Direct LULCC Flux ($\text{g C/m}^2/\text{yr}$) averaged over the historical time period (1850 – 2014). The distribution and magnitude of the Direct Flux is identical across all simulations in this study.



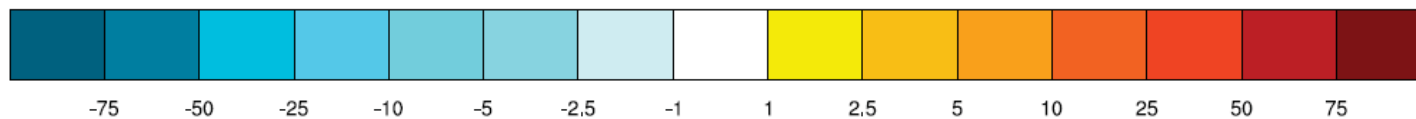
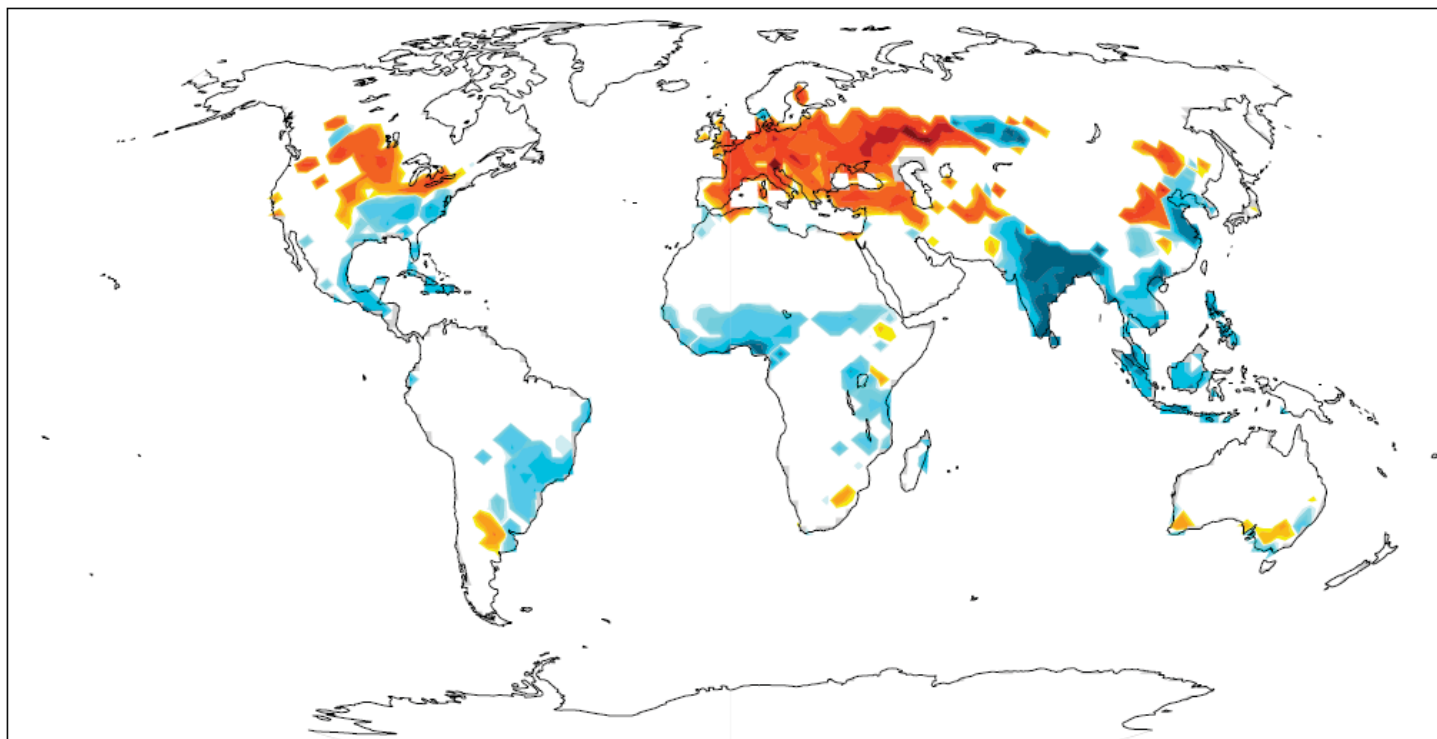
Supplementary Figure S-12. Geographical distribution of annual mean Indirect LULCC Flux ($\text{g C/m}^2/\text{yr}$) averaged over the historical time period (1850 – 2014) for the three main simulations: generic crops (GC) (A); CLM 5.0 default (CLM5) (B); all management practices (AM) (C).



Supplementary Figure S-13. Bar plots showing the cumulative difference over the historical time period (1850 – 2015) for components of the Indirect Flux (Δ NPP, Δ HR, Δ Fire, Δ CropProdC) between LULCC on (LU) and LUC off (NOLU) runs of two simulations: all management practices (AM) (A) and all management without tillage (AM – Tillage) (B).

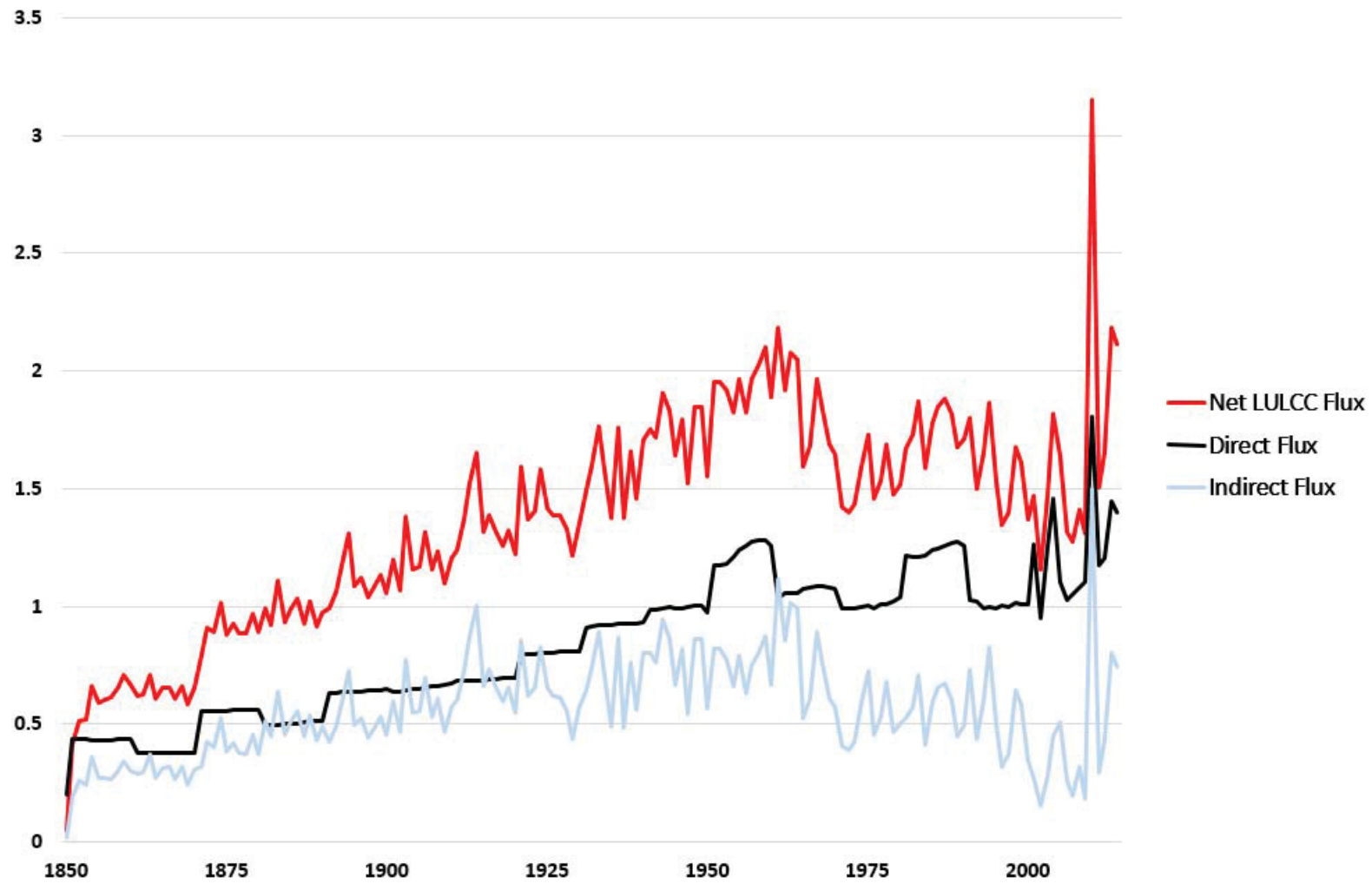


Supplementary Figure S-14. Geographical distribution of the cumulative difference in soil organic carbon (SOC) per hectare of cropland (Mg C/ha) over the historical time period (1850 – 2015) for CLM 5.0 default minus generic crops (CLM5 – GC) simulations.

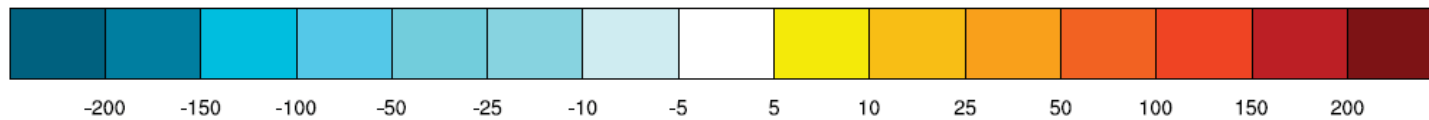
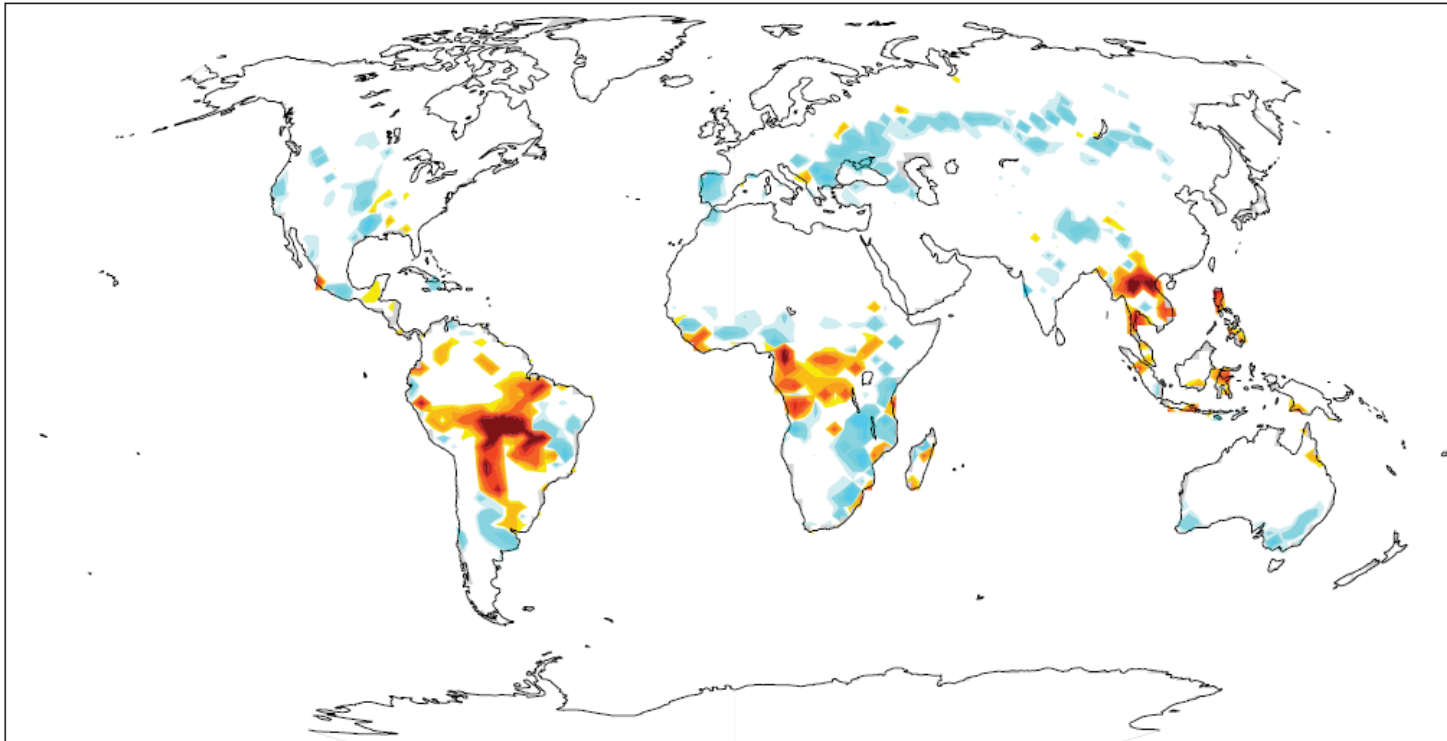


Total SOM Carbon per hectare of cropland (Mg C ha⁻¹)

Supplementary Figure S-15. Plot showing the annual change in Net LULCC Flux, Direct Flux, and Indirect Flux for the all management (AM) simulation over the historical time period (1850 – 2015).



Supplementary Figure S-16. Geographical distribution of annual mean flux due to wildfire ($\Delta\text{Fire}_{\text{LU-NOLU}}$) ($\text{g C/m}^2/\text{yr}$) averaged over the 2010 – 2015 time interval for the all management simulation.



Carbon Losses due to Wildfire ($\text{g C m}^{-2} \text{ yr}^{-1}$)

Supplementary Figure S-17. Plot showing the annual change in $\Delta HR_{LU-NOLU}$, $\Delta Fire_{LU-NOLU}$, $\Delta NPP_{LU-NOLU}$, and $\Delta CropProdC_{LU-NOLU}$ for the all management (AM) simulation over the historical time period (1850 – 2015).

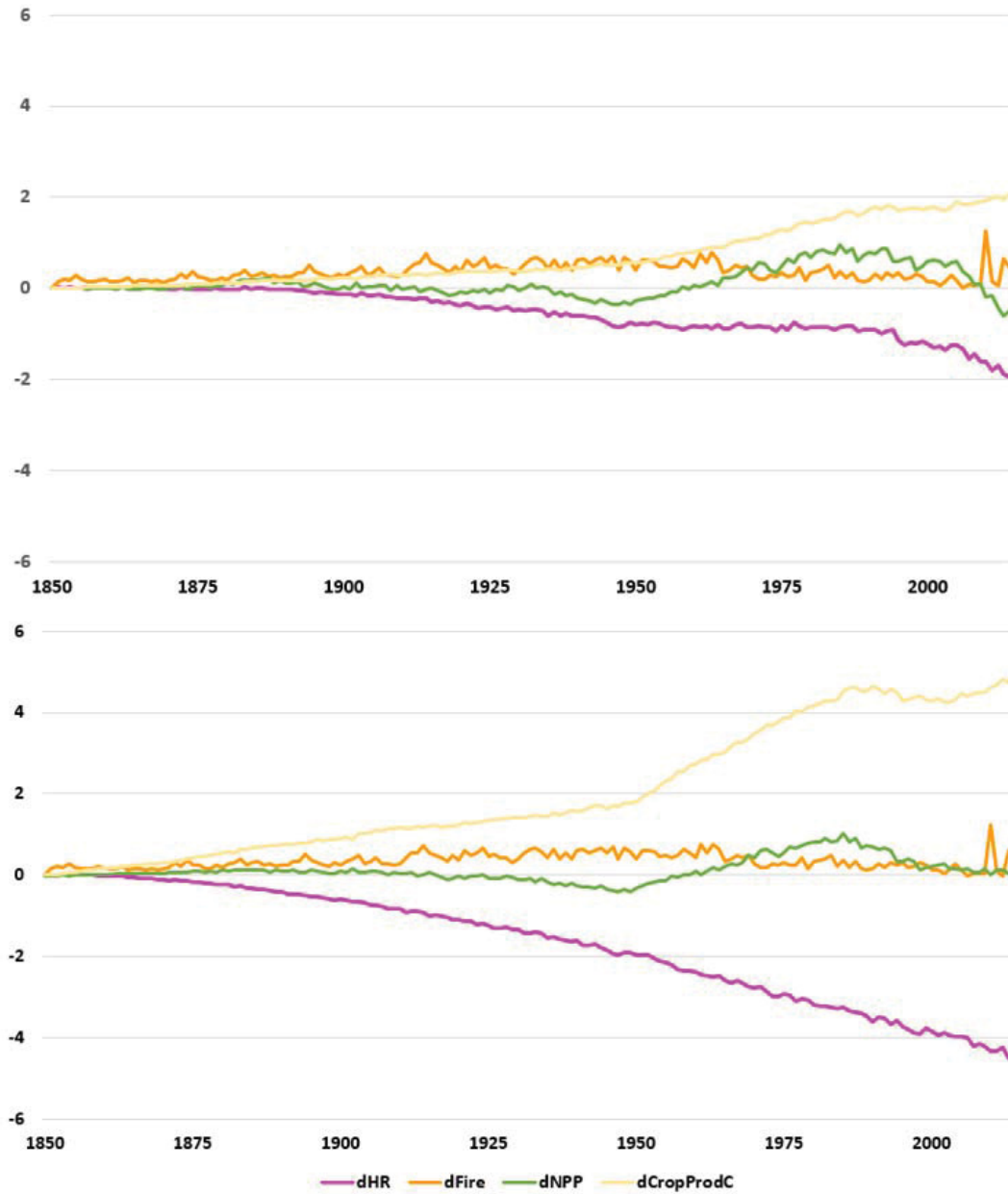
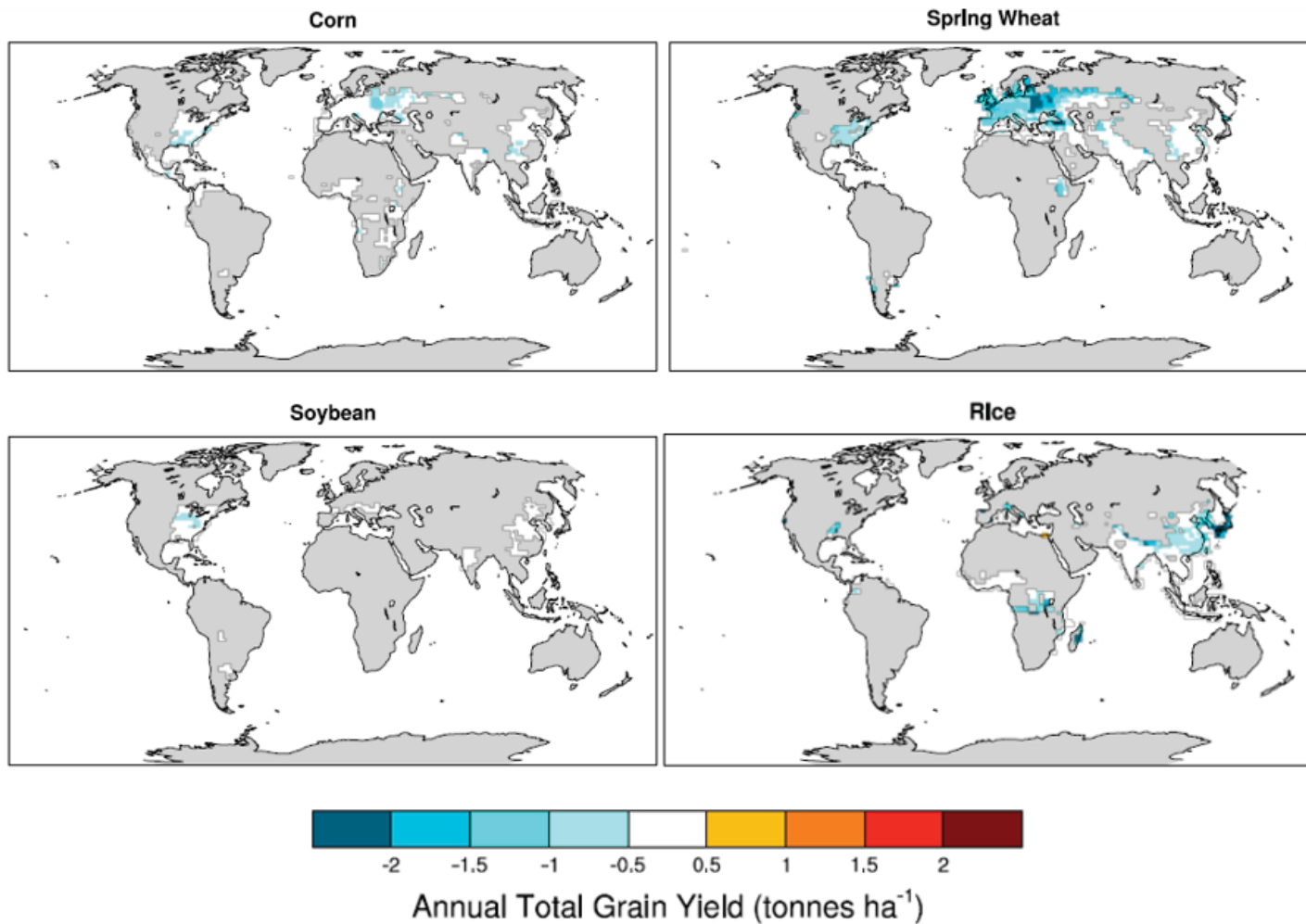
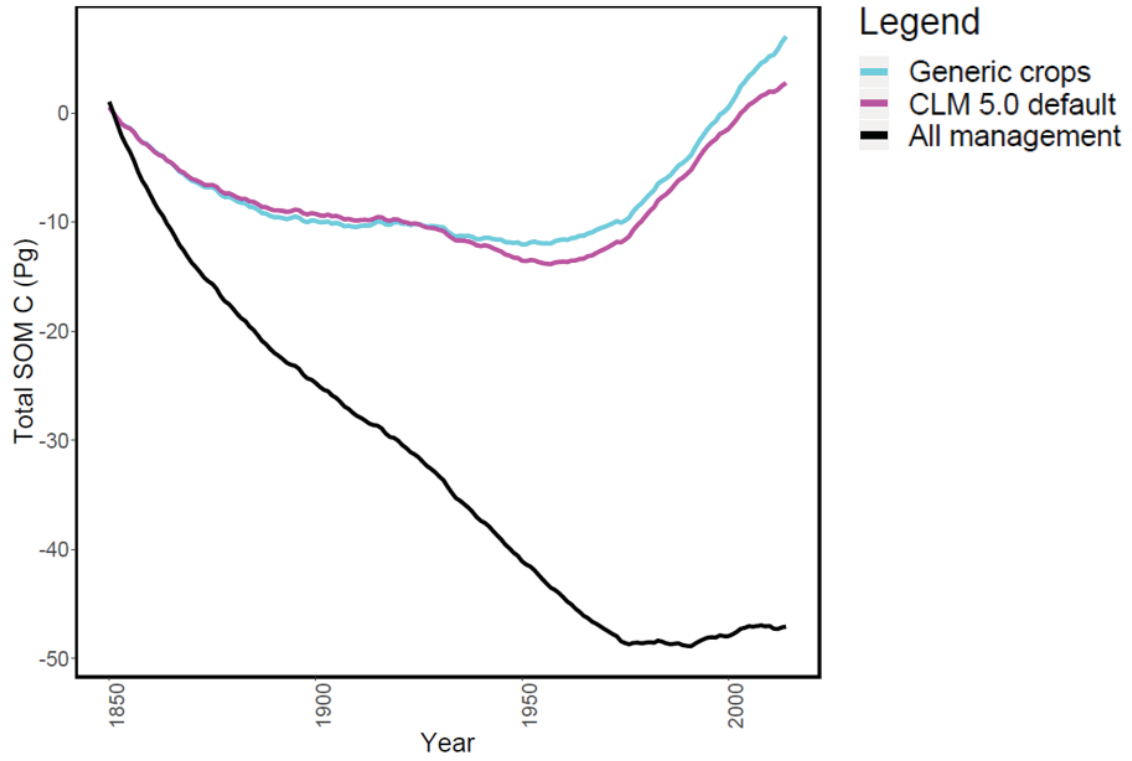


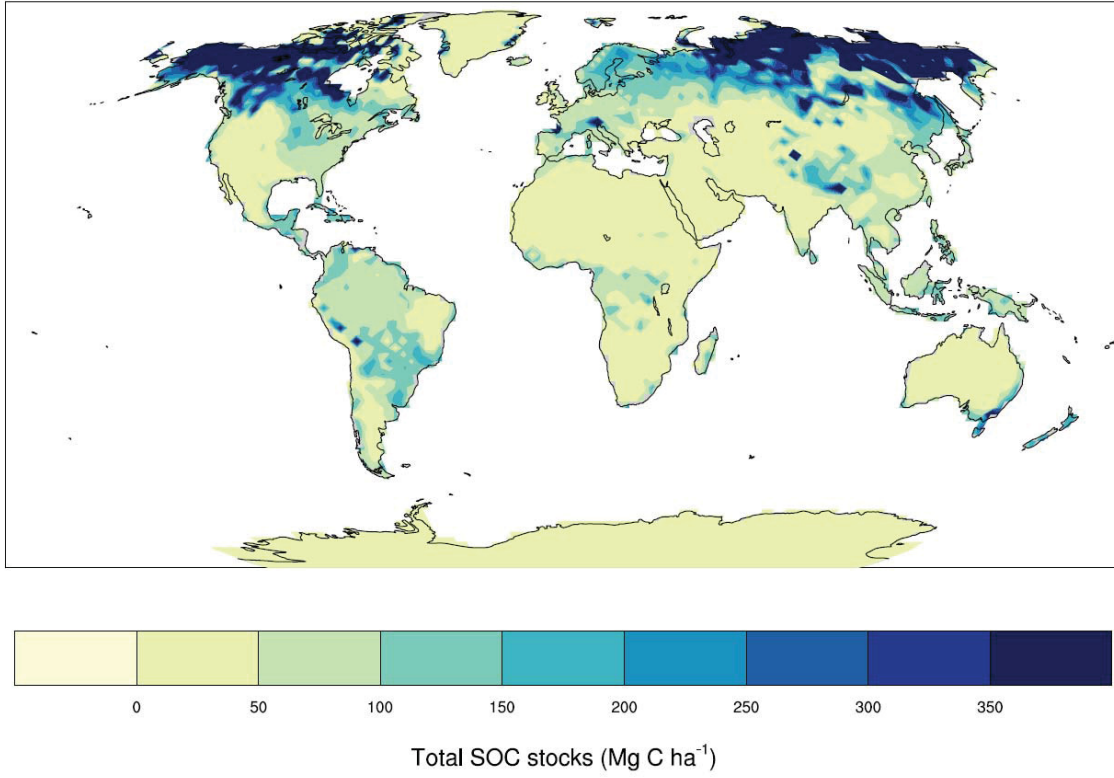
Figure S-18. Geographical distribution of the average difference in grain yields (tonnes/ha) for major cereal crops between the full management (AM) and CLM 5.0 default (CLM5) simulations for the 2000 – 2015 time interval. Grain yields for the 2000 – 2015 interval were used to capture the cumulative legacy effects of all crop management practices historically.



Supplementary Figure S-19. Plot showing the annual change in absolute cumulative global SOC stocks for LULCC on (LU) simulations only over the historical time period (1850 – 2015) for the three main simulations.



Supplementary Figure S-20. Map showing the initial distribution of average soil organic carbon stocks (Mg C/ha) in 1850 (i.e. prior to implementation of intensive tillage practices) for each individual grid cell in the Community Land Model.



CHAPTER 5. CONCLUSIONS AND RECOMMENDATIONS

Remote sensing of tillage and crop residue management practices

In the remote sensing study in this dissertation, the performance of the minimum Normalized Difference Tillage Index (minNDTI) method was below average compared to previous studies, despite using next generation sensors (Landsat 8 OLI and Sentinel-2A MSI) and standardized data procured from the NASA Harmonized Landsat 8 Sentinel-2 Project (HLS). Relatively poor performance of the minNDTI method was at least partially attributable to self-imposed methodological restrictions, but we found that it is still difficult to obtain good time-series cloud-free imagery at the beginning of the planting window, when tillage operations are performed. Combining Landsat 8 and Sentinel-2 raises new issues related to revisit frequency, which varies between 0-10 days, and makes obtaining a consistent a time-series more difficult (Li and Roy, 2017). These issues could be ameliorated once imagery from the Sentinel-2B sensor becomes available to provide a consistent 5-day revisit frequency for Sentinel-2, but the availability of Sentinel-2B will not resolve Sentinel-2A issues with data gaps and cloud masks for multiple scenes (Claverie et al., 2018).

Future work on mapping tillage and crop residue practices at broader scales using these sensors should be expanded to other locations and years (we focused on only a single location in this study). However, methods that can accurately map tillage without intensive field data collection and which can be extrapolated to different locations, as well as for different years at the same location, have not yet been developed (Zheng et al., 2014). Mapping tillage practices at scales useful as inputs for environmental and Earth system models, such as SWAT and CLM, will therefore require considerably more effort in terms of ground-truthing and coordination across multiple locations and years to obtain regional to national scale data on these practices. At present, the best option for inputs to environmental and Earth system models appears to be globally gridded data based on relatively crude national-level inventories of tillage practices (Prestele et al., 2018), the basis of which has been shown elsewhere to be unreliable in terms of accurately estimating crop residue cover and tillage intensity (Zheng et al., 2013a).

Soil carbon sequestration and climate change mitigation potential of ‘no-till’ adoption based on Earth system modeling

This study was among the first to assess the impacts of intensive tillage (IT) practices at the global scale using the land component of an Earth system model, and the first to examine adoption of NT practices globally within an ESM framework. We found that increases in SOC sequestration due to NT adoption for RCP 8.5 over the 2015 – 2100 interval ranged between 6.6 – 14.4 Pg C, and that accumulation of SOC following NT adoption depended heavily on magnitude of losses in the corresponding IT scenario over the historical time period (1850 – 2015). The gain in SOC under NT was equivalent to approximately one year of current emissions from fossil fuels, which is an order of

magnitude lower than targets set out by UNFCCC initiatives, such as ‘4 per 1000’. Adjusting for areas where NT has already been adopted had minimal impact on these numbers, presumably because NT is practiced on a very small fraction of cropland globally (<7%). The highest gains in SOC with NT adoption were heavily concentrated in temperate regions of developed countries, indicating any policy initiatives aimed at increasing SOC and mitigation should target these areas.

These results were largely in line with more recent field-research and analyses of NT impacts on SOC (Angers and Eriksen-Hamel, 2008; Powlson et al., 2014), which indicate that the capacity of NT to store additional SOC relative to intensive tillage is more limited than early studies indicated and optimistic policies might expect (Lal, 2004; Minasny et al., 2017; Baveye et al., 2018). Additionally, for the two scenarios in which NT was simulated, the gains in SOC from NT adoption were heavily concentrated in temperate latitudes, and in North America specifically. Simulated SOC sequestration due to NT on a per hectare basis in the ‘high’ scenario for this region was much larger than even the most optimistic reports from field studies of NT adoption in this region (Lal et al., 2015; Syswerda et al., 2011; Hollinger et al., 2005), indicating that the climate change mitigation potential of NT is likely to be closer to that of the “low” NT scenario. Since SOC gains in the NT scenarios were proportional to losses in the historical IT scenario, this could indicate that the historical losses attributable to IT and associated decomposition multipliers for the ‘high’ intensity scenario may also be unrealistic.

Given that there are multiple reasons to think results obtained in the study in Chapter 2 are optimistic, it seems unlikely that NT will represent a panacea for climate change mitigation purposes. Research should focus on additional management strategies with proven or more promising returns to SOC on agricultural land, such as cover crops or simply setting aside less profitable land (Brandes et al., 2015; Liebman and Schulte, 2015; Poeplau and Don, 2015).

Although this study points to a relatively small effect for both intensive and conservation tillage practices on SOC, tillage in this study was simulated in an idealized manner as merely a change in decomposition rates, whereas other studies have emphasized the complexity of processes governing SOC storage under different tillage practices. Accounting for these processes, such as NT and residue management impacts on albedo and soil water-holding capacity, is likely to lead to divergent changes in SOC depending on climate and other edaphic factors (Virto et al., 2012; Pittelkow et al., 2015). Future work should therefore seek to improve process-understanding of tillage and residue management practices and work toward implementation of these processes in existing ESMs to more accurately capture the true impact of tillage (Erb et al., 2017). However, simple or idealized implementation of tillage practices should be possible for most current generations ESMs (Pongratz et al., 2018), and should be included as a standard practice in future model intercomparison projects, such as the Land Use Model Intercomparison Project (LUMIP) (Lawrence et al., 2016). Minimally, it is hoped that this research will set the foundation for permanent inclusion of tillage as a standard management practice in future versions of the CLM.

Effects of including full range of crop management practices on LULCC emissions and SOC in the an Earth system model

The study in Chapter 3 was the first to implement the full range of crop management practices and examine their impacts on LULCC emissions and SOC in an ESM. We found that including the full range of management practices led to an increase in LULCC emissions of 29.2 – 38.3 Pg C over the historical time period (1850 – 2014), which represented an increase of 15-20% compared to simulations with generic crops and current CLM 5.0 defaults, respectively. This implies that ESMs that exclude important crop management practices from ESMs, including many of those contributing to Coupled Model Intercomparison Project 6 (CMIP6), may underestimate LULCC emissions, leading to underestimation of the corresponding residual land sink and inappropriate actions with respect to climate change mitigation and adaptation on croplands.

We found that crop residue harvest had the largest impact on LULCC emissions (18 Pg C), followed by grain harvest (9 Pg C), and soil tillage (5 Pg C). By contrast, the effects of irrigation and fertilization on the LULCC flux were minimal despite their importance to crop yields, presumably because all aboveground crop biomass was harvested in these simulations. All changes in cumulative LULCC Flux were attributable to the Indirect or “legacy” flux on cropped soils, and this research also contributes to a small but growing body evidence regarding the importance of the Indirect Flux or “legacy flux” due to crop and other land management activities on LULCC emissions (Wesemael et al., 2010; Houghton et al., 2012; Pongratz and Caldeira, 2012; Pongratz et al., 2014)

Although we simulated both crop residue harvest and tillage practices in an extreme and simplistic manner in this study, multiple lines of evidence indicate that the CLM, which currently only includes grain harvest, may be underestimating the importance of biomass C removals via crop harvest (Haberl et al., 2007; Lombardozzi et al., 2019). The true impact of crop management practices on emissions from LULCC is therefore likely between those simulated in simulations with all management practices activated and those simulated using CLM 5.0 default management practices. However, this work highlights the need to more accurately simulate the effects of crop residue and grain harvest by developing globally gridded datasets for crop residue harvest and improving grain yield simulations, even if gridded data for residue harvest rates are created at the national to regional scale using crude harvest factors (i.e., “simple implementation”, as described by Pongratz et al., 2018).

Changes in SOC due to implementation of the full range of crop management practices followed a similar pattern to those for LULCC emissions, as their inclusion reduced SOC stocks on croplands by 33 – 39 Pg C globally. Adding more crop management practices to the CLM resulted in net cumulative decreases in SOC for virtually all locations globally, whereas previous work has shown unexpected increases for some locations (Lombardozzi et al., 2019). Changes in SOC due to additional crop management practices were similar in magnitude to those found in a recent analysis on the historical impacts of agricultural globally for most locations, though the magnitude of losses exceeded those reported elsewhere for some locations. The temporal pattern of SOC

change over the historical time period for simulations with the full range of crop management practices also showed a more realistic pattern, as SOC stocks declined precipitously for much of the 20th century before stabilizing at a new, lower level (Guo and Gifford, 2002; Poeplau et al., 2011). By contrast, simulations with generic crops and CLM 5.0 default management practices showed an unexpected net accumulation in SOC over the same time period.

The effects of individual management practices on SOC were similar in magnitude to those reported for the LULCC Flux above, with crop product harvest and tillage having the largest impact on SOC stocks. The geographical distribution of gains and losses due to individual management practices was nearly identical for most management practices, as areas with high initial SOC contents tended to both lose and gain more SOC depending on the management practice. This phenomenon was also found in Chapter 2 with respect to adoption of NT practices, and implies that soils with high initial SOC prior to historical, intensive cropping practices may also have greater potential to gain SOC through changes in management (Stewart et al., 2008, Castellano et al., 2015).

Future work should focus on improving process-level understanding and seek to include the full range of crop management practices in major ESMs to better capture the effects of crop management on emissions from LULCC and management-induced changes in SOC. Crop modeling in ESMs should continue to focus on accurately simulating of grain yield, particularly since harvested grain is likely to represent the largest removal of C from many cropland ecosystems. Soil tillage is probably a small but still important contributor to changes in SOC and LULCC fluxes, and more research ought to refine its implementation in ESMs, as discussed in the preceding section. We did not assess the impact of replacing potential natural vegetation with crops, but productivity differences between natural vegetation and crop could be a major driver of changes in LULCC flux and SOC following land cover change (Haberl et al., 2007).

REFERENCES

- Abdalla, K., Chivenge, P., Ciais, P., & Chaplot, V. (2016). No-tillage lessens soil CO₂ emissions the most under arid and sandy soil conditions: results from a meta-analysis. *Biogeosciences*, 13(12), 3619–3633. <https://doi.org/10.5194/bg-13-3619-2016>
- Abdalla, M., Osborne, B., Lanigan, G., Forristal, D., Williams, M., Smith, P., & Jones, M. B. (2013). Conservation tillage systems: a review of its consequences for greenhouse gas emissions. *Soil Use and Management*, 29(2), 199–209. <https://doi.org/10.1111/sum.12030>
- Angers, D. A., & Eriksen-Hamel, N. S. (2008). Full-inversion tillage and organic carbon distribution in soil profiles: A meta-analysis. *Soil Science Society of America Journal*, 72(5), 1370–1374. <https://doi.org/10.2136/sssaj2007.0342>
- Arneth, A., Sitch, S., Pongratz, J., Stocker, B. D., Ciais, P., Poulter, B., et al. (2017). Historical carbon dioxide emissions caused by land-use changes are possibly larger than assumed. *Nature Geoscience*, 10(2), 79-+. <https://doi.org/10.1038/NGEO2882>
- Bagley, J. E., Miller, J., & Bernacchi, C. J. (2015). Biophysical impacts of climate-smart agriculture in the Midwest United States. *Plant, Cell & Environment*, 38(9), 1913–1930. <https://doi.org/10.1111/pce.12485>
- Bai, X., Huang, Y., Ren, W., Coyne, M., Jacinthe, P.-A., Tao, B., et al. (2019). Responses of soil carbon sequestration to climate-smart agriculture practices: A meta-analysis. *Global Change Biology*, 25(8), 2591–2606. <https://doi.org/10.1111/gcb.14658>
- Baveye, P. C., Berthelin, J., Tessier, D., & Lemaire, G. (2018). The “4 per 1000” initiative: A credibility issue for the soil science community? *Geoderma*, 309(Supplement C), 118–123. <https://doi.org/10.1016/j.geoderma.2017.05.005>
- Beeson, P. C., Daughtry, C. S. T., Hunt, E. R., Akhmedov, B., Sadeghi, A. M., Karlen, D. L., & Tomer, M. D. (2016). Multispectral satellite mapping of crop residue cover and tillage intensity in Iowa. *Journal of Soil and Water Conservation*, 71(5), 385–395. <https://doi.org/10.2489/jswc.71.5.385>
- Bernacchi, C. J., Hollinger, S. E., & Meyers, T. (2005). The conversion of the corn/soybean ecosystem to no-till agriculture may result in a carbon sink. *Global Change Biology*, 11(11), 1867–1872. <https://doi.org/10.1111/j.1365-2486.01050.x>
- Bonan, G. B., & Doney, S. C. (2018). Climate, ecosystems, and planetary futures: The challenge to predict life in Earth system models. *Science*, 359(6375), eaam8328. <https://doi.org/10.1126/science.aam8328>

- Bonan, G. B., Lombardozzi, D. L., Wieder, W. R., Oleson, K. W., Lawrence, D. M., Hoffman, F. M., & Collier, N. (2019). Model Structure and Climate Data Uncertainty in Historical Simulations of the Terrestrial Carbon Cycle (1850–2014). *Global Biogeochemical Cycles*, 0(ja).
<https://doi.org/10.1029/2019GB006175>
- Brandes, E., McNunn, G. S., Schulte, L. A., Bonner, I. J., Muth, D. J., Babcock, B. A., et al. (2016). Subfield profitability analysis reveals an economic case for cropland diversification. *Environmental Research Letters*, 11(1), 014009.
<https://doi.org/10.1088/1748-9326/11/1/014009>
- Cai, Z. (2019, January). Vegetation Observation in the Big Data Era: Sentinel-2 data for mapping the seasonality of land vegetation. Lund University, Faculty of Science, Department of Physical Geography and Ecosystem Science. Retrieved from
[https://portal.research.lu.se/portal/en/publications/vegetation-observation-in-the-big-data-era\(fb651a5f-5339-4644-b87e-4a51037b1da7\).html](https://portal.research.lu.se/portal/en/publications/vegetation-observation-in-the-big-data-era(fb651a5f-5339-4644-b87e-4a51037b1da7).html)
- Castellano, M. J., Mueller, K. E., Olk, D. C., Sawyer, J. E., & Six, J. (2015). Integrating plant litter quality, soil organic matter stabilization, and the carbon saturation concept. *Global Change Biology*, 21(9), 3200–3209.
<https://doi.org/10.1111/gcb.12982>
- Chang, K.-H., Warland, J., Voroney, P., Bartlett, P., & Wagner-Riddle, C. (2013). Using DayCENT to Simulate Carbon Dynamics in Conventional and No-Till Agriculture. *Soil Science Society of America Journal*, 77(3), 941–950.
<https://doi.org/10.2136/sssaj2012.0354>
- Ciais, P., Sabine, C., Bala, G., Bopp, L., Brovkin, V., Canadell, J., et al. (2013). Carbon and other biogeochemical cycles. *Climate change 2013: the physical science basis. Contribution of Working Group I to the Fifth Assessment Report of the Intergovernmental Panel on Climate Change*. Cambridge University Press Cambridge United Kingdom and New York NY USA, 465–570.
- Claverie, M., Ju, J., Masek, J. G., Dungan, J. L., Vermote, E. F., Roger, J.-C., et al. (2018). The Harmonized Landsat and Sentinel-2 surface reflectance data set. *Remote Sensing of Environment*, 219, 145–161.
<https://doi.org/10.1016/j.rse.2018.09.002>
- Corbeels, M., de Graaff, J., Ndah, T. H., Penot, E., Baudron, F., Naudin, K., et al. (2014). Understanding the impact and adoption of conservation agriculture in Africa: A multi-scale analysis. *Agriculture, Ecosystems & Environment*, 187, 155–170.
<https://doi.org/10.1016/j.agee.2013.10.011>
- Corbeels, M., Cardinael, R., Naudin, K., Guibert, H., & Torquebiau, E. (2019). The 4 per 1000 goal and soil carbon storage under agroforestry and conservation agriculture

- systems in sub-Saharan Africa. *Soil and Tillage Research*, 188, 16–26.
<https://doi.org/10.1016/j.still.2018.02.015>
- Creutzig, F., Ravindranath, N. H., Berndes, G., Bolwig, S., Bright, R., Cherubini, F., et al. (2015). Bioenergy and climate change mitigation: an assessment. *Global Change Biology Bioenergy*, 7(5), 916–944. <https://doi.org/10.1111/gcbb.12205>
- Daughtry, C. S. T. (2001). Discriminating crop residues from soil by shortwave infrared reflectance. *Agronomy Journal*, 93(1), 125–131.
<https://doi.org/10.2134/agronj2001.931125x>
- Daughtry, C. S. T., Hunt, E. R., Doraiswamy, P. C., & McMurtrey, J. E. (2005). Remote Sensing the Spatial Distribution of Crop Residues. *Agronomy Journal*; Madison, 97(3), 864–871. Retrieved from
<https://search.proquest.com/docview/194537112/citation/6D1B5527C2FD4670PQ/1>
- Daughtry, C. S. T., Graham, M. W., Stern, A. J., Quemada, M., Hively, W. D., & Russ, A. L. (2018). Landsat-8 and Worldview-3 Data for Assessing Crop Residue Cover. In *IGARSS 2018 - 2018 IEEE International Geoscience and Remote Sensing Symposium* (pp. 3844–3847).
<https://doi.org/10.1109/IGARSS.2018.8519473>
- Davin, E. L., Seneviratne, S. I., Ciais, P., Olioso, A., & Wang, T. (2014). Preferential cooling of hot extremes from cropland albedo management. *Proceedings of the National Academy of Sciences of the United States of America*, 111(27), 9757–9761. <https://doi.org/10.1073/pnas.1317323111>
- del Grosso, J. S., Parton, W. J., Mosier, A. R., Walsh, M. K., Ojima, D. S., & Thornton, P. E. (2006). DAYCENT National-Scale Simulations of Nitrous Oxide Emissions from Cropped Soils in the United States. *Journal of Environmental Quality*, 35(4), 1451–1460. <https://doi.org/10.2134/jeq2005.0160>
- Derpsch, R., Friedrich, T., Kassam, A., & Li, H. (2010). Current Status of Adoption of No-till Farming in the World and Some of its Main Benefits. *International Journal of Agricultural and Biological Engineering*, 3(1), 1–25.
<https://doi.org/10.25165/ijabe.v3i1.223>
- Dirmeyer, P. A., Dolman, A. J., & Sato, N. (1999). The Pilot Phase of the Global Soil Wetness Project. *Bulletin of the American Meteorological Society*, 80(5), 851–878. [https://doi.org/10.1175/1520-0477\(1999\)080<0851:TPPOTG>2.0.CO;2](https://doi.org/10.1175/1520-0477(1999)080<0851:TPPOTG>2.0.CO;2)
- Don, A., Schumacher, J., & Freibauer, A. (2011). Impact of tropical land-use change on soil organic carbon stocks - a meta-analysis. *Global Change Biology*, 17(4), 1658–1670. <https://doi.org/10.1111/j.1365-2486.2010.02336.x>

- Elzen, M. G. J. den, Fransen, T., Rogner, H. H., Luderer, G., Rogelj, J., Schaeffer, R., et al. (2013). The emissions gap report 2013 - A UNEP Synthesis Report. United Nations Environment Programme. Retrieved from <https://research.wur.nl/en/publications/the-emissions-gap-report-2013-a-unep-synthesis-report>
- Erb, K.-H., Luyssaert, S., Meyfroidt, P., Pongratz, J., Don, A., Kloster, S., et al. (2017). Land management: data availability and process understanding for global change studies. *Global Change Biology*, 23(2), 512–533. <https://doi.org/10.1111/gcb.13443>
- FAOSTAT (2015) Statistical Databases. Available at: <http://faostat.fao.org>
- Fujisaki, K., Perrin, A.-S., Desjardins, T., Bernoux, M., Balbino, L. C., & Brossard, M. (2015). From forest to cropland and pasture systems: a critical review of soil organic carbon stocks changes in Amazonia. *Global Change Biology*, 21(7), 2773–2786. <https://doi.org/10.1111/gcb.12906>
- Fujisaki, K., Chevallier, T., Chapuis-Lardy, L., Albrecht, A., Razafimbelo, T., Masse, D., et al. (2018). Soil carbon stock changes in tropical croplands are mainly driven by carbon inputs: A synthesis. *Agriculture, Ecosystems & Environment*, 259, 147–158. <https://doi.org/10.1016/j.agee.2017.12.008>
- Gassman, P., Reyes, M., Green, C., & Arnold, J. (2007). Soil and Water Assessment Tool: Historical Development, Applications, and Future Research Directions, The (Center for Agricultural and Rural Development (CARD) Publications). Center for Agricultural and Rural Development (CARD) at Iowa State University. Retrieved from <https://econpapers.repec.org/paper/iascpaper/07-wp443.htm>
- Guo, L. B., & Gifford, R. M. (2002). Soil carbon stocks and land use change: a meta analysis. *Global Change Biology*, 8(4), 345–360. <https://doi.org/10.1046/j.1354-1013.2002.00486.x>
- Haberl, H., Erb, K. H., Krausmann, F., Gaube, V., Bondeau, A., Plutzer, C., et al. (2007). Quantifying and mapping the human appropriation of net primary production in earth's terrestrial ecosystems. *Proceedings of the National Academy of Sciences*, 104(31), 12942–12947. <https://doi.org/10.1073/pnas.0704243104>
- Hansis, E., Davis, S. J., & Pongratz, J. (2015). Relevance of methodological choices for accounting of land use change carbon fluxes. *Global Biogeochemical Cycles*, 29(8), 1230–1246. <https://doi.org/10.1002/2014GB004997>
- Harris, Z. M., Spake, R., & Taylor, G. (2015). Land use change to bioenergy: A meta-analysis of soil carbon and GHG emissions. *Biomass and Bioenergy*, 82, 27–39. <https://doi.org/10.1016/j.biombioe.2015.05.008>

- Hartman, M. D., Merchant, E. R., Parton, W. J., Gutmann, M. P., Lutz, S. M., & Williams, S. A. (2011). Impact of historical land-use changes on greenhouse gas exchange in the. *Ecological Applications*, 21(4), 1105–1119.
- Hively, W. D., Lamb, B. T., Daughtry, C. S. T., Shermeyer, J., McCarty, G. W., & Quemada, M. (2018). Mapping Crop Residue and Tillage Intensity Using WorldView-3 Satellite Shortwave Infrared Residue Indices. *Remote Sensing*, 10(10), 1657. <https://doi.org/10.3390/rs10101657>
- Hollinger, S. E., Bernacchi, C. J., & Meyers, T. P. (2005). Carbon budget of mature no-till ecosystem in North Central Region of the United States. *Agricultural and Forest Meteorology*, 130(1–2), 59–69. <https://doi.org/10.1016/j.agrformet.2005.01.005>
- Houghton, R. A., & Nassikas, A. A. (2017). Global and regional fluxes of carbon from land use and land cover change 1850–2015. *Global Biogeochemical Cycles*, 31(3), 456–472. <https://doi.org/10.1002/2016GB005546>
- Houghton, R. A., House, J. I., Pongratz, J., van der Werf, G. R., DeFries, R. S., Hansen, M. C., et al. (2012). Carbon emissions from land use and land-cover change. *Biogeosciences*, 9(12), 5125–5142. <https://doi.org/10.5194/bg-9-5125-2012>
- Hurt, G. C., Chini, L. P., Frolking, S., Betts, R. A., Feddema, J., Fischer, G., et al. (2011). Harmonization of land-use scenarios for the period 1500–2100: 600 years of global gridded annual land-use transitions, wood harvest, and resulting secondary lands. *Climatic Change*, 109(1–2), 117–161. <https://doi.org/10.1007/s10584-011-0153-2>
- Jain, A. K., West, T. O., Yang, X., & Post, W. M. (2005). Assessing the impact of changes in climate and CO₂ on potential carbon sequestration in agricultural soils. *Geophysical Research Letters*, 32(19). <https://doi.org/10.1029/2005GL023922>
- Lal, R. (2003). Global potential of soil carbon sequestration to mitigate the greenhouse effect. *Critical Reviews in Plant Sciences*, 22(2), 151–184. <https://doi.org/10.1080/713610854>
- Lal, R. (2004). Soil carbon sequestration to mitigate climate change. *Geoderma*, 123(1), 1–22. <https://doi.org/10.1016/j.geoderma.2004.01.032>
- Lal, R., Reicosky, D. C., & Hanson, J. D. (2007). Evolution of the plow over 10,000 years and the rationale for no-till farming. *Soil and Tillage Research*, 93(1), 1–12. <https://doi.org/10.1016/j.still.2006.11.004>
- Lal, Rattan. (2015). Sequestering carbon and increasing productivity by conservation agriculture. *Journal of Soil and Water Conservation*, 70(3), 55A–62A. <https://doi.org/10.2489/jswc.70.3.55A>

- Lawrence, D. M., Hurtt, G. C., Arneeth, A., Brovkin, V., Calvin, K. V., Jones, A. D., et al. (2016). The Land Use Model Intercomparison Project (LUMIP) contribution to CMIP6: rationale and experimental design. *Geoscientific Model Development*, 9(9), 2973–2998. <https://doi.org/10.5194/gmd-9-2973-2016>
- Lawrence, P. J., Lawrence, D. M., & Hurtt, G. C. (2018). Attributing the Carbon Cycle Impacts of CMIP5 Historical and Future Land Use and Land Cover Change in the Community Earth System Model (CESM1). *Journal of Geophysical Research: Biogeosciences*, 123(5), 1732–1755. <https://doi.org/10.1029/2017JG004348>
- Le Quéré, C. Andrew, R. M., Friedlingstein, P., Sitch, S., Hauck, J., Pongratz, J., et al. (2018). Global Carbon Budget 2018. *Earth System Science Data (Online)*, 10(4). <https://doi.org/10.5194/essd-10-2141-2018>
- Leite, L. F. C., Mendonca, E. D., Machado, P., Fernandes, E. I., & Neves, H. C. L. (2004). Simulating trends in soil organic carbon of an Acrisol under no-tillage and disc-plow systems using the Century model. *Geoderma*, 120(3–4), 283–295. <https://doi.org/10.1016/j.geoderma.2003.09.010>
- Levis, S., Hartman, M. D., & Bonan, G. B. (2014). The Community Land Model underestimates land-use CO₂ emissions by neglecting soil disturbance from cultivation. *Geoscientific Model Development*, 7(2), 613–620. <https://doi.org/10.5194/gmd-7-613-2014>
- Levis, Samuel, Bonan, G. B., Kluzek, E., Thornton, P. E., Jones, A., Sacks, W. J., & Kucharik, C. J. (2012). Interactive Crop Management in the Community Earth System Model (CESM1): Seasonal Influences on Land-Atmosphere Fluxes. *Journal of Climate*, 25(14), 4839–4859. <https://doi.org/10.1175/JCLI-D-11-00446.1>
- Li, J., & Roy, D. P. (2017). A Global Analysis of Sentinel-2A, Sentinel-2B and Landsat-8 Data Revisit Intervals and Implications for Terrestrial Monitoring. *Remote Sensing*, 9(9), 902. <https://doi.org/10.3390/rs9090902>
- Liebman, M., & Schulte, L. A. (2015). Enhancing agroecosystem performance and resilience through increased diversification of landscapes and cropping systems. *Elem Sci Anth*, 3(0), 000041. <https://doi.org/10.12952/journal.elementa.000041>
- Lipper, L., McCarthy, N., Zilberman, D., Asfaw, S., & Branca, G. (2018). Climate smart agriculture: building resilience to climate change. *Natural Resource Management and Policy (USA) Eng No. 52*. Retrieved from <http://agris.fao.org/agris-search/search.do?recordID=XF2018001082>
- Lombardozi, D. L., Bonan, G. B., Levis, S., & Lawrence, D. M. (2018). Changes in Wood Biomass and Crop Yields in Response to Projected CO₂, O₃, Nitrogen

- Deposition, and Climate. *Journal of Geophysical Research: Biogeosciences*, 123(10), 3262–3282. <https://doi.org/10.1029/2018JG004680>
- Lugato, E., Bampa, F., Panagos, P., Montanarella, L., & Jones, A. (2014). Potential carbon sequestration of European arable soils estimated by modelling a comprehensive set of management practices. *Global Change Biology*, 20(11), 3557–3567. <https://doi.org/10.1111/gcb.12551>
- Lugato, E., Leip, A., & Jones, A. (2018). Mitigation potential of soil carbon management overestimated by neglecting N₂O emissions. *Nature Climate Change*, 8(3), 219–223. <https://doi.org/10.1038/s41558-018-0087-z>
- Luo, Z., Wang, E., & Sun, O. J. (2010). Can no-tillage stimulate carbon sequestration in agricultural soils? A meta-analysis of paired experiments. *Agriculture Ecosystems & Environment*, 139(1–2), 224–231. <https://doi.org/10.1016/j.agee.2010.08.006>
- Luysaert, S., Jammot, M., Stoy, P. C., Estel, S., Pongratz, J., Ceschia, E., et al. (2014). Land management and land-cover change have impacts of similar magnitude on surface temperature. *Nature Climate Change*, 4(5), 389–393. <https://doi.org/10.1038/nclimate2196>
- Mandanici, E., & Bitelli, G. (2016). Preliminary Comparison of Sentinel-2 and Landsat 8 Imagery for a Combined Use. *Remote Sensing*, 8(12), 1014. <https://doi.org/10.3390/rs8121014>
- Manies, K., Harden, J., Kramer, L., & Parton, W. (2000). Parameterizing Century to model cultivated and noncultivated sites in the loess region of western Iowa.
- McDermid, S. S., Mearns, L. O., & Ruane, A. C. (2017). Representing agriculture in Earth System Models: Approaches and priorities for development. *Journal of Advances in Modeling Earth Systems*, 9(5), 2230–2265. <https://doi.org/10.1002/2016MS000749>
- Meehl, G. A., Washington, W. M., Arblaster, J. M., Hu, A., Teng, H., Tebaldi, C., et al. (2012). Climate System Response to External Forcings and Climate Change Projections in CCSM4. *Journal of Climate*, 25(11), 3661–3683. <https://doi.org/10.1175/JCLI-D-11-00240.1>
- Metherell, A.K., L.A. Harding, C.V. Cole, W.J. Parton. 1993. CENTURY, Soil Organic Matter Model Environment. Technical Documentation. Agroecosystem Version 4.0, Great Plains System Research Unit, Technical Report No. 4. USDA-ARS, Fort Collins, Colorado, USA.
- Minasny, B., Malone, B. P., McBratney, A. B., Angers, D. A., Arrouays, D., Chambers, A., et al. (2017). Soil carbon 4 per mille. *Geoderma*, 292(Supplement C), 59–86. <https://doi.org/10.1016/j.geoderma.2017.01.002>

- Monfreda, C., Ramankutty, N., & Foley, J. A. (2008). Farming the planet: 2. Geographic distribution of crop areas, yields, physiological types, and net primary production in the year 2000. *Global Biogeochemical Cycles*, 22(1), GB1022. <https://doi.org/10.1029/2007GB002947>
- Morrison, J. E., Huang, C.-C., Lightle, D. T., & Daughtry, C. S. T. (1993, November 1). Residue measurement techniques. Retrieved May 20, 2019, from <http://link.galegroup.com/apps/doc/A14774461/AONE?sid=google scholar>
- Nagler, P. L., Daughtry, C. S. T., & Goward, S. N. (2000). Plant Litter and Soil Reflectance. *Remote Sensing of Environment*, 71(2), 207–215. [https://doi.org/10.1016/S0034-4257\(99\)00082-6](https://doi.org/10.1016/S0034-4257(99)00082-6)
- Neale R. B., Gettleman A., Park S., Chen C., Lauritzen P. H., Williamson D. L., et al. (2012). Description of the NCAR Community Atmosphere Model (CAM 5.0) NCAR Technical Note 1–289.
- Oleson, K., Lawrence, D. M., Bonan, G. B., et al. (2013). Technical description of version 4.5 of the Community Land Model (CLM). NCAR Technical Note, 434pp.
- Palm, C., Blanco-Canqui, H., DeClerck, F., Gatere, L., & Grace, P. (2014). Conservation agriculture and ecosystem services: An overview. *Agriculture Ecosystems & Environment*, 187, 87–105. <https://doi.org/10.1016/j.agee.2013.10.010>
- Parton, W. J. (1996). The CENTURY model. In *Evaluation of Soil Organic Matter Models* (pp. 283–291). Springer, Berlin, Heidelberg. https://doi.org/10.1007/978-3-642-61094-3_23
- Parton, W. J., Gutmann, M. P., Merchant, E. R., Hartman, M. D., Adler, P. R., McNeal, F. M., & Lutz, S. M. (2015). Measuring and mitigating agricultural greenhouse gas production in the US Great Plains, 1870–2000. *Proceedings of the National Academy of Sciences*, 112(34), E4681–E4688. <https://doi.org/10.1073/pnas.1416499112>
- Peng, B., Guan, K., Chen, M., Lawrence, D. M., Pokhrel, Y., Suyker, A., et al. (2018). Improving maize growth processes in the community land model: Implementation and evaluation. *Agricultural and Forest Meteorology*, 250–251, 64–89. <https://doi.org/10.1016/j.agrformet.2017.11.012>
- Pittelkow, C. M., Liang, X., Linquist, B. A., van Groenigen, K. J., Lee, J., Lundy, M. E., et al. (2015). Productivity limits and potentials of the principles of conservation agriculture. *Nature*, 517(7534), 365–368. <https://doi.org/10.1038/nature13809>


- Poeplau, C., & Don, A. (2015). Carbon sequestration in agricultural soils via cultivation of cover crops – A meta-analysis. *Agriculture, Ecosystems & Environment*, 200, 33–41. <https://doi.org/10.1016/j.agee.2014.10.024>
- Poeplau, C., Don, A., Vesterdal, L., Leifeld, J., Van Wesemael, B., Schumacher, J., & Gensior, A. (2011). Temporal dynamics of soil organic carbon after land-use change in the temperate zone - carbon response functions as a model approach. *Global Change Biology*, 17(7), 2415–2427. <https://doi.org/10.1111/j.1365-2486.2011.02408.x>
- Pongratz, J., Reick, C. H., Houghton, R. A., & House, J. I. (2014). Terminology as a key uncertainty in net land use and land cover change carbon flux estimates. *Earth System Dynamics*, 5(1), 177–195. <https://doi.org/10.5194/esd-5-177-2014>
- Pongratz, Julia, & Caldeira, K. (2012). Attribution of atmospheric CO₂ and temperature increases to regions: importance of preindustrial land use change. *Environmental Research Letters*, 7(3), 034001. <https://doi.org/10.1088/1748-9326/7/3/034001>
- Pongratz, Julia, Dolman, H., Don, A., Erb, K.-H., Fuchs, R., Herold, M., et al. (2018). Models meet data: Challenges and opportunities in implementing land management in Earth system models. *Global Change Biology*, 24(4), 1470–1487. <https://doi.org/10.1111/gcb.13988>
- Portmann, F. T., Siebert, S., & Döll, P. (2010). MIRCA2000—Global monthly irrigated and rainfed crop areas around the year 2000: A new high-resolution data set for agricultural and hydrological modeling. *Global Biogeochemical Cycles*, 24(1). <https://doi.org/10.1029/2008GB003435>
- Powlson, D. S., Stirling, C. M., Jat, M. L., Gerard, B. G., Palm, C. A., Sanchez, P. A., & Cassman, K. G. (2014). Limited potential of no-till agriculture for climate change mitigation. *Nature Climate Change*, 4(8), 678–683. <https://doi.org/10.1038/nclimate2292>
- Prestele, R., Alexander, P., Rounsevell, M. D. A., Arneth, A., Calvin, K., Doelman, J., et al. (2016). Hotspots of uncertainty in land-use and land-cover change projections: a global-scale model comparison. *Global Change Biology*, 22(12), 3967–3983. <https://doi.org/10.1111/gcb.13337>
- Prestele, R., Hirsch, A. L., Davin, E. L., Seneviratne, S. I., & Verburg, P. H. (2018). A spatially explicit representation of conservation agriculture for application in global change studies. *Global Change Biology*, 24(9), 4038–4053. <https://doi.org/10.1111/gcb.14307>
- Pugh, T. a. M., Arneth, A., Olin, S., Ahlstrom, A., Bayer, A. D., Goldewijk, K. K., et al. (2015). Simulated carbon emissions from land-use change are substantially

- enhanced by accounting for agricultural management. *Environmental Research Letters*, 10(12), 124008. <https://doi.org/10.1088/1748-9326/10/12/124008>
- Qin, Z., Dunn, J. B., Kwon, H., Mueller, S., & Wander, M. M. (2016). Soil carbon sequestration and land use change associated with biofuel production: empirical evidence. *Global Change Biology Bioenergy*, 8(1), 66–80. <https://doi.org/10.1111/gcbb.12237>
- Quemada, M., Hively, W. D., Daughtry, C. S. T., Lamb, B. T., & Shermeyer, J. (2018). Improved crop residue cover estimates obtained by coupling spectral indices for residue and moisture. *Remote Sensing of Environment*, 206, 33–44. <https://doi.org/10.1016/j.rse.2017.12.012>
- Quemada, Miguel, & Daughtry, C. S. T. (2016). Spectral Indices to Improve Crop Residue Cover Estimation under Varying Moisture Conditions. *Remote Sensing*, 8(8), 660. <https://doi.org/10.3390/rs8080660>
- Le Quéré, C., Andrew, R. M., Friedlingstein, P., Sitch, S., Hauck, J., Pongratz, J., et al. (2018). Global Carbon Budget 2018. *Earth System Science Data*, 10(4), 2141–2194. <https://doi.org/10.5194/essd-10-2141-2018>
- Sanderman, J., Hengl, T., & Fiske, G. J. (2017). Soil carbon debt of 12,000 years of human land use. *Proceedings of the National Academy of Sciences*, 114(36), 9575–9580. <https://doi.org/10.1073/pnas.1706103114>
- Schob, D. E. (1973). Sodbusting on the Upper Midwestern Frontier, 1820-1860. *Agricultural History*, 47(1), 47–56. Retrieved from <http://www.jstor.org/stable/3741260>
- Seneviratne, S. I., Phipps, S. J., Pitman, A. J., Hirsch, A. L., Davin, E. L., Donat, M. G., et al. (2018). Land radiative management as contributor to regional-scale climate adaptation and mitigation. *Nature Geoscience*, 11(2), 88. <https://doi.org/10.1038/s41561-017-0057-5>
- Serbin, G., Hunt, E. R., Daughtry, C. S. T., McCarty, G. W., & Doraiswamy, P. C. (2009). An Improved ASTER Index for Remote Sensing of Crop Residue. *Remote Sensing*, 1(4), 971–991. <https://doi.org/10.3390/rs1040971>
- Smith, P., Martino, D., Cai, Z., Gwary, D., Janzen, H., Kumar, P., et al. (2008). Greenhouse gas mitigation in agriculture. *Philosophical Transactions of the Royal Society B-Biological Sciences*, 363(1492), 789–813. <https://doi.org/10.1098/rstb.2007.2184>
- Smith, P., Bustamante, M., Ahammad, H., Clark, H., Dong, H., Elsiddig, E. A., et al. (2014). Agriculture, Forestry and Other Land Use (AFOLU). In O. Edenhofer, R. PichsMadrugá, Y. Sokona, J. C. Minx, E. Farahani, S. Kadner, et al. (Eds.),

- Climate Change 2014: Mitigation of Climate Change. Contribution of Working Group III to the Fifth Assessment Report of the Intergovernmental Panel on Climate Change. Cambridge: Cambridge Univ Press.
- Soussana, J.-F., Lutfalla, S., Ehrhardt, F., Rosenstock, T., Lamanna, C., Havlík, P., et al. (2017). Matching policy and science: Rationale for the ‘4 per 1000 - soils for food security and climate’ initiative. *Soil and Tillage Research*.
<https://doi.org/10.1016/j.still.2017.12.002>
- Stewart, C. E., Plante, A. F., Paustian, K., Conant, R. T., & Six, J. (2008). Soil Carbon Saturation: Linking Concept and Measurable Carbon Pools. *Soil Science Society of America Journal*, 72(2), 379–392. <https://doi.org/10.2136/sssaj2007.0104>
- Stockmann, U., Adams, M. A., Crawford, J. W., Field, D. J., Henakaarchchi, N., Jenkins, M., et al. (2013). The knowns, known unknowns and unknowns of sequestration of soil organic carbon. *Agriculture Ecosystems & Environment*, 164, 80–99.
<https://doi.org/10.1016/j.agee.2012.10.001>
- Storey, J. C., Roy, D. P., Masek, J., Gascon, F., Dwyer, J. L., & Choate, M. J. (2016). A note on the temporary misregistration of Landsat-8 Operational Land Imager (OLI) and Sentinel-2 Multi Spectral Instrument (MSI) imagery. *Remote Sensing of Environment*, 186, 2. <https://doi.org/10.1016/j.rse.2016.08.025>
- Syswerda, S. P., Corbin, A. T., Mokma, D. L., Kravchenko, A. N., & Robertson, G. P. (2011). Agricultural Management and Soil Carbon Storage in Surface vs. Deep Layers. *Soil Science Society of America Journal*, 75(1), 92–101.
<https://doi.org/10.2136/sssaj2009.0414>
- Thoma, D. P., Gupta, S. C., & Bauer, M. E. (2004). Evaluation of optical remote sensing models for crop residue cover assessment. *Journal of Soil and Water Conservation*, 59(5), 224–233. Retrieved from
<http://www.jswnonline.org/content/59/5/224>
- Tittonell, P., Gérard, B., & Erenstein, O. (2015). Tradeoffs around crop residue biomass in smallholder crop-livestock systems – What’s next? *Agricultural Systems*, 134, 119–128. <https://doi.org/10.1016/j.agry.2015.02.003>
- Tomer, M. D., & James, D. E. (2004). Do Soil Surveys and Terrain Analyses Identify Similar Priority Sites for Conservation? *Soil Science Society of America Journal*, 68(6), 1905–1915. <https://doi.org/10.2136/sssaj2004.1905>
- Tomer, M. D., Moorman, T. B., James, D. E., Hadish, G., & Rossi, C. G. (2008). Assessment of the Iowa River’s South Fork watershed: Part 2. Conservation practices. *Journal of Soil and Water Conservation*, 63(6), 371–379.
<https://doi.org/10.2489/jswc.63.6.371>

- USDA - National Agricultural Statistics Service. 2016. Crop condition and progress reports. Washington, DC. Available online:
https://www.nass.usda.gov/Statistics_by_State/Iowa/Publications/Crop_Progress_&_Condition/index.php (accessed on 30 May 2019).
- USDA - National Agricultural Statistics Service. 2017. Crop condition and progress reports. Washington, DC. Available online:
https://www.nass.usda.gov/Statistics_by_State/Iowa/Publications/Crop_Progress_&_Condition/index.php (accessed on 30 May 2019).
- USDA-Natural Resource Conservation Service. 2006a. Tillage Practice Guide: A Guide to USDA-NRCS Practice Standards 329 No-till/Strip Till/Direct Seed & 345 Mulch Till. Available online:
http://www.nrcs.usda.gov/Internet/FSE_DOCUMENTS/nrcs142p2_020719.pdf (accessed on 15 July 2019).
- USDA-Natural Resource Conservation Service. 2006b. Land resource regions and major land resource areas of the United States, the Caribbean, and Pacific Basin. Available online:
https://www.nrcs.usda.gov/Internet/FSE_DOCUMENTS/nrcs142p2_050898.pdf (accessed on 30 May 2019).
- van Deventer, A. P., Ward, A. D., Gowda, P. H., & Lyon, J. G. (1997). Using thematic mapper data to identify contrasting soil plains and tillage practices. *Photogrammetric Engineering and Remote Sensing*, 63(1), 87–93.
- Virto, I., Barre, P., Burlot, A., & Chenu, C. (2012). Carbon input differences as the main factor explaining the variability in soil organic C storage in no-tilled compared to inversion tilled agrosystems. *Biogeochemistry*, 108(1–3), 17–26.
<https://doi.org/10.1007/s10533-011-9600-4>
- Wesemael, B. van, Paustian, K., Meersmans, J., Goidts, E., Barancikova, G., & Easter, M. (2010). Agricultural management explains historic changes in regional soil carbon stocks. *Proceedings of the National Academy of Sciences*, 107(33), 14926–14930. <https://doi.org/10.1073/pnas.1002592107>
- Wirsenius, S. (2000). Human use of land and organic materials: modeling the turnover of biomass in the global food system. Retrieved from <http://agris.fao.org/agris-search/search.do?recordID=XF2015034666>
- Wirsenius, S. (2003). Efficiencies and biomass appropriation of food commodities on global and regional levels. *Agricultural Systems*, 77(3), 219–255.
[https://doi.org/10.1016/S0308-521X\(02\)00188-9](https://doi.org/10.1016/S0308-521X(02)00188-9)
- Zheng, B., Campbell, J. B., Serbin, G., & Daughtry, C. S. T. (2013). Multitemporal remote sensing of crop residue cover and tillage practices: A validation of the

- minNDTI strategy in the United States. *Journal of Soil and Water Conservation*, 68(2), 120–131. <https://doi.org/10.2489/jswc.68.2.120>
- Zheng, Baojuan, Campbell, J. B., & de Beurs, K. M. (2012). Remote sensing of crop residue cover using multi-temporal Landsat imagery. *Remote Sensing of Environment*, 117, 177–183. <https://doi.org/10.1016/j.rse.2011.09.016>
- Zheng, Baojuan, Campbell, J. B., Shao, Y., & Wynne, R. H. (2013). Broad-Scale Monitoring of Tillage Practices Using Sequential Landsat Imagery. *Soil Science Society of America Journal*, 77(5), 1755. <https://doi.org/10.2136/sssaj2013.03.0108>
- Zheng, Baojuan, Campbell, J. B., Serbin, G., & Galbraith, J. M. (2014). Remote sensing of crop residue and tillage practices: Present capabilities and future prospects. *Soil and Tillage Research*, 138, 26–34. <https://doi.org/10.1016/j.still.2013.12.009>

Link	Icon	Licenses	Author <u>allows</u> users to	Author <u>requires</u> users to	Author <u>restricts</u> users from
Link		CC BY-NC-ND (CC BY Non-Commercial, No Derivative Works)	Copy, distribute, display, and perform verbatim (unchanged) copies of the work for non-commercial purposes.	Attribute or credit the author as requested.	Remixing or creating derivatives of the work. Copying, distributing, displaying, performing, and remixing the work for commercial purposes.